ELASTO-VISCOPLASTIC MODELLING OF ROCK EXCAVATIONS

by

Maged Kamal Rizkalla

A thesis

submitted to the School of Graduate Studies

in Partial Fulfilment of the Requirements

for the Degree

Master of Engineering

Department of Mining and Metallurgical Engineering

McGill University

June 1991

ABSTRACT

The first part of the thesis describes the concepts of viscoplasticity as a continuum plasticity theory highlighting different kinds of yield functions, plastic potentials and viscoplastic constitutive laws.

A 2-dimensional elasto-viscoplastic finite element model for stress/stability analysis of mining excavations has been developed for use on microcomputers. An iterative explicit time stepping scheme is implemented. The program uses automatic time-step calculator based on equations giving a limit on the time step in an attempt to prevent numerical instability when common forms of isotropic yield functions and plastic potentials are used in the viscoplastic solution. When the input data are read parallel to the analysis undertaken the user can simulate compound behaviour by stopping the analysis, examining the results graphically and restarting it again and possibly implementing a certain decision in the subsequent appended input. This also imposes no limit on the number of time stations at which instantaneous changes like elements cut, elements backfilled, loads added or simply outputs are required. The program is equipped with graphical pre- and post- processors.

RÉSUMÉ

La première partie de cette thèse porte sur les notions de viscoplasticité comme théorie de la plasticité des milieux continus où sont mis en évidence plusieurs types de fonctions de fluage, de potentiels de plasticité et de lois constitutives de viscoplasticité.

Un modèle d'élasto-viscoplasticité bidimensionnel à éléments finis pour l'analyse des contraintes et de la stabilité dans les cavités minières a été élaboré pour être utilisé sur micro-ordinateur. Le modèle utilise un élément isoparamétrique quadrilatéral à quatre noeuds et un schéma itératif explicite d'intégration dans l'intervalle de temps. Pour empêcher l'instabilité numérique de la solution, le programme utilise des équations qui limitent l'intervalle; cela assure la stabilité numérique de la solution pour les formes courantes de fonctions de fluage isotropiques et de potentiels de plasticité servant à la formulation d'une loi de viscoplasticité. Lorsque les données d'introduction sont lues parallèlement à l'analyse entreprise, l'utilisateur peut simuler le comportement composé en stoppant l'analyse, en procédant à l'examen graphique des résultats, puis en reprenant l'analyse; il peut même intégrer une décision dans les données qui seront ajoutées par la suite. Cela n'impose pas de limites quant au nombre de points dans le temps auxquels des modifications instantanées (éléments sectionnés, éléments remblayés ou charges appliquées) sont apportées, ou auxquels des données doivent être extraites. Le programme comporte des pré et post-processeurs graphiques.

ACKNOWLEDGEMENTS

First of all, I give thanks to my Lord Jesus Christ for guiding me through this work and giving me the light to see through the subject of this study.

I wish to express my appreciation to my supervisor Professor H. S. Mitri for his continuing encouragement and support throughout the period of my study. Without his help, this work would not have come to its current state of development. He offered technical support and made available all the necessary hardware for the program development. Thanks are also given to all members of the Numerical Modelling Group particularly my colleagues Phanuwat Suriyachat and Keyvan Fotoohi with whom I shared a friendly work environment which was essential for production.

TABLE OF CONTENTS

LIST OF FIGURES

NOTATION

Note that bold letters represent vectors or matrices

$\boldsymbol{\sigma}$ stress vector

$=\{\sigma_x\ \sigma_y\ \sigma_z\ \tau_{xy}\ \tau_{yz}\ \tau_{zx}\}^T$

σ_{ij} stress at plane i in the direction of j

σ_1, σ_2, σ_3 are the principal stresses

J_1 first stress invariant

$= \sigma_1 + \sigma_2 + \sigma_3 = \sigma_x + \sigma_y + \sigma_z = 3\ \sigma_m$

σ_m mean stress or hydrostatic stress

$= J_1/3$

s_{ij} deviatoric stress at plane i in j direction

$= \sigma_{ij} - \sigma_m$

$J_{2D}^{1/2}$ second deviatoric stress invariant

$$(\tfrac{1}{2}s_{ij}s_{ij})^{1/2} = \sqrt{\frac{1}{2}s_x^2+\frac{1}{2}s_y^2+\frac{1}{2}s_z^2+\tau_{xy}^2+\tau_{yz}^2+\tau_{zx}^2}$$

σ $= J_{2D}^{1/2}$

J_{3D} third deviatoric stress invariant

$= 1/3\ s_{ij}s_{jk}s_{kl}$

$\cap$ Lode's angle

$$= \frac{1}{3}\sin^{-1}\left[-3\frac{\sqrt{3}}{2}\frac{J_{3D}}{J_{2D}^{\frac{3}{2}}}\right] \quad \text{and} \quad -\pi/6 \leq \cap \leq \pi/6$$

ϵ or ϵ_t total strain vector

$= \{\epsilon_x\ \epsilon_y\ \epsilon_z\ \gamma_{xy}\ \gamma_{yz}\ \gamma_{zx}\}^T$

ϵ_{xy} $=\gamma_{xy}/2$

$\epsilon_{xy}^{e}=\tau_{xy}/2G$

ϵ_{vp} viscous strain vector

ϵ^{P} plastic strain vector

ϵ^{I} inelastic strain vector which correspond to ϵ_{vp} or ϵ^{P}

$\dot{\epsilon}_{vp}$ viscoplastic strain rate = $\frac{d\epsilon_{vp}}{dt}$

ϵ_{v} volumetric strain = $\epsilon_x+\epsilon_y+\epsilon_z$

ϵ_{m} mean plastic strain

and $\epsilon_m^{e} = \sigma_m/(3K)$

ϵ_{ij} strain at plane i in the direction of j

ϵ_1, ϵ_2, ϵ_3 are the principal strains

e_{ij} deviatoric strain at plane i in j direction

$=\epsilon_{ij}-\epsilon_m$ and $e_{ij}^{e} = s_{ij}/2G$

ϵ_{d} deviatoric strain invariant corresponding to $J_{2D}^{1/2}$

$$=(\tfrac{1}{2}e_{ij}e_{ij})^{1/2}= \sqrt{\frac{1}{2}e_x^2+\frac{1}{2}e_y^2+\frac{1}{2}e_z^2+\epsilon_{xy}^2+\epsilon_{yz}^2+\epsilon_{zx}^2}$$

σ_T $=\sigma_1+\sigma_3$

σ_d $=|\sigma_1-\sigma_3|/2$ When x-y is the plane of maximum and minimum stresses= $\sqrt{\left(\frac{\sigma_x-\sigma_y}{2}\right)^2+\tau_{xy}^2}$

ϵ_T $=\epsilon_1+\epsilon_3$

ϵ_d $=|\epsilon_1-\epsilon_3|/2$ when x-y is the plane of maximum and

	minimum strains= $\sqrt{\left(\frac{\epsilon_x-\epsilon_y}{2}\right)^2+\epsilon_{xy}^2}$
E	Young's modulus
G	shear modulus = $\frac{E}{2(1+\nu)}$
K	bulk modulus = $\frac{E}{3(1-2\nu)}$
F	yield function
Q	plastic potential
k	hardening variable
ψ	angle of internal friction
C	cohesion
D	elasticity matrix
K	global stiffness matrix
t	time
Δt_n	time increment between t_n and t_{n+1}
H	rate of softening or hardening used in incremental plasticity
b	body force/unit volume (e.g the own weight)
s	vector of surface loading / unit surface of the element side (shear and pressure)
$d\Omega$	infinitesimal volume and $\int_\Omega (\quad) d\Omega$ is the integration of a function over the elements volume
$d\Gamma$	infinitesimal area and $\int_\Gamma (\quad) d\Gamma$ integration of a function over the side surface area of an element .

CHAPTER 1

INTRODUCTION

1.1 GENERAL

The prediction of stresses and strains around excavations is one of the major objectives of rock mechanics studies . Most of the rock mechanics problems involving stress calculation and mine stability are so complicated that closed form solutions are difficult to derive and that numerical methods have to be employed. The rapid development of personal computers in the last two decades has made it easy for numerical modelling techniques like finite elements and boundary elements to play an important role in rock mechanics. Usually, the finite element is the preferable numerical modelling technique for solving rock mechanics stabilty problems, because of being a differential method which offers its ability to handle materials of nonlinear behaviour and makes it possible to account for time dependent effects step by step. This report is focusing on the use of vicoplasticity in the finite element. The reader is referred to References [1] and [2] for a description of the different numerical methods in general and to Reference [3] for details on the finite element method in particular.

1.1.1 ELASTO-VISCOPLASTICITY

The theory of elasticity has found wide spread use in rock mechanics studies for solving problems of linearized material behaviour. Plasticity is a continuum theory and its use arises when the non-linear stress-strain behaviour or the time dependent behaviour has to be considered.

The theory of elasticity together with the theory of viscoplasticity or the incremental theory of plasticity are used in a numerical modelling technique like the finite element method to calculate the stresses and deformations induced after excavation. The incremental theory of plasticity is used to model the instantaneous elastoplastic behaviour, while the theory of viscoplasticity is used to model the time-dependent behaviour. Physically, the instantaneous and time-dependent plasticity cannot be treated separately. The apparent difference is that the former occurs at a high rate sometimes higher than the loading rate, e.g compressible porous media initially under low hydrostatic pressure and for unstable (softening) parts of the rock mass.

The main subject of this study is the theory of elasto-viscoplasticity which can also be used to model problems of instantaneous or viscous elastoplasticity. References [4], [3], [5] present a comprehensive description of plasticity.

1.1.2 CREEP LAWS

In order to model the short term stress strain response in

viscoplasticity, the time is used as a fictitious variable and the rate of viscoplastic strain is chosen on an arbitrary scale [4]. On the other hand, the creep behaviour is a phenomenon frequently met when dealing with geotechnical problems involving weak rocks , salt rocks or rocks rich in clay minerals,etc. [6]. The importance of this phenomenon is magnified when dealing with the stability or the closure of deep mine openings excavated in ductile halite or potash. The great interest arose from the challenge of embedding in a safe and permanent way the nuclear radioactive waste in deep viscous rocksalt for which the creep phenomenon is very apparent.

Several experimental and analytical approaches have been presented to formulate creep laws. Reference [6] presents an exhaustive review of creep laws of rock in general and of rocksalt in particular. In most cases, these are scalar functions relating the total creep strain or its rate with the affecting parameters mainly; the acting stress, time (case of time hardening creep laws) or strain , temperature and other environmental variables like the humidity. It should be noted that in the numerical modelling of nonlinear creep behaviour, we are most concerned with the rate of creep as a function of the variables with time which are the stress and the strain (case of strain hardening creep laws) or the time itself (case of time hardening creep laws).

1.1.3 YIELD FUNCTIONS AND PLASTIC POTENTIALS

A great portion of rock mechanics studies in the last two decades was aimed for the description of yield functions for different rock types under different stress conditions [7], [8], [9]. The yield function checks if the yield (or creep) occurs, while the material parameters included in it, together with those involved in the creep law itself, as being functions of the viscoplastic strain or the plastic work reflect the hardening or softening behaviour (primary or tertiary creep)[10],[11]. To obtain the components of the strain rate, a plastic potential is used.

Some aspects of the inelastic behaviour cannot be modelled by the conventional linear yield conditions like Mohr-Coulomb or Drucker Prager especially when the yield condition is used as a plastic potential. This led to the development of special forms of yield functions and plastic potentials which attempt to model the compound paths of the stress-strain behaviour as well as the observed components of the inelastic strain rate especially its volumetric changes (e.g. [11],[12],[13]).

Several papers in the recent years deal with anisotropic yield functions and the anisotropic evolution of these yield surfaces in the acting stresses space [14],[9].

1.2 SCOPE OF WORK

The plan of this study can be summarized in a point form as

follows ;

1) LITERATURE REVIEW

a) After revising the finite element modelling of elastic behavior of rock excavations , study the plasticity theories; incremental theory of plasticity and elasto-viscoplasticity and their use in the finite element method with the related concepts of yield functions and plastic potentials.

b) From the plasticity theories the theory of viscoplasticity is chosen to model time dependent and time independent plasticity.

c) Review the recent developments of yield functions, plastic potentials, and constitutive creep laws.

d) Review of creep laws applicable to soft rock in general and rocksalt in particular.

e) Review of the numerical procedure of implementing the viscoplasticity in the finite element method. This subject is rarely available in the literature but References [4],[3] present its basic concepts.

2)-**Writing an elasto-viscoplastic 2D finite element computer program** . And considering the numerical stabilty and accuracy of its proposed iterative explicit time integration scheme.

3) Modification of an existing graphical pre- and postprocessors to account for time dependent input and output.

1.3 PROGRAM VISA2D

The developed numerical model is a 2-D finite element program using the theory of elasto-viscoplasticiy to model the effect of short term and time dependent behaviour on stresses and deformations around compound layouts of surface or underground mine excavations.

The program uses the continuum theory of elasto-viscoplasticity thus to overcome the inhomogeneity of the surrounding rock several material types can be used. It uses the classical 4 node-isoparametric elements with four integration points and it handles different types of loading , like own weight , nodal loading , surface loading and the initial or premining stresses. At any time station , the user can specify instantaneous changes. These could be added loads or additional cut or fill. The program can be stopped at any time and the analysis may be restarted at that time station later. The program models the combined effect of elastoplasticity and creep by first performing the viscoplasticity as an artifice to elastoplastic behaviour then it starts assessing creep. This approach is suited for its iterative explicit time integration scheme , while the approach used in Reference [22] is a useful tool for an implicit scheme. Several yield functions and creep laws can easily be adopted in the developed numerical model.

In writing the program , it was focused on reducing the running time , increasing the limit on the number of elements

it can handle, and making the program user-friendly and flexible. The program is written using many of the powerful features of MicroSoft Fortran version 5.0 [15] which deals efficiently with the 80286 processors and 287 coprocessors. The numerical model has a preprocessor for mesh generation and three graphics programs for checking the input data and interpreting results. **PRESAP** is a preprocessor used to generate the required finite element mesh by reading a simple free format input data file in which the user just divides the problem into zones representing distinct conditions of rock types and intensity of elements. This data file written by the user is compatible with the data files used by program **MSAP2D** [16]. One graphics program is used to check this free format user-created data file , the second is used to check the actual mesh data of nodal points and elements connectivity mesh created by the preprocessor . The third is used to give the graphical interpretation of stresses and deformations around openings as well as the material behavior.

The program uses an automatic time stepping calculator formulated based on the same concept of Reference [17] for explicit stepping scheme.

1.4 THESIS OUTLINE

The basic concepts of viscoplasticity as a continuum plasticity theory are explained in Section 2.1 highlighting yield functions , and plastic potentials with reference to

the incremental theory of plasticity and viscous elasto-plasticity.

Section 2.2 and Section 2.3 discuss some types of yield functions and plastic potentials while Section 2.4 presents different kinds of creep and viscoplastic constitutive laws which can be or already implemented in the developed computer program.

The numerical algorithm of an iterative explicit time integration scheme implemented in program **VISA2D** and its flow chart are described in Section 3.2 . Section 3.3 derives the equations used for the numerical stability of a fully explicit stepping scheme. A description of the input data are given in Sections 4.2, 4.3 . Three illustrative examples will be discussed in section 4.4 of this report representing ; a simple axisymmetric problem , the effect of face advance and creep on the deformations and stresses around the longitudinal section of a circular tunnel in axisymmetric ground conditions and finally an elastoplastic solution of a circular tunnel by the theory of viscoplasticity then the report ends by conclusions.

CHAPTER 2

ELASTO-VISCOPLASTICITY AS A CONTINUUM

PLASTICITY THEORY

2.1 BASIC CONCEPTS OF PLASTICITY:

One use of plasticity theories arises when the post yield behaviour of the material has to be considered. This is the case when analyzing excavations in soft rock or when problems involving large deformations of rock mass are encountered Examples of such problems inlude rock mass caving, slope instability involving rock of weak quality and soil layers or backfill. Other important uses arise when dealing with creeping rocks of viscous nature like potash.

The theory of plasticity is a continuum theory like the theory of elasticity i.e a constitutive model (composed of the two theories) assigned to a specific zone (or element) describes it as being uniform or homogeneous. This assumption deteriorates if the considered zone is intact and traversed by one discontinuity. In this case another constitutive model should be assigned to the discontinuity itself. However if the relative scale of spacing between discontinuities and rock mass of the considered zone is small the domain might be considered homogeneous and in this case one constitutive model may describe this zone of composite

material [18]. The theory of plasticity involves a number of important concepts that can only be briefly introduced here. Readers are advised to consult Reference [4],[5],[3],[1] for more detail.

2.1.1 YIELD FUNCTIONS AND PLASTIC POTENTIALS

The state of stress under which the plastic flow occurs satisfies what is called a yield function or yield criterion such that :

$$F(\boldsymbol{\sigma},\boldsymbol{\epsilon}^P) \geq 0.0 \quad (\textit{viscoplasticity})$$
$$\textit{or}$$
$$F(\boldsymbol{\sigma},\boldsymbol{\epsilon}^P) = 0.0 \quad (\textit{incremental plasticity})$$

Where $\boldsymbol{\sigma}$ is the stress vector and $\boldsymbol{\epsilon}^P$ is the plastic or viscoplastic strain vector. In some cases the yield function might be simplified as follows :

$$F(\boldsymbol{\sigma},\boldsymbol{\epsilon}^P) = f(\boldsymbol{\sigma}) - Y(\boldsymbol{\epsilon}^P) \qquad (2.1)$$

where $f(\boldsymbol{\sigma})$ is an expression of the acting stresses and Y is the yield strength which varies with the evolution of viscoplastic strain [3]. Once plastic yielding has taken place the relation between stresses and strains might not be unique. A flow rule is the relation between the state of stress at which viscoplastic strain occurs and the rate of that strain vector. At early stages of plasticity theory one of the assumptions was to relate the plastic strain rate in a certain direction with the deviatoric stress in this direction [5],[3]. Later the concept of the plastic potential (Q) was

developed, see equation 2.7,2.11 where Q is an expression of the acting stresses and might as well depend on the plastic strain. It represents a convex surface in the stress space which means that the plastic work is positive because the normal to this surface is parallel to the direction of the inelastic strain rate.

It is also accepted that this surface would be that of the yield condition which implies that $F \equiv Q$. The reason of this assumption might be clear if one considers yielding of specimen under shear stress. By using an associative flow rule (normality condition $F \equiv Q$) ,the yield function would serve as :

1-A stress condition to check if yield (or creep) occurs.

2-Gives the direction of the plastic strain rate vector (see Figure 2.1).

3- The material constants in the yield function , as being dependent on the viscoplastic strain , govern the behavior pattern in the stress-strain curve or in deformation-time curve , thus simulating the hardening , softening or perfect plasticity [12],[18] (see Figure 2.4b and Figure 2.7b) .

Isotropic yield functions are used for isotropic rock mass. In this case the yield condition is independent of the direction of the acting stresses but depends on the principal stresses at the point.

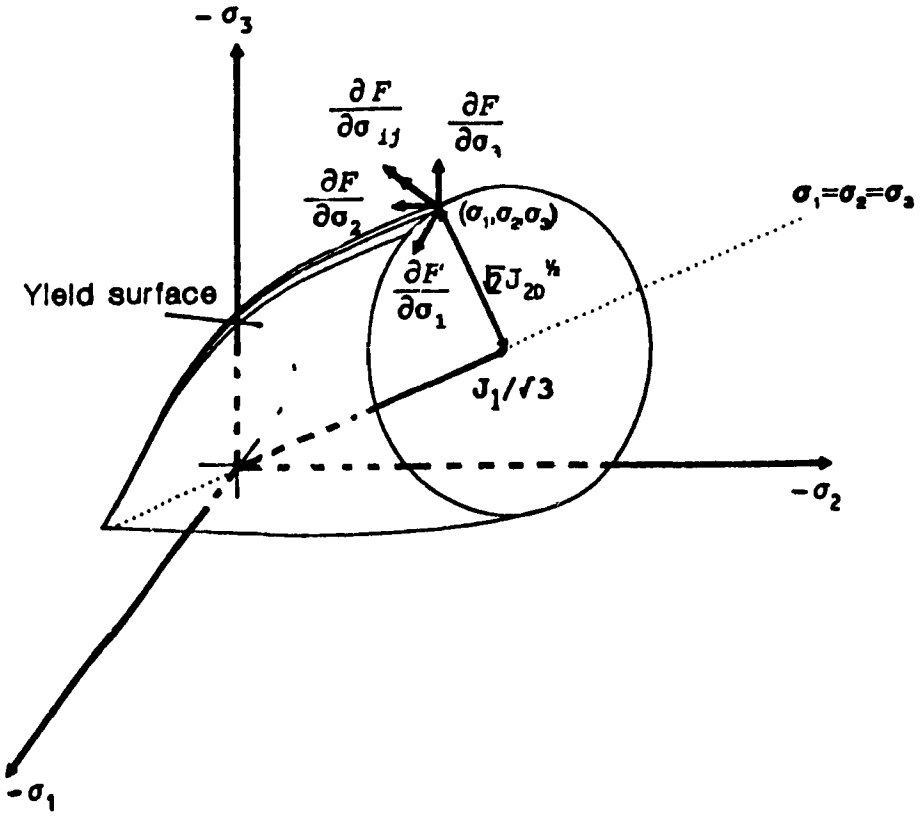

A plot of the yield surface of an isotropic material in the principal stress space
(Figure 2.1)

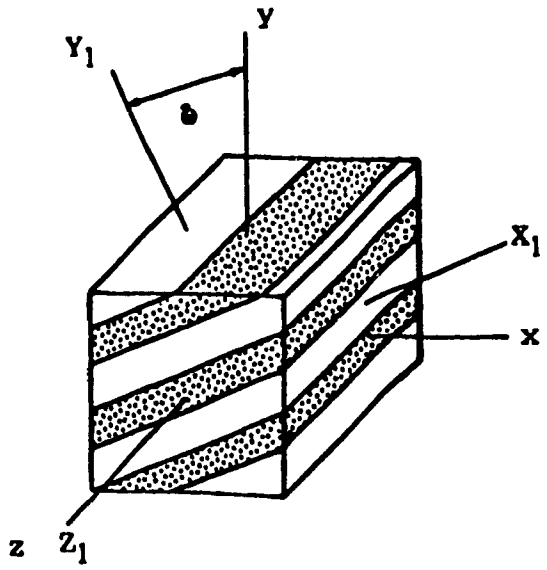

$$F=F(\sigma_x,\sigma_y,\sigma_z,\tau_{xy},\tau_{yz},\tau_{xz},\omega)$$

Orientation of planes of weakness dictating an anisotropic yield condition
(Figure 2.2)

For anisotropic rock or the case of one or more parallel

sets of joints , an anisotropic yield function which depends on the direction of loading with respect to a plane of weakness is used [1],[14],[19], see equation 2.31.
Isotropic hardening keeps the yield function isotropic and the stress condition remains in the principal stress space [20],[13]. References [8],[11],[9] give examples of anisotropic hardening which convert the yield condition to an anisotropic one dependent on the direction of the past plastic strain to include Bauscinger effect [18].

In the following review isotropic yield functions and plastic potentials are the main subject however the yield functions discussed in Sections 2.4 and 2.5 are anisotropic. Mohr-Coulomb yield condition considers only the plane of maximum and minimum principal stresses σ_1, σ_3 relating the maximum shear with the normal stress [5] (see Figure 2.3a);

$$F(\sigma, \epsilon_{vp}) = |\sigma_1 - \sigma_3| + (\sigma_1 + \sigma_3) * \sin\psi - 2C\cos\psi \qquad (2.2)$$

where ψ is the angle of internal friction and c is the cohesion and 2C cosψ may correspond to $Y(\epsilon_{vp})$ in equation 2.1 as a material parameter function of the inelastic strain.
Other yield functions like Drucker-Prager relate the deviatoric and hydrostatic stress invariants to the material constants c and ψ as follows :

$$F = \sqrt{3}\sqrt{J_{2D}} + \frac{2\sin\psi}{3-\sin\psi} J_1 - \frac{6c\cos\psi}{3-\sin\psi} \qquad (2.3)$$

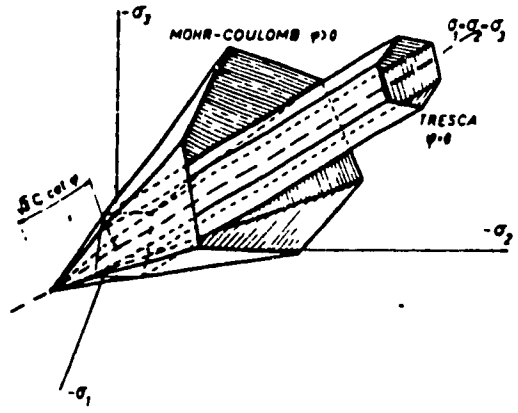

Mohr coulomb C-φ yield surface [4]
(Figure 2.3 a)

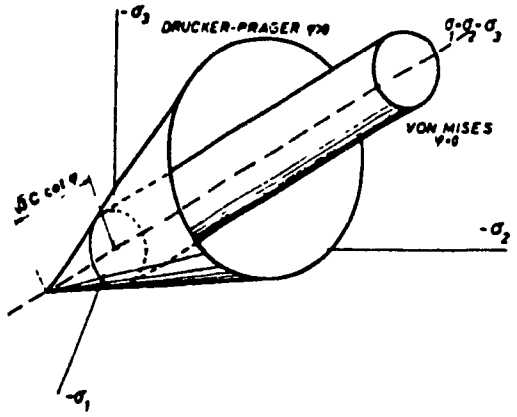

Drucker-Prager C-φ yield surface [4]
(Figure 2.3 b)

To consider the post yield behavior Equations 2.2,2.3 have to be thought of as follows (see Figure 2.3):

$$F(\sigma, \varepsilon_{vp}) = |\sigma_1 - \sigma_3| + \alpha_1 (\sigma_1 + \sigma_2) - Y_1(\varepsilon_{vp}) \quad (2.4\ a)$$

$$F(\sigma, \varepsilon_{vp}) = \sqrt{J_{2D}} + \alpha_2 J_1 - Y_2(\varepsilon_{vp}) \quad (2.4\ b)$$

where α_1 , α_2, Y_1, Y_2 material constants controlling the role of the yield function and plastic potential as seen in more detail in Sections 2.2, 2.3.

2.1.2 THE INCREMENTAL THEORY OF PLASTICITY:

Two major continuum theories are used to quantify and model the plastic behaviour these are :

1) The theory of elasto-viscoplasticity, This is implemented in program **VISA2D** which is reviewed in the following subsection and therefore is the main subject of this study.

2) The incremental theory of plasticity. This theory is widely used for the short term stress-strain behavior as will be briefly reviewed only in this subsection (see References [1],[3],[5]).

In this theory the relation between the instantaneous plastic strain increments and the stress increments is determined from Drucker's consistency Condition :

$$F(\sigma, \varepsilon^p) = 0.0 \quad at\ yield$$
$$\rightarrow dF = \frac{\partial F}{\partial \sigma} d\sigma + \frac{\partial F}{\partial \varepsilon^p} d\varepsilon^p = 0.0 \quad (2.5)$$

This means that when the loading energy exceeds the elastic energy at the initial yield point Y_o a plastic strain increment takes place causing hardening or softening effect on the material behavior. For example in the simple case represented in Figure 2.4a , hardening means that each $d\epsilon^p$ allows for an increase in the yield strength of the friction slider. In other words when the yield strength of the material can no longer sustain the applied load (or energy) , $d\epsilon^p$ occurs and the strength is changed by an increment - $\frac{\partial F}{\partial \epsilon^p} d\epsilon^p$ (in equation 2.5) which then allows $d\sigma$ to satisfy Drucker consistency condition:

$$d\epsilon^p \rightarrow \frac{\partial F}{\partial \epsilon^p} d\epsilon^p \rightarrow d\sigma \text{ satisfying; } \frac{\partial F}{\partial \sigma} d\sigma = -\frac{\partial F}{\partial \epsilon^p} d\epsilon^p \qquad (2.6)$$

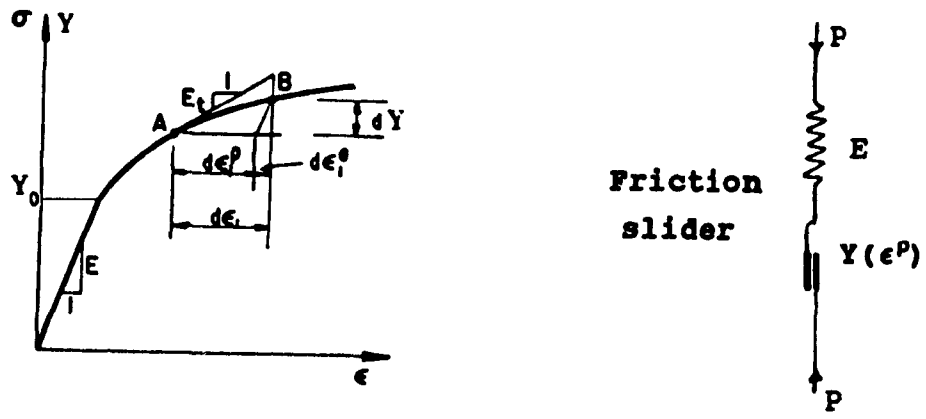

Elasto-plastic behaviour under uniaxial compression
(Figure 2.4 a)

, and so on for the successive strain and stress increments to

give the nonlinear behavior shown in Figure 2.4.

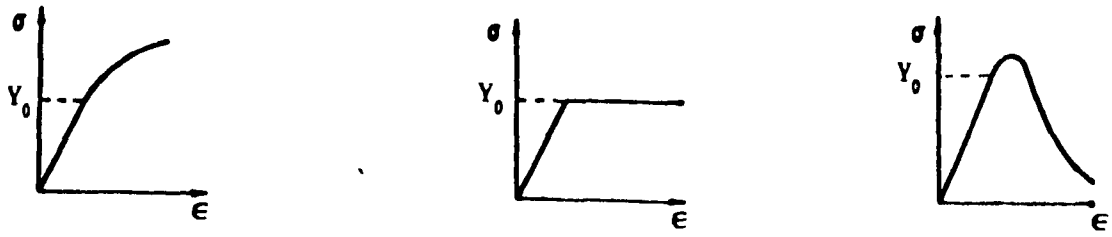

$\frac{\partial F}{\partial \epsilon_{vp}} < 0.0$ hardening

$\frac{\partial F}{\partial \epsilon_{vp}} = 0.0$ perfect plasticity (Figure 2.4 b)

$\frac{\partial F}{\partial \epsilon_{vp}} > 0.0$ softening

By using a flow rule , the relation between each component of the plastic strain and the stress increment vectors can be formulated as in equation 2.7.

$$d\epsilon^P = d\epsilon^P_{ij} = d\lambda \frac{\partial Q}{\partial \sigma_{ij}} \qquad (2.7)$$

where Q is the plastic potential and the increment $d\lambda$ is given when Drucker's consistency condition is applied as follows;

$$d\epsilon^P = d\lambda \frac{\partial Q}{\partial \sigma} = \left(\frac{\left(\frac{\partial F}{\partial \sigma} \cdot d\sigma \right)}{H} \right) \frac{\partial Q}{\partial \sigma} \qquad (2.8)$$

where H is a scalar quantifying the hardening or softening caused by $d\epsilon^P/d\lambda$; $H = -\frac{\partial F}{\partial \epsilon^P} \frac{\partial Q}{\partial \sigma}$ or if k is the strain hardening variable $H = -\frac{\partial F}{\partial k} \frac{dk}{d\lambda}$ and $dk/d\lambda$ is determined according to the flow rule used. For some yield functions H may by $d\sigma_1/d\epsilon^P$ in a uniaxial test (see Figure 2.5). Because $d\sigma$ vector is unknown the relation between $d\epsilon^P$ and $d\sigma$ is given

as follows;

$$d\epsilon^p = \frac{1}{H}\left[\frac{\partial Q}{\partial \sigma}\frac{\partial F}{\partial \sigma}^T\right] d\sigma \qquad (2.9)$$

In equation 2.9 , using the yield function as a plastic potential gives a symmetric stress strain matrix leading to symmetric global stiffness matrix, thus reducing significantly the time and storage size. When H is positive it reflects hardening behavior while when H is negative the softening behavior is simulated in which case we might face non uniqueness of the solution. This problem is overcome in the theory of viscoplasticity described in the following Section.

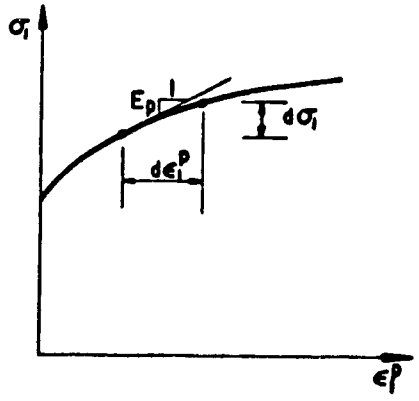

$$\frac{dF}{dk} = \frac{\frac{dF}{d\sigma_1}}{\frac{dk}{d\epsilon_1^p}}\frac{d\sigma_1}{d\epsilon_1^p} = \frac{\frac{dF}{d\sigma_1}}{\frac{dk}{d\epsilon_1^p}}E_p$$

Determination of the $\partial F/\partial k$ using uniaxial compression test
(Figure 2.5)

2.1.3 ELASTO-VISCOPLASTICITY THEORY:

The elasto-viscoplasticity theory developed by Zeinkiewicz and Cormeau [4], has been adopted in the present study. The elasto viscoplastic behaviour could be described by the behaviour of the dashpot inside the mechanical model shown in Figure 2.6 Each component of the creep strain vector is obtained using the a plastic potential which for associative viscoplasticity is the yield function (F) itself [3].

$$F(\sigma, \varepsilon^p) = f(\sigma) - Y(\varepsilon^p) \tag{2.10}$$

$F \geq 0.0$ → elasto-viscoplastic i.e

$$\dot{\varepsilon}_{vp_{ij}} = \phi \frac{\partial Q}{\partial \sigma_{ij}} \tag{2.11}$$

$F < 0.0$ → elastic

$\dot{\varepsilon}_{vp} = 0.0$

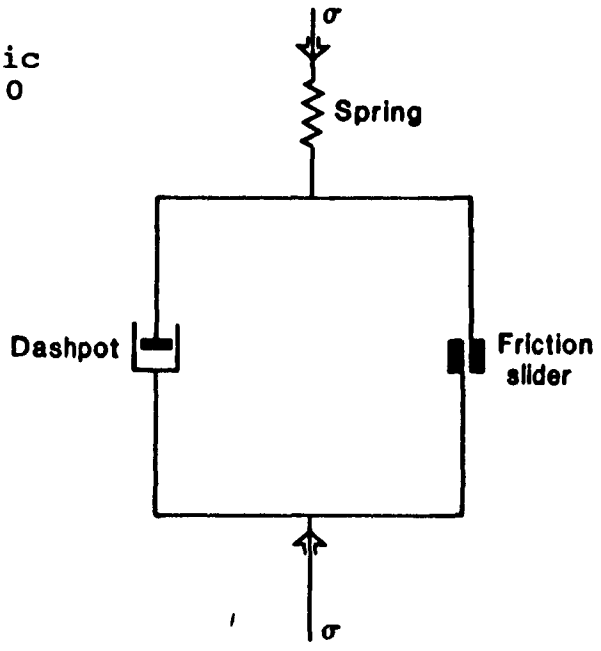

Simple elasto-viscoplastic mechanical model (Figure 2.6)

The model behaves elastically under instantaneous loading

allowing for the acting stresses $f(\sigma)$ to build up elastically over the yield threshold Y in equation 2.10 , which is a simplified form of a yield function. Then the viscoplastic strain starts under the effect of the dynamic yield function $F > 0.0$ [11] , see Figure 2.7 . The rate of viscoplastic strain is defined experimentally by a the positive scalar expression of ϕ which is a function of the dynamic yield function , the viscoplastic strain (or the inelastic work [10]), time and several other variables like the temperature ,humidity,etc. In a uniaxial compression test, this function may be the uniaxial plastic strain (depending on the plastic potential Q) and F may be ,or linearly related to, the uniaxial acting stress, while in a conventional triaxial test ϕ and F could be ,or linearly related to, the differential strain $(\epsilon_1-\epsilon_2)$ and differential stress respectively $(\sigma_1-\sigma_2)$.

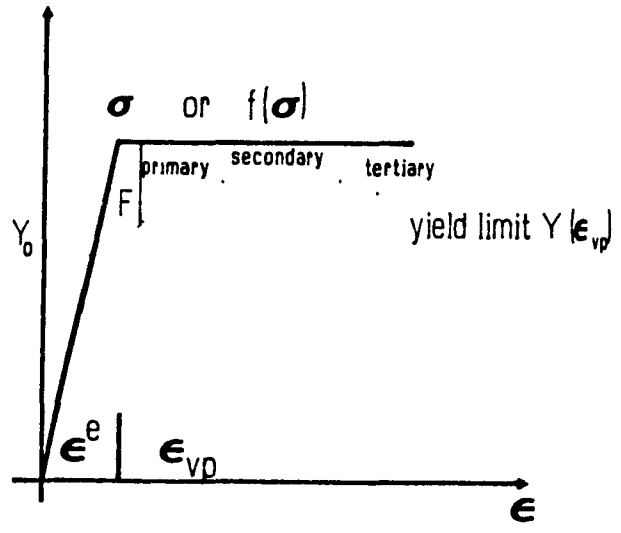

Viscoplastic strain under constant stress
(Figure 2.7a)

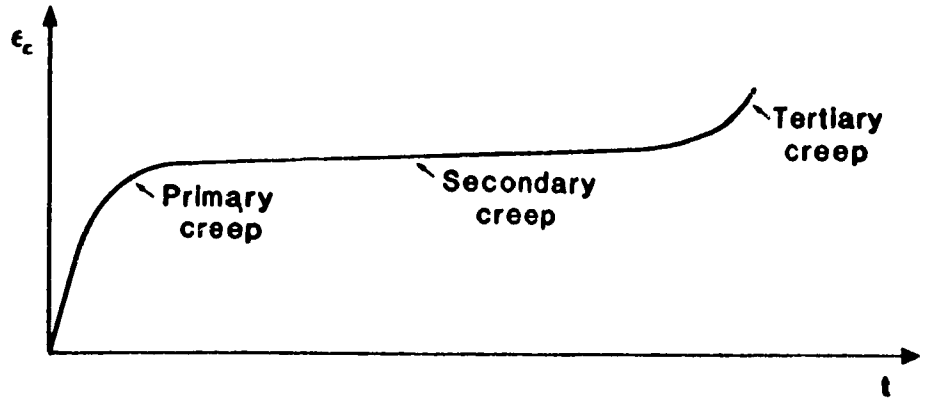

The typical three phases of creep behavior
(Figure 2.7b)

The strain hardening or softening effect (see Figure 2.7a) might appear in the material constants of the yield function or directly in the creep law itself.

$\frac{\partial \phi}{\partial t}$ or $\frac{\partial \phi}{\partial \epsilon_{vp}} < 0.0 \rightarrow$ primary creep (hardening)

$\frac{\partial \phi}{\partial t}$ or $\frac{\partial \phi}{\partial \epsilon_{vp}} = 0.0 \rightarrow$ secondary creep (perfect plasticity)

$\frac{\partial \phi}{\partial t}$ or $\frac{\partial \phi}{\partial \epsilon_{vp}} > 0.0 \rightarrow$ tertiary creep (softening)

If the time variable t replaces the strain variable ϵ_{vp} in the function ϕ , the creep law is called time-hardening creep law and in such creep experiments the value of the creep threshold Y might be assumed = 0.0.

Figure 2.9 presents a comparison between the theory of elasto-viscoplasticity and the incremental theory of plasticity when used to model the elastoplastic or the short term stress strain behaviour during a conventional triaxial

test and assuming that stresses are applied in small increments and remains constant. The incremental theory of plasticity assumes that the plastic strain occurs instantaneously followed by the elastic response . This assumption is at variance with experiment and is at best a convenient mathematical fiction [4].

$$\textit{The total strain } d\epsilon = d\epsilon^{I} + d\epsilon^{e} \qquad (2.12)$$

Equation 2.12 shows that both time dependent and time independent inelastic strain mechanisms ($d\epsilon^{I}$) , their effect is to be added to the elastic strain $d\epsilon^{e}$ causing a relaxation or loss of the stored elastic strain energy at a point if $d\epsilon_{total} < d\epsilon^{I}$. According to Reference [15], the study of creep (time dependent or viscous strain) is curried out in two kinds of experiments; the "short term" creep is studied by a universal testing machine with fast applied incremental loading followed by time intervals of several minutes during which the stress is kept constant and the "long term " creep is studied with standard apparatus like conventional creep tests.

Viscous deformation
with relaxation
(Figure 2.8)

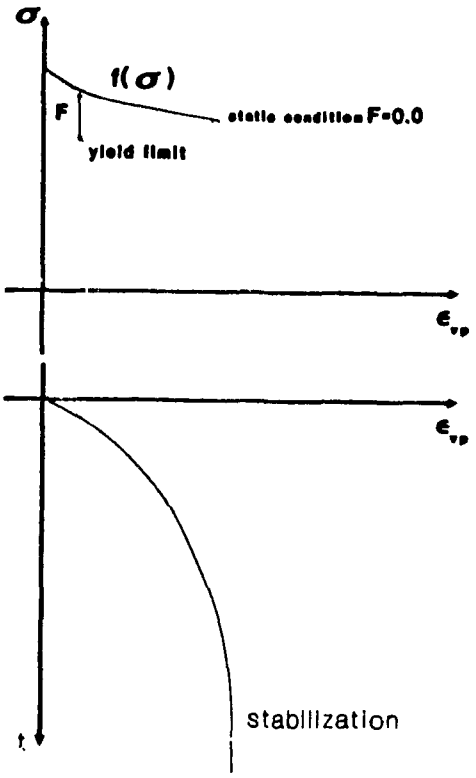

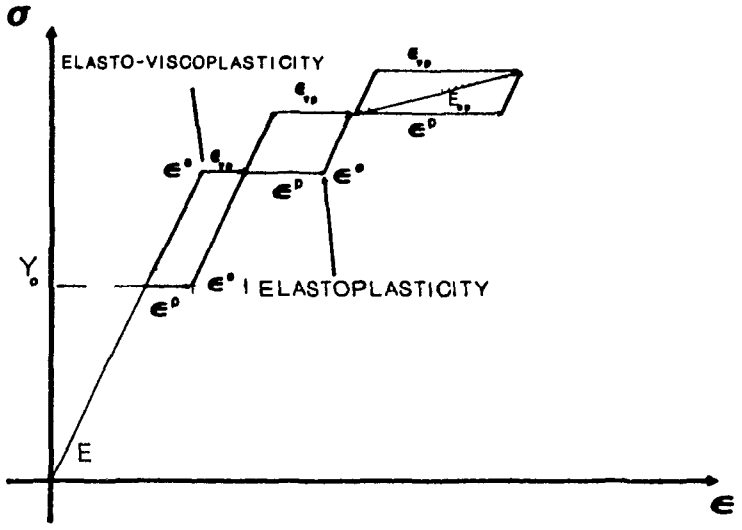

Comparison between instantaneous and viscous plasticity
(Figure 2.9)

2.2 NON-LINEAR YIELD FUNCTIONS:

Yield functions like Mohr-coulomb or Drucker-Prager (when presented in equations 2.4a,b are linear relations between the deviatoric and hydrostatic stresses and if a similar plastic potential is used , the viscoplastic flow will always be accompanied by constant ratio of dilation (volume increase) to deviatoric strain [14].

Hoek and Brown [2] (equation 2.13) developed an empirical non-linear failure condition which is a good tool to check the peak conditions after which unstable behaviour may occur. It is mainly a failure criterion and not a yield function as its constants are obtained experimentally to satisfy a peak condition, but they are not checked to whether this condition is used as a plastic potential nor are they functions of the inelastic strains or inelastic work (see Figure 2.10).

$$\sigma_1 = \sigma_3 + \sqrt{m\sigma_c\sigma_3 + s\sigma_c^2} \quad \ldots\ldots \quad (2.13)$$

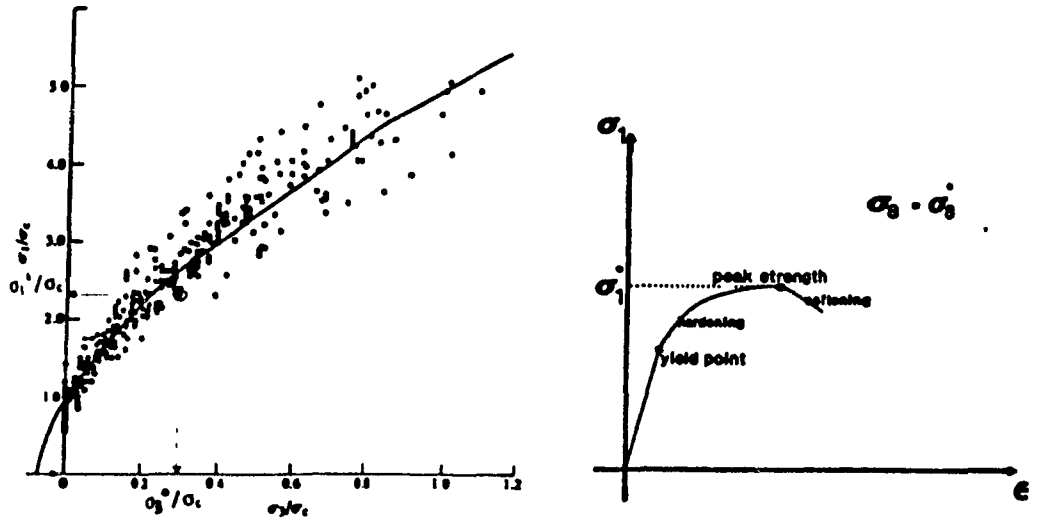

Normalized peak strength envelope for sandstones
(Figure 2.10) [2]

where σ_c is the uniaxial stress of the intact rock, m and s are constants that depend on the properties of the rock and the extent to which it has been broken before it is subjected to failure stresses.

It has been stated in several papers, e.g [13],[22],that unless dilatancy and compressibility are accurately modelled , the constitutive equation is not appropriate for rock-like materials.

Reference [12] gives an example of a non-linear yield function giving a non-linear dilatant plastic strain. It uses two plastic strain variables to model hardening followed by softening behaviour. This yield function was proposed for modelling elastoplastic behavior of hard rock under moderate stresses. As the progressive fracturing induces the weakening of material, there is also the hardening effect related to inhomogeneity of microdeformations associated with irreversible strain. The rate of plastic dilatancy is directly linked to microdamage and softening mechanisms:

$$\dot{\beta} = a\,\dot{\epsilon}_m^P \qquad (2.14\ a)$$

where ß is a microdamage and softening parameter , a is a positive constant. On the other hand, it is the rate of deviatoric strain invariant which is related to hardening mechanisms, or the closure of microcracks;

$$\dot{k} = (\dot{e}_{ij}^P\ \dot{e}_{ij}^P)^{\frac{1}{2}} \qquad \ldots\ldots \qquad (2.14b)$$

where e_{ij}^p is the deviatoric plastic strain . k may also be the inelastic work of the deviatoric stresses s_{ij} :

$$\dot{k} = s_{ij}\, \dot{e}_{ij}^p \qquad (2.14c)$$

where $\dot{e}_{ij}^p$ and $\dot{\epsilon}_m^p$ are obtained using the yield function (equation 2.15a) as a plastic potential.

$$F(\sigma, k, \beta) = J_{2D} - 2p(k,\beta)(J_1^\circ - J_1) \qquad (2.15a)$$

where p(k,ß) is a material function controlling the rate of hardening and softening and J_1° is a constant :

$$p(k,\beta) = p_o + z_1 k - z_2 \beta^2 \qquad (2.15b)$$

and p_o, z_1, z_2 are positive constants determined experimentally. In equation 2.15 , the nonlinear yield function includes the effect of the second deviatoric stress invariant $J_{2D}^{1/2}$ squared (see Figure 2.1), as well as the hydrostatic stress J_1 ,while the two inelastic strain variables (ϵ_m^p ,k) appear in the function P(k,ß) .

The vanishing of plastic ductility under tensile stresses, justifies the existence of a rupture surface as a function of the stresses only. The brittle rupture condition is shown in equation 2.16 .

$$F^*(\sigma) = (J_1 - J^*)^2 - J_{2D}\gamma^2 - \delta^2 = 0.0 \qquad (2.16)$$

where J^* , γ , δ are constants independent of the strain history.

The configuration of the rupture and yield loci in the stress

invariants space is shown in Figure 2.11 a.

The yield surface is represented by a set of parabolas giving

$\dot{\epsilon}_v^p = \Phi \frac{\partial F}{\partial \sigma_{ii}} - 3\Phi \frac{\partial F}{\partial J_1} - 3\Phi\,(2p(k,\beta))$ so that the viscoplastic strain $\dot{\epsilon}_{vp}$ is always accompanied by volume increase (dilatant) and as the surface expands by the increase of p(k,ß) the ratio of dilatant to deviatoric deformations increases.

The intersection of the initial yield parabola (for $p(k,\beta) = p_o$) and the rupture curve (equation 2.16) occurs at points F_1, F_2 representing simple shear states. For stress paths having tensile hydrostatic stress brittle rupture occurs (O C_2), while when the stress path is accompanied by low hydrostatic pressure , limited ductility happens with hardening effect , followed by brittle rupture when the stress path intersects the rupture surface, see Figure 2.11-a) .

The ductile curve (Figure 2.11 (d,e)) is simulated by this yield function if the applied stress path is accompanied by higher values of hydrostatic stress. In Figure 2.11a (path O A D E) , the initial expansion of the yield surface means a predominating hardening effect , while the softening takes place when the effect of volumetric dilatancy becomes prevailing. In this case there is no contribution of the brittle rupture condition . The transition from hardening to softening (or to unstable behaviour) means that the rock mass has become highly rearranged so that the softening effect of dilatancy (β) becomes more than the hardening of the

deviatoric component of the inelastic strain increments (k).

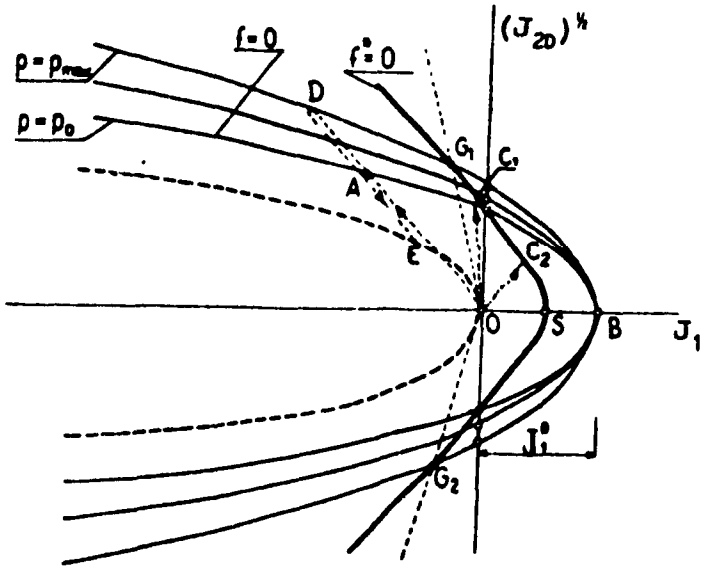

Configuration of the rupture and yield loci
in the stress invariants space
(Figure 2.11a)[12]

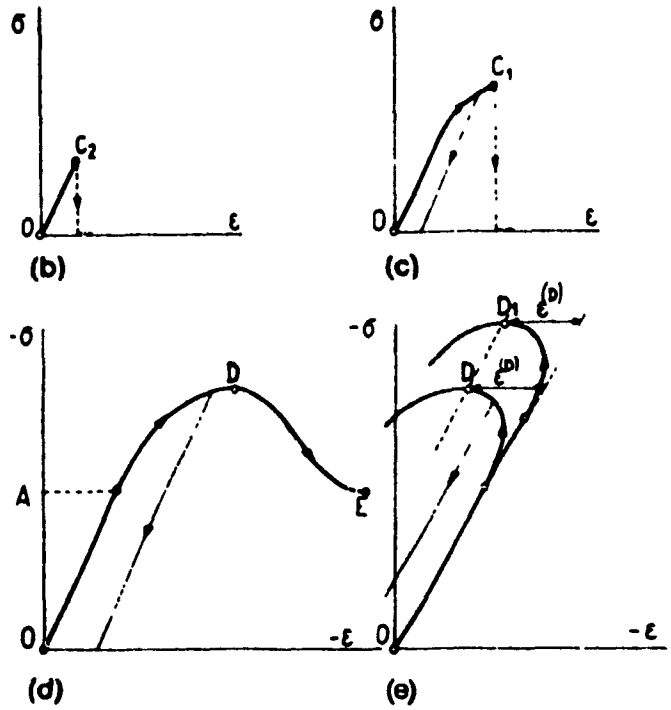

Stress strain relations during path: $OC_2, OC_1, OADE$
(Figure 2.11 b,c,d,e)[12]

In equation 2.15b, $p(k,\beta)$ is function of the $(-\beta^2)$ making the effect of an increment $d\beta$ on $dp(k,\beta)$ increases with the growth of the plastic strain.

This model is suited for viscous elastoplastic analysis of hard rock showing ductile or brittle behaviour [12]. It also seems to be good for creep analysis, as the three phases of the creep behaviour can be established even under constant stress i.e constant flow rule (by considering the effect of $p(k,\beta)$ in equation 2.15b).

2.3 DILATANT-COMPACTING YIELD FUNCTIONS:

Some rocks cannot be described by a dilatant yield function like that described earlier (equation 2.15), in that over certain pressure ranges the initial yield point decreases with subsequent increases in the confining pressure, at which a transition from dilatant deformation to compaction or volume decrease takes place (see Figure 2.13). This concept first was treated by adding "end caps" to the dilatant yield function. However, a discontinuous yield condition makes the numerical modelling difficult and not flexible enough. Equation 2.19 [23] is a continuous yield function based on the critical state concept developed for soil-like materials [23], [11]. The idea of this theory comes from the theory of work dissipation [23]. For conventional triaxial test one may define the hydrostatic pressure and deviatoric stresses as in equations 2.17 (see Figure 2.12) :

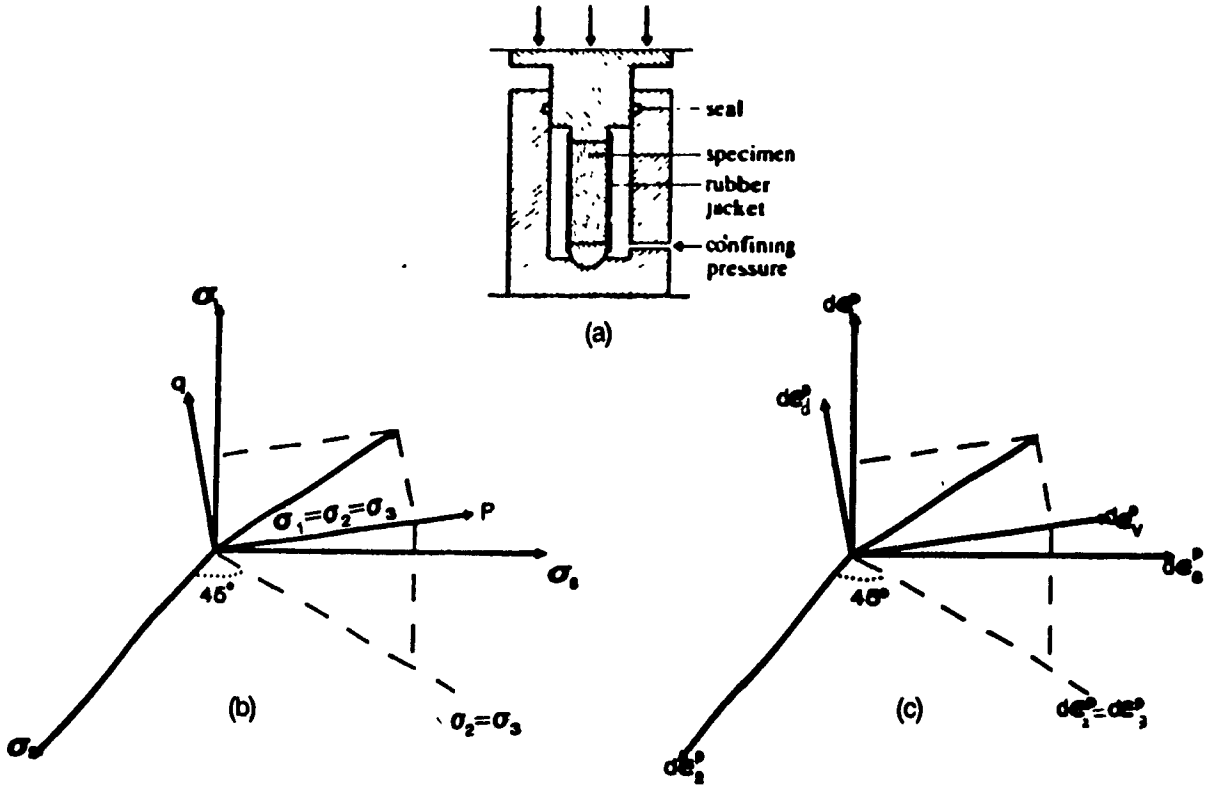

Triaxial compression in the principal stress and strain space [20] (Figure 2.12)

$$p = \frac{1}{\sqrt{3}} (\sigma_1 + 2\sigma_3)$$
$$q = \frac{2}{\sqrt{6}} (\sigma_1 - \sigma_3) \qquad (2.17\ a)$$

and the corresponding viscoplastic strain increments as:

$$d\varepsilon_v^p = \frac{1}{\sqrt{3}} (d\varepsilon_1^p + 2\, d\varepsilon_3^p)$$
$$d\varepsilon_d^p = \frac{2}{\sqrt{6}} (d\varepsilon_1^p - d\varepsilon_3^p) \qquad (2.17\ b)$$

and assuming the plastic potential depending on p,q (or $J_1, J_{20}^{1/2}$) only , the loading power could be described in the

plane of p-q as follows :- $q\,d\epsilon_d^p + p\,d\epsilon_v^p$

and for a frictional material this power is dissipated in friction work only :

$$q\,d\epsilon_d^p + p\,d\epsilon_v^p - M^* p\,|d\epsilon_d^p| - \frac{p}{p_c}(q_c\,d\epsilon_d^p) \qquad (2.18)$$

where $M^* = q_c/p_c$ is a simple friction constant relating the deviatoric and hydrostatic stresses at the critical state where no inelastic volume change takes place. Equation 2.18 means that the volumetric work ($p\,d\epsilon_v^p$) in case of compaction increases the friction and for dilation decreases the friction work by a factor of (p/p_c). By integrating equation 2.18 [23], [20] after putting $dq/dp = d\epsilon_v^p/d\epsilon_d^p$ as a property of the required plastic potential Q;

$Q = \frac{q}{M^* p} + \ln\frac{p}{p_c} - 1$ (see Figure 2.13 a) and noting that q and p are proportional to $\bar{\sigma} = J_{2D}^{1/2}$, J_1 respectively we reach the form of yield function F ≡ Q as follows (see Figure 2.13 c) ;

$$F = \frac{\bar{\sigma}}{\mu^* J_1} + \ln\frac{J_1}{J_s} \qquad (2.19)$$

where μ^* is a friction constant relating the deviatoric stress invariant $J_{2D}^{1/2}$ and J_1 at the critical state (i.e when the volumetric viscoplastic strain is zero) and J_s is the hydrostatic yield limit.

When F > 0.0 the viscoplastic strain occurs , while when F <

0.0 ,the behaviour is elastic. Figure 2.13c indicates that ,for associative plasticity , when a point is subjected to J_* and r_* the value of F is positive and the plastic strain increment is normal to the revolutionary surface :

$$Q = F = \frac{\bar{\sigma}}{\mu^* J_1} + \ln \frac{J_1}{J_d^*} = 0.0 \qquad (2.20a)$$

where Q is the plastic potential and J_d is a constant satisfying the equality.

If a soil specimen , subjected to hydrostatic pressure J_{cr} ,is sheared till $\bar{\sigma}_{cr}$ so that $(\bar{\sigma}_{cr}/J_{cr}) = \mu^*$ (see Figure 2.13c) the resulting behaviour has no volumetric viscoplastic strain and is perfectly plastic. Higher values of applied $(\bar{\sigma}/J_1)$ at yielding give softening behaviour accompanying the dilatant viscoplastic strain and lower values give compaction and hardening behaviour.

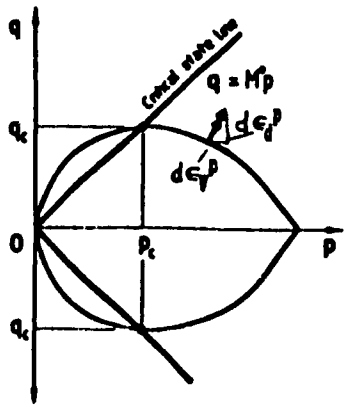

Yield curve and critical state on p-q plane [20]

(Figure 2.13 a)

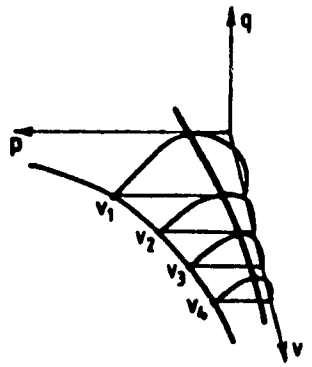

Family of yield surfaces function of the change in volume [20]
(Figure 2.13 b)

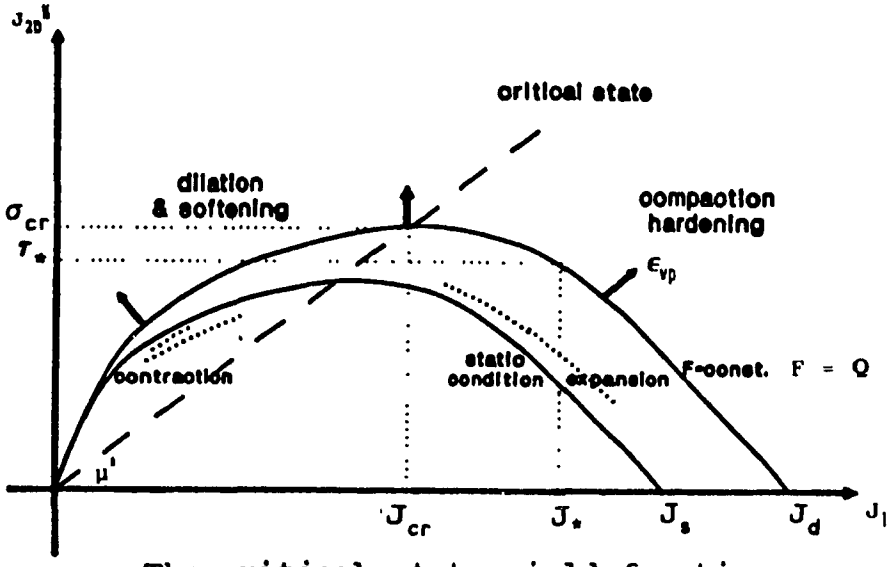

The critical state yield function
for soil like materials
(Figure 2.13 c)

In equation 2.19 J_s is a material parameter which may be constant , or function of the volumetric inelastic strain and simulates the hardening and softening responses as expansion and contraction of a static yield surface defined by ;

$$F_{static} = \frac{\sqrt{J_{2D}}}{\mu^* J_1} + \ln \frac{J_1}{J_s^*} = 0.0 \qquad (2.20\ b)$$

Equation 2.21b uses the critical state yield function , equation 2.21a , in the creep law (ϕ) to simulate the viscous behaviour(consolidation) of clay in case of isotropic hardening and using the effective mean stress σ_m' in place of J_1 (effective means net stress in case any pore water pressure exists).

$$F = \frac{\sqrt{2J_{2D}}}{\mu \sigma_m'} + \ln \frac{\sigma_m'}{\sigma_{my}^s} - A\epsilon_v^p \qquad (2.21\ a)$$

$$\phi(F) = C_o \exp b_o \left[\frac{\sqrt{2J_{2D}}}{\mu \sigma_m'} + \ln \frac{\sigma_m'}{\sigma_{my}^s} - A\epsilon_v^p \right] \qquad (2.21\ b)$$

$$\dot{\epsilon}_{vp_{ij}} = \phi \frac{\partial F}{\partial \sigma_{ij}} \qquad (2.21\ c)$$

where b_o , C_o and A are constants, ϵ_v^p is the volumetric viscoplastic strain and σ_m' is the effective mean stress. Each component of the viscoplastic strain vector is obtained using the dynamic yield function as a plastic potential , equation 2.21 c . The critical state concept is mainly applied to model short term (elastoplastic) behaviour of frictional media like soil [20],[23], backfill and it is possible to use it to model the behaviour of rock having initial cohesion but this cohesion drops to 0.0 after very small plastic deformation (like cemented back fill). It has its application for time dependent behavior of frozen soils , clay and consolidation analysis of clay-like soils [11] important for settlement of foundations or slope stability. It is interesting here to note that the hardening simulated by the expansion of the static yield surface is physically accepted as it is towards the high hydrostatic stress while the material remains the non-tension one.

This general concept is the origin of dilatant-compacting yield function used to model rock behaviour.The difference here lies in that to model intact rock behaviour (or partially fractured) the assumption of work dissipation might be expressed as follows;

$$q\,d\epsilon_d^p + p\,d\epsilon_v^p = M^* p\,|d\epsilon_d^p| + const. \qquad (2.22)$$

where M^* is the friction constant. This means that at p=0.0

(i.e no hydrostatic pressure) there is still a way of internal work dissipation, which might be due to the cohesion , viscoelastic mechanisms and the ductility,etc. On the other hand, the assumption that the dilatant behaviour corresponds to softening or that zero plastic volume change gives perfect plasticity is not valid because for rock the deviatoric strain (representing the shape change) may cause hardening or at least eliminates some or all of the softening effect caused by dilation or micro cracks. Instead of depending on the work dissipation theory ,researchers [13],[14] assume yield functions in a polynomial form of the stress invariants Equation 2.23 is an isotropic dilatant compacting yield function;

$$J_{2D} + \alpha_1 J_1 + \alpha_2 J_1' - A \qquad (2.23)$$

where α_1, α_2, A are material parameters.

Equation 2.24 [13], is another example of this type of yield functions relating $(\sigma_1-\sigma_3)$and $(\sigma_1+\sigma_3)$ when considering the state of stress on the plane of maximum and minimum principal stresses ;

$$F = (\sigma_1-\sigma_3)^2 + n^2(\sigma_1+\sigma_3)^2 + 4n^2c(\sigma_1+\sigma_3) + 4c^2(n^2-\tan^2\theta) \qquad (2.24)$$

where n,c,tanθ are parameters governing the location and shape of the set of ellipses represented by F=0.0 whose major axis is directed along the line of hydrostatic stresses [13]. Using this family of dilatant compacting yield functions (see Figure 2.14) ; apart from the experimental stress-strain characteristics , the field state of stress governs ;

* Softening or hardening (point 1 compared with point 2)

* The rate of hardening or softening (point 2 compared with point 3)

* For the incremental loading of elasto-plastic behaviour (see Figure 2.9) for which the state of stress is at (or near) the static yield surface (i.e $Q \equiv F_{(static)} = 0.0$), the expansion or contraction of this surface simulates non-linear hardening and softening as the ratio of the viscous strain increments $d\epsilon_v^p : d\epsilon_d^p$ changes (e.g it increases with surface expansion to decrease the rate of hardening).

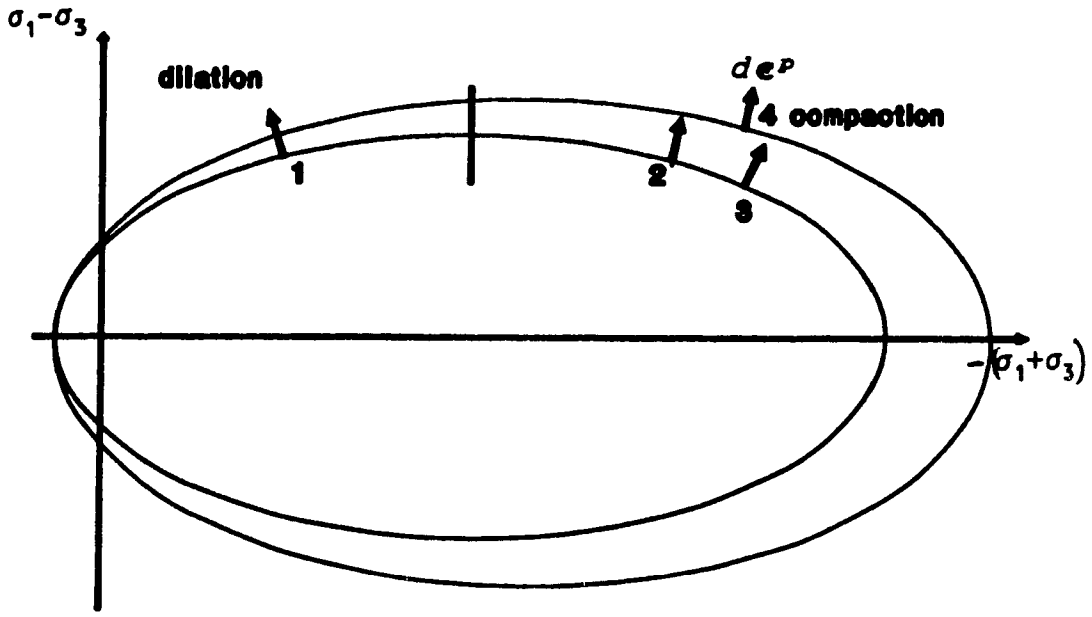

Dilatant compacting yield curve (Equation 2.24)
(Figure 2.14)

Equation 2.25 [24] is a yield function proposed for soft rock

(e.g. soapstone);

$$F = J_{2D} - \left(-\frac{\alpha}{\alpha_o} J_1^n + \gamma J_1^2\right)\left(1 - \beta S_r\right)^m$$

$$\text{where } S_r = \frac{J_{3D}^{1/3}}{J_{2D}^{1/3}} \quad , \quad \alpha = \frac{a_1}{\xi^{\eta_1}} \quad , \quad \beta = \beta_o e^{-\beta_1 J_1} \qquad (2.25)$$

Where $\alpha_o, n, m, \gamma, \eta_1$ and a_1 are constants, ξ is the trace of total plastic strain= $\int (d\epsilon^p_{ij}\, d\epsilon^p_{ij})^{\frac{1}{2}}$. The effect of the third deviatoric stress invariant J_{3D} is more apparent for low hydrostatic stresses when $\beta = \beta_o e^{-\beta_1 J_1}$ where β_o, β_1 are constants. This effect causes the yield limit of the deviatoric stress invariant J_{2D} to be lower in case of triaxial extension i.e when $(\sigma_2 = \sigma_3 > \sigma_1)$ than it is for triaxial compression $(\sigma_1 > \sigma_2 = \sigma_3)$ (see Figure 2.15a).

In equation 2.25, α is chosen function of the total plastic strain trajectory which simulates successive hardening or expansion of the yield surface in the course of the plastic strain. At point 1 (see Figure 2.15a) where the plastic strain increments are 100% deviatoric ($d\epsilon_v^p = 0.0$), the rock still exhibits hardening behaviour . At point 2 the plastic strain increment is dilatant ($d\epsilon_v^p > 0.0$) , this dilation according to the equation of α, has no softening effect, so the yield function continues to expand , but its expansion is only towards the high hydrostatic compression . This means that the behaviour is perfectly plastic at points higher than the ultimate envelope in Figure 2.15c (these points correspond to stress states of low ratio of hydrostatic to deviatoric stresses). The softening or contraction of the yield surface

is not modelled by the parameters of this yield conditions. The value of n in equation 2.25 representing the power of J_1 has a control on the shape of yield curve (Figure 2.15b) and consequently controls the ratio between the volumetric and the deviatoric plastic strain increments , thus used to fit this yield function (when used as a plastic potential) to the experimentally observed plastic strain [24].

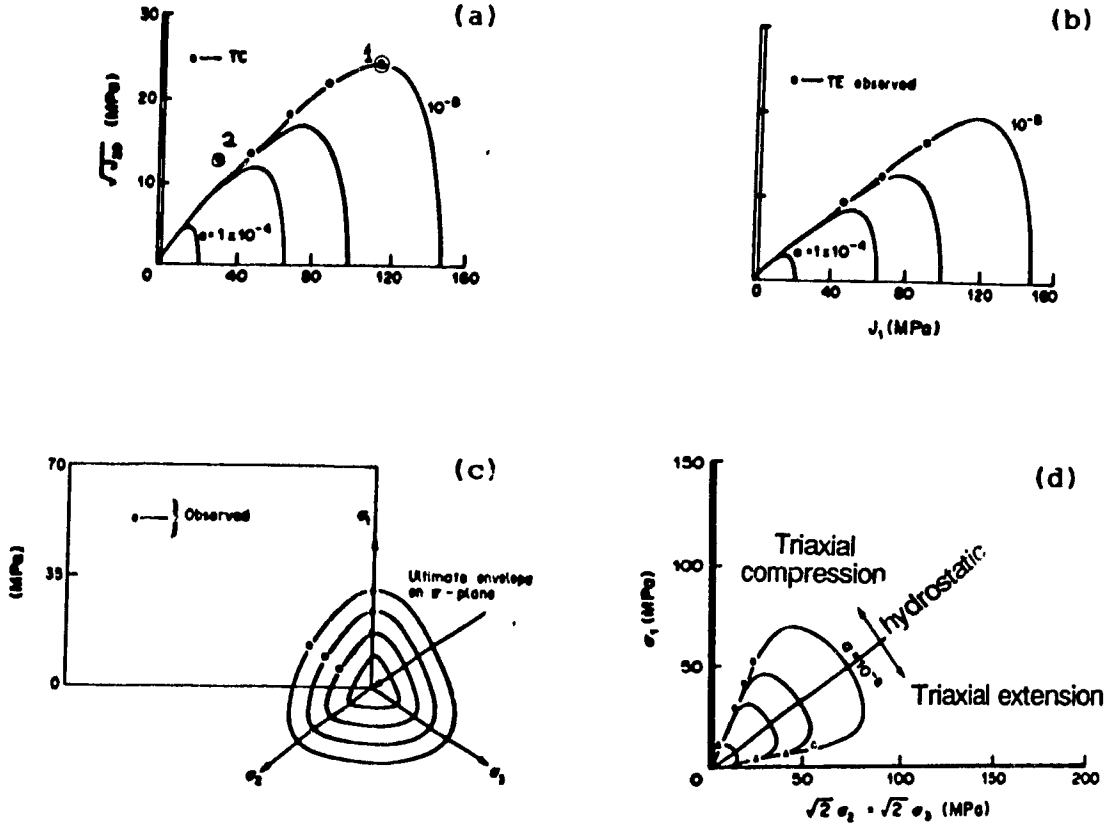

Plots of F (Equation 2.25) for different stress paths (Figure 15) [24]

2.3 CREEP AND VISCOPLASTIC CONSTITUTIVE LAWS

When viscoplasticity is used to predict elasto-plastic behaviour, the function ϕ in equation 2.11 represents , not the exact viscoplastic rate , but a rate proportional to the stress condition $\phi = \lambda F$ (compared to other points in the rock-mass) where λ is called the fluidity parameter and may be chosen = 1 because the time here is used as a fictitious variable i.e the time increments Δt is chosen such that $\Delta \epsilon_{vp} = \dot{\epsilon}_{vp} \Delta t$ does not exceed a certain limit which causes numerical instability (see Section 3.3), similar to the initial strain approach [4]. However in case of incremental viscoplasticity λ takes a real number so that ϕ simulate the real viscous rate. In reference [10] the incremental viscoplasticity is simulated using a work hardening creep law.

In case of creep or time-dependent deformations the value of ϕ, the creep rate at time t, should be modelled by equation 2.11. The empirical approach takes the form of the creep laws and their constants by best fitting interpolation of the data obtained from a series of laboratory creep tests . Popular forms of the empirical creep laws are the time power and exponential laws [25],[26] (the environmental effects like temperature , humidity appear in the constants):

$$\epsilon_c(t) = B\, t^m \sigma^n \quad \ldots\ldots \quad (2.26a)$$

$$\epsilon_c(t) = B\,(1-e^{-mt})\,\sigma^n \quad \ldots\ldots \quad (2.26b)$$

where B,m,n are constants, σ is usually the axial stress in a uniaxial creep test or the differential stress in a conventional triaxial creep test, while ϵ_c is the vertical creep strain ϵ_1 or the differential creep strain $(\epsilon_1-\epsilon_2)$. Other creep laws may take an exponential strain hardening form [27] (see also equation 2.21);

$$\begin{array}{ll} \dot{\epsilon}_c = \dot{\epsilon}_{s.cr.}\, e^{A(1-\epsilon_c/\epsilon_{ta})} & \text{if } \epsilon_c < \epsilon_{ta} \\ \text{and} & \\ \dot{\epsilon}_c = \dot{\epsilon}_{s.cr.} & \text{if } \epsilon_c > \epsilon_{ta} \end{array} \quad \ldots \quad (2.26b)$$

where A is a constant and $\dot{\epsilon}_{s.cr.}$ is the secondary creep rate where no hardening or softening occur which is function of stresses(i.e $\dot{\epsilon}_{s.cr.}=f(\sigma)$ or $=A_1\,\sigma^n$) and the effect of stresses appears also in the limit at which the secondary creep starts (see Figure 2.7b); $\epsilon_{ta}=m_1(\sigma/G)^m$ where m_1 and m are constants. While some authors suggest logarithmic forms others use mixed forms as listed in reference [6].

When a **rheological** approach is adopted , a **mechanical system** of springs ,dashpots , sliders or friction blocks is built up in a certain arrangement to exhibit a time dependent behaviour similar to that of the material studied (see Figure 2.16). In this case the mechanical model suggested for the material imposes the form of the creep law while the parameters or the constants involved have to be determined experimentally by curve fitting.

This approach seems to have the flexibility to be applied to different rock types in different conditions [6],[21].

It is common for creep laws to assume a zero yield limit or creep threshold . Several authors state that a rock-like material loaded starting from a stress-free state or low premining stresses (initial stresses) possesses a near zero yield limit [28],[10],[29].

Figure 2.16 shows two popular mechanical models; Zener and Burger [6] with their equations. These models are one dimensional and some researchers like Serata [29] implements them to model two separate components of the isotropic creep strain; the mean strain ϵ_m and the second deviatoric strain invariant $\epsilon_d=(\frac{1}{2}\ e_{ij}e_{ij})^{\frac{1}{2}}$. If $\bar{\sigma} = (J_{2D})^{\frac{1}{2}}$ (the stress corresponding to ϵ_d) $< C_o$ according to Figure 2.17 Zener model is used for ϵ_m, ϵ_d as follows (Figure 2.16-a defines the constants):

$$e_d = \frac{\bar{\sigma}}{2G} + \frac{\bar{\sigma}}{2G_2}\left(1-e^{(-(2G_2/2\eta_2)\,t)}\right) \qquad (2.27a)$$

$$e_m = \frac{\sigma_m}{3K} + \frac{\sigma_m}{3K^*}\left(1-e^{(-(3K^*/3\eta^*)\,t)}\right) \qquad (2.27b)$$

but if $\bar{\sigma} > C_o$ according to Figure 2.17, Burger model is used for ϵ_d only (i.e no volumetric creep) as follows ;

$$e_d = \frac{\bar{\sigma}}{2G} + \frac{\bar{\sigma}}{2G_3}\left(1-e^{(-(2G_3/2\eta_3)\,t)}\right) + \frac{\bar{\sigma}}{2\eta_4}\,t \qquad (2.28)$$

To determine the form of the creep rate function ϕ using an experimental or a mechanical model , a yield function and a plastic potential are assumed to relate ϕ (see equation 2.11) with the measured strain component (like $\dot{\epsilon}_m, \dot{\epsilon}_d$ in equations 2.27) during a creep test and also to relate the applied

uniaxial or triaxial state of stress to three dimensional state of field stresses.

If the theory of elasto-viscoplasticity is used to model the time dependent behaviour of the mechanical model of Figure 2.17 , one would put a compound creep rate law as follows;

$$If\ \bar{\sigma} \leq C_0\ ;$$
$$\dot{\epsilon}_{vp_{ij}} = \phi_1(F_1, t)\ \frac{\partial Q_1}{\partial \sigma_{ij}} + \phi_2(F_2, t)\ \frac{\partial Q_2}{\partial \sigma_{ij}} \qquad (2.29a)$$

where the yield function $F_1=\bar{\sigma}$ and $F_2=\sigma_m$ with no creep thresholds imposed (viscoelastic) and using a plastic potential $Q_1=\bar{\sigma}=(J_{2D})^{1/2}=(\frac{1}{2}\ s_{ij}s_{ij})^{1/2}$=const. . This gives a flow rule of pure deviatoric strain $\dot{\epsilon}_{vpij} = \frac{1}{2}\ \phi_1\ s_{ij}/(J_{2D})^{1/2}$ and consequently $\dot{\epsilon}_{dvp}=\frac{1}{2}\phi_1$, while $Q_2=\sqrt{(\sigma_m)^2}$ =const. chosen to give pure volumetric strain gives $\dot{\epsilon}_m=\phi_2/3$ (of the same sign of σ_m) thus the equations of the creep rates are :

$$\phi_1 = 2\ \frac{\partial \epsilon_{d_{vp}}}{\partial t} = 2\ \frac{F_1}{2\eta_2}\ e^{(-(G_2/\eta_2)\ t)}$$
$$\phi_2 = 3\ \frac{\partial \epsilon_{m_{vp}}}{\partial t} = 3\ \frac{F_2}{3\eta^*}\ e^{(-(K_2/\eta^*)\ t)} \qquad (2.29b)$$

And if $\bar{\sigma}$ is checked to be > C_0 the following law is used;

$$\dot{\epsilon}_{vp_{ij}} = \phi_3(F_1, t)\ \frac{\partial Q_1}{\partial \sigma_{ij}} \qquad (2.30a)$$

where ϕ_3 = 2 times $\dot{\epsilon}_{dvp}$ given by equation 2.28 because Q_1 which gives no volumetric plastic strain is still used ;

$$\phi_3 = 2\ \frac{\partial \epsilon_{d_{vp}}}{\partial t} = 2\left(\frac{F_1}{2\eta_2}\ e^{(-(G_2/\eta_2)\ t)} + \frac{F_1}{2\eta_4}\right) \qquad (2.30b)$$

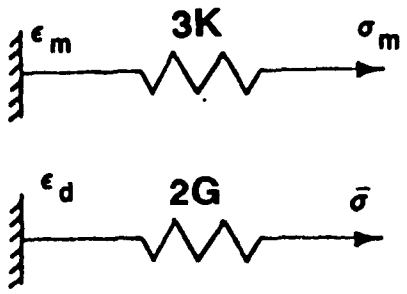

$\sigma_m = 3K\ \epsilon_m$ and $\bar{\sigma} = 2G\ \epsilon_d$

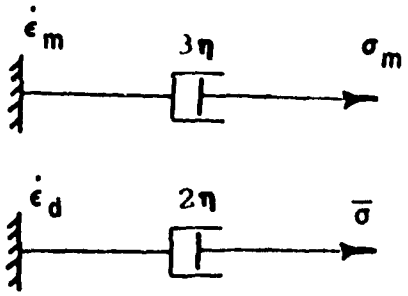

$\sigma_m = 3\eta\ \dot{\epsilon}_m$ and $\bar{\sigma} = 2\eta\ \dot{\epsilon}_d$

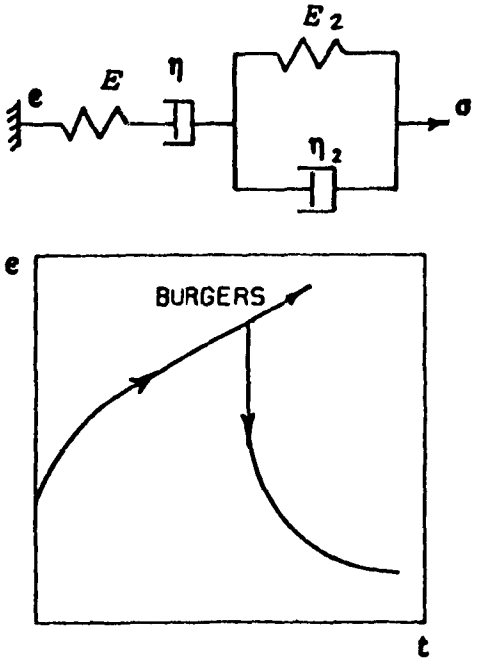

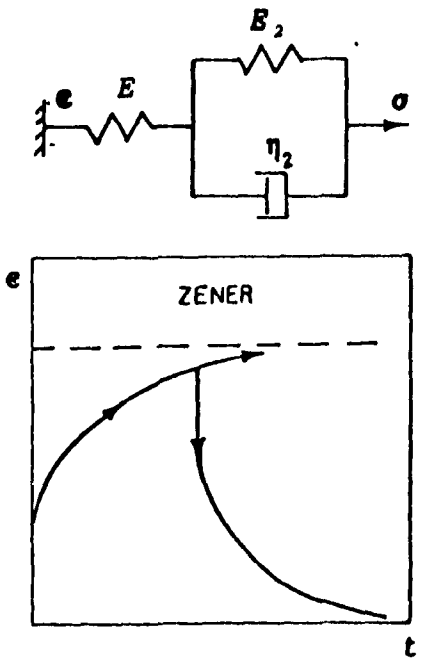

$$e = \frac{\sigma}{E} + \frac{\sigma}{E_2}\left(1 - e^{(-(E_2/\eta_2)\,t)}\right) + \frac{\sigma}{\eta}\,t$$

Burger model

$$e = \frac{\sigma}{E} + \frac{\sigma}{E_2}\left(1 - e^{(-(E_2/\eta_2)\,t)}\right)$$

Zener model

(Figure 2.16)[6]

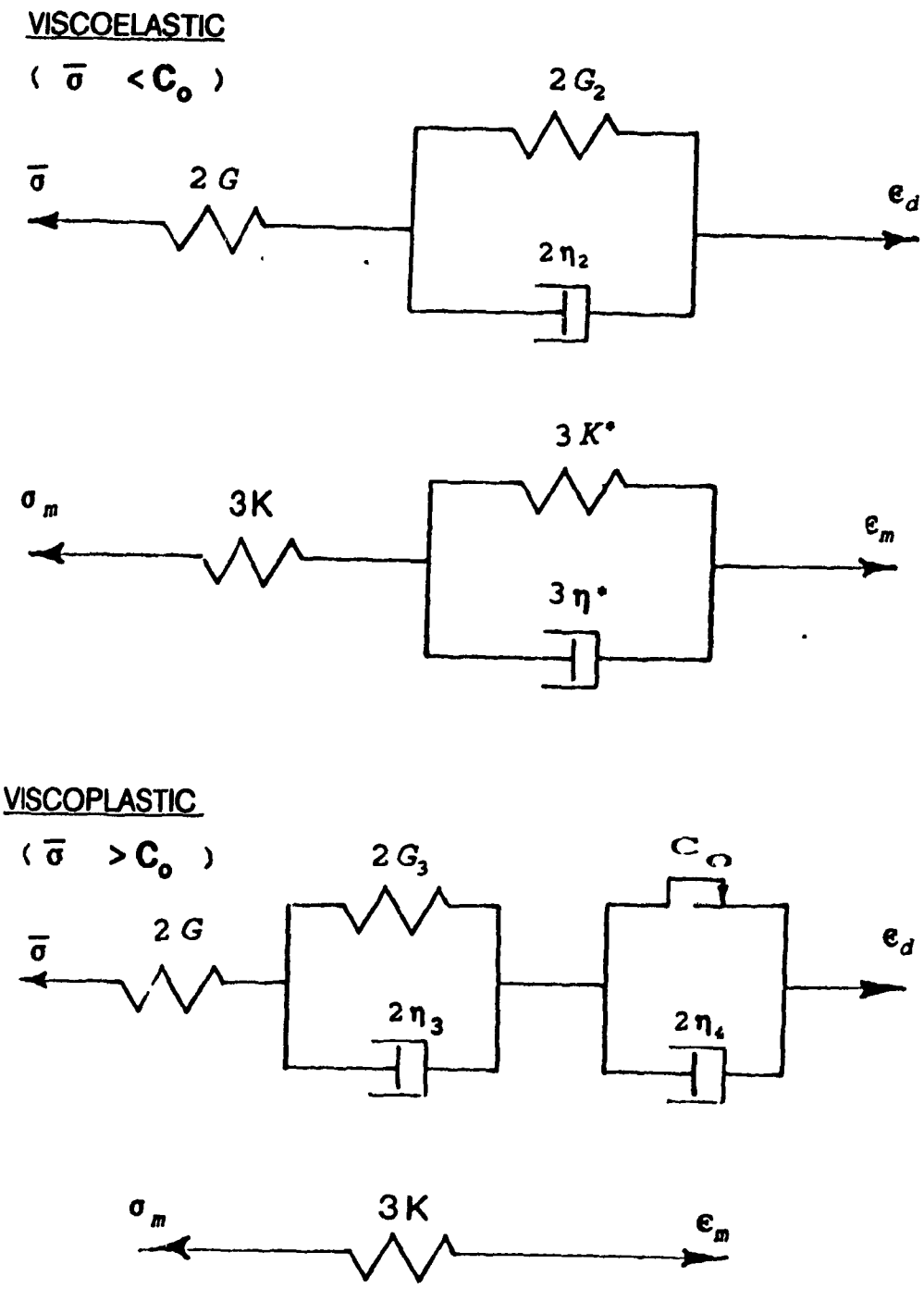

Rheological model for rocksalt [29]
(Figure 2.17)

Figure 2.18 compares between the prediction of a time-hardening creep law : $\phi=f(t,\sigma)$ and strain-hardening creep law :$\phi=f(\sigma,\epsilon_{vp})$ for nonlinear creep where the stress σ changes with time. It can be noted that time hardening creep laws are not well suited to modelling the stress history. Work-hardening creep laws ($\phi=f(\sigma,\int\sigma d\epsilon_{vp})$) is the best approach in such cases.

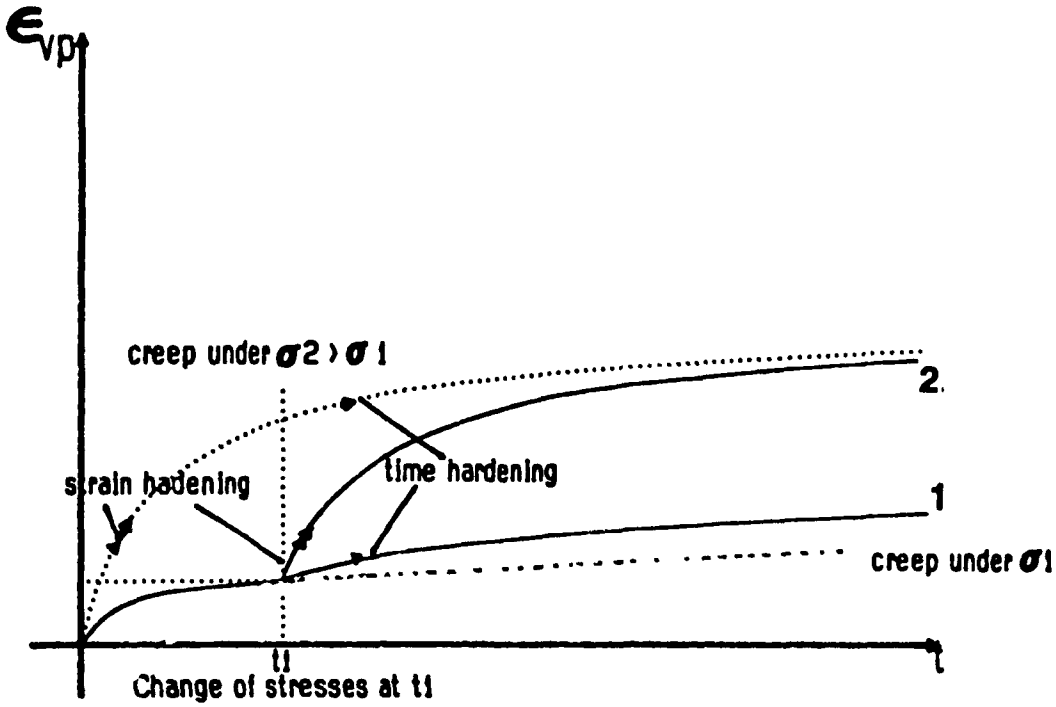

Curve 1 is the prediction using time hardening law and curve 2 is the prediction using strain hardening law when the stress is incremented.
(Figure 2.18)

To adopt an empirical or mechanical model in the theory of viscoplasticity described in Section 2.1.3, the model (like that of Figure 2.19) has to be divided to a system having a stiffness of an instantaneous elastic response (system 1)

attached serially to another system (system 2) which cannot be strained instantaneously but is giving a viscous strain rate (described by a creep law as in equation 2.29) and its viscous strain $\dot{\epsilon}_{vp}$ (being viscoplastic or viscoelastic) is to be added serially to $\dot{\epsilon}_e$ to give the total strain i.e $\dot{\epsilon}_t=\dot{\epsilon}_{vp}+\dot{\epsilon}_e$. If at time t, an element of the rock mass is confined so that $\Delta\epsilon_t$ is less than $\Delta\epsilon_{vp}$ the viscoplastic strain ($\Delta\epsilon_{vp}$) will cause a relaxation in the elastic energy $\dot{\epsilon}_e$.

Reference [6] presents a comprehensive survey of creep laws used for rock in general and rocksalt in particular.

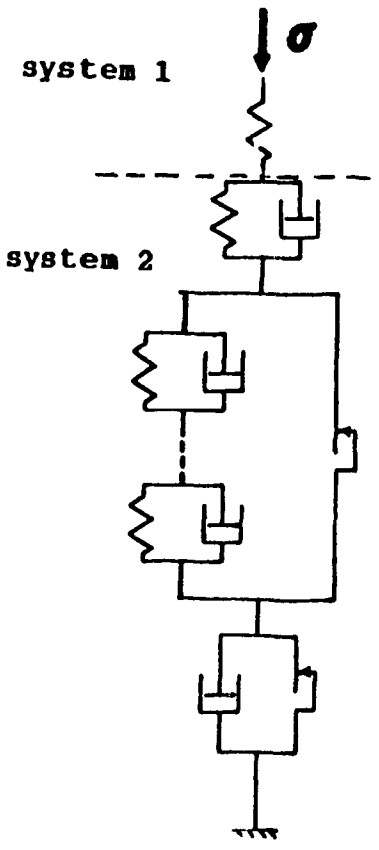

Analyzing a mechanical model by considering : an elastic part and viscous part.
(Figure 2.19)

2.4 RHEOLOGICAL ANALOGUE OF ROCK ZONE INTERSECTED BY PARALLEL JOINT SETS

In the iterative explicit scheme described in Section 3.2 it is possible to incorporate the rheological model describing a rock mass transversed by sets of parallel joints (Figure 2.20) [1],[19].

If σ_n is the stress normal to the joint surface , τ is the resultant of shear stresses parallel to the joint surface k ;

$$If \quad \sigma_{n_k} \leq 0.0$$

$$F_k = \left[|\tau| + \sigma_n \tan\theta_k - C_k\right]_{(joint\ set\ k)} > 0.0 \qquad (2.31a)$$

where θ_k is the joint friction angle and C_k is the apparent cohesion ;

$$Q_k = \left[\sqrt{\tau^2} + \sigma_n \tan\psi_k - Const \ -0.0 \ \right]_{(joint\ set\ k)} \qquad (2.31b)$$

$$\dot{\epsilon}_{vp_k} = \lambda_k F_k \frac{\partial Q_k}{\partial \sigma_{ij}} \qquad (2.31c)$$

where ψ_k is the dilation angle and λ_k is a fluidity parameter of the parallel joint set k (depends on surface condition and the number of parallel joint per unit length). λ_k may be assumed unity in an elastoplastic solution.

The yield function and plastic potential used to describe this model are anisotropic. The yield limit monitors the yielding along the shear parallel to the joint surface k (τ_k) The logic of having the form of the plastic potential near to that of the yield function appears obviously when equation

2.31b is used as a plastic potential thus giving inelastic shear deformation parallel to the joint surface, while the dilation is controlled by the value of tan (ψ_k). Equations 2.31 are used if the stress normal to the joint surface is compression i.e $\sigma_n \leq 0.0$. If $\sigma_n > 0.0$ it would not be true and a viscoplastic no-tension model is <u>added</u> to redistribute the stresses and relief the tension ;

$$F_2 = [\sigma_n]_k \quad > 0.0 \qquad (2.32\ a)$$

$$Q_2 = [\sigma_n - const. = 0.0]_{joint\ k} \qquad (2.32\ b)$$

$$\dot{\epsilon}_{vp_k} = \lambda_k F_{1_k} \frac{\partial Q_{1_k}}{\partial \sigma_{ij}} + \lambda_k F_{2_k} \frac{\partial Q_{2_k}}{\partial \sigma_{ij}} \qquad (2.32\ c)$$

where F_1 and Q_1 are the yield function and plastic potential of equations 2.31a,b respectively. F_1, Q_1 might preferably be $(\tau_k^2)^{1/4}$ as in equation 2.34b depending on the opening of joints at this point In both cases the total viscoplastic rate is ; $\dot{\epsilon}_{vp} = \sum_{k=1}^{n} \dot{\epsilon}_{vp_k} + \dot{\epsilon}_{vp\ of\ intact\ rock}$. Equations 2.31, 2.32 are anisotropic yield functions which are dependent on the direction of a set of parallel planes of weakness. Other types of anisotropic yield functions are discussed in References [9],[10].

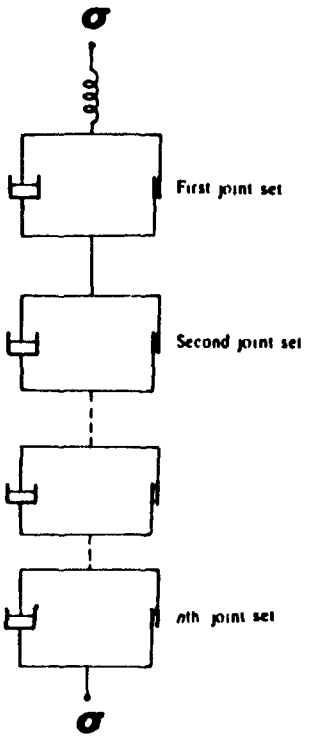

Rheological analogue of multilaminate model
of jointed rock mass
(Figure 2.20)

2.5 TIME DEPENDENT NO TENSION MODEL:

Reference [1] proposed a time dependent no tension model given by equation 2.33 to relieve the false tension exceeding the tension resistance at a point ;

$$F = \sigma_1 - \sigma_m + \frac{2}{3}\bar{\sigma}\sin\left(\cap + \frac{2\pi}{3}\right) \qquad (2.33\ a)$$

$$Q = \sigma_1 - const. = 0.0 \qquad (2.33\ b)$$

where σ_1 is the maximum principal stress (tension) , σ is the second deviatoric stress invariant and $\cap$ is the lode angle.

Another way of handling the excessive tension is proposed here ; If the total stress $\sigma_T = \sigma_x + \sigma_y$ (in the x-y plane) at a point is positive (tension) and exceeds the tension resistance , the maximum principal stress is calculated (which is the tension) and the direction it makes α_o as well (assuming a plane problem). Then two associative viscoplastic mechanisms with two yield functions are assumed;

The first , see equation 2.34 a, is a viscoplastic relaxation of the tension in a direction normal to the plane of α_o (α_o once calculated remains constant throughout the analysis).

The second ,equation 2.34 b, is for the shear acting parallel to the joint (assumed to be locally created after the tension failure) i.e the two yield functions are simulating a free surface created (and localized at the gauss point) at angle α_o with the horizontal:

$$F_1 = \sigma_n > 0 \quad i.e \ (tension) \qquad (2.34\ a)$$

$$F_2 = \sqrt{\tau^2} \qquad (2.34\ b)$$

$$\dot{\epsilon}_{vp_{ij}} = \phi(F_1)\ \frac{\partial \sigma_n}{\partial \sigma_{ij}} + \phi(F_2)\ \frac{\partial \sqrt{\tau^2}}{\partial \sigma_{ij}} \qquad (2.34\ c)$$

This approach presented here is more convenient because the direction of the tension failure α_o once existed is considered constant throughout the analysis and not changing with direction of the maximum principal stress which is the case of equations 2.33 (especially for the case of incremental loading). Equations 2.34 are also easy to implement in the plane strain or axisymmetric problems modelled by the developed program for which the planes of principal stresses are predefined.

In both approaches ϕ (F)=λF or another form chosen to give the same sensitivity to a change in stress (i.e $\partial\phi/\partial$F) as those of the viscoplastic creep laws implemented for the surrounding rock (important for an explicit time integration scheme). Equations 2.34 are anisotropic yield conditions and plastic potentials. Using an anisotropic yield function in the numerical modelling of <u>associative</u> viscoplasticity depending on an implicit time integration scheme does not violate the symmetry of the global stiffness matrix .

CHAPTER 3

NUMERICAL ALGORITHM

3.1 INTRODUCTION

The developed numerical model **VISA2D** is a 2-D finite element program using the theory of elasto-viscoplasticiy to model the effect of short term and time dependent behaviour on stresses and deformations around compound layouts of surface or underground mine excavations. It uses the classical 4 node-isoparametric elements with four integration points and it handles different types of loading , like own weight , nodal loading , surface loading and the initial or premining stresses. At any time station , the user can specify instantaneous changes. These could be added loads or additional cut or fill. The program can be stopped at any time and the analysis may be restarted at that time station later. The program uses the continuum theory of elasto-viscoplasticity thus to overcome the inhomogeneity of the surrounding rock several material types can be used. Several yield functions and creep laws can easily be adopted in the developed numerical model.

In this chapter, the finite element formulation of its elasto-viscoplastic numerical algorithm is explained in detail through Section 3.2 which describes the flow chart of the

developed computer program . Section 3.3 explains the numerical stability of a fully explicit time integration scheme.

3.2 NUMERICAL ALGORITHM OF THE ITERATIVE EXPLICIT TIME STEPPING SCHEME IMPLEMENTED IN PROGRAM VISA2D:

This Section describes how the numerical model uses the finite element and the theory of viscoplasticity to integrate the inelastic strain rate over the successive time increments by using an iterative explicit scheme .

With the viscous strain rate expressed by equation 2.11, we can define a strain increment $\Delta\epsilon_{vp}^{n}$ occurring in a time interval $\Delta t_n = t_{n+1}-t_n$ as follows;

$$\Delta\epsilon_{vp}^{n} = (\dot{\epsilon}_{vp}^{n}(1-\Theta) + \dot{\epsilon}_{vp}^{n+1}\Theta)\,\Delta t_n \qquad (3.1)$$

For $\Theta = 0.0$ we obtain the Euler time integration scheme which is also referred to as 'fully explicit' since the viscoplastic strain increment is completely determined from conditions at time t_n. On the other hand, $\Theta = 1$ gives a fully implicit scheme with the strain increment being determined from $\dot{\epsilon}_{vp}^{n+1}$. The case of $\Theta=1/2$ results in the so called implicit trapezoidal scheme or Crank-Nicolson rule. The value of Θ lies from 0.6 to .9 which is dictated by the shape of the $\dot{\epsilon}_{vp}$-t at the critical points (see Figure 3.1d) and also from equation 3.28.

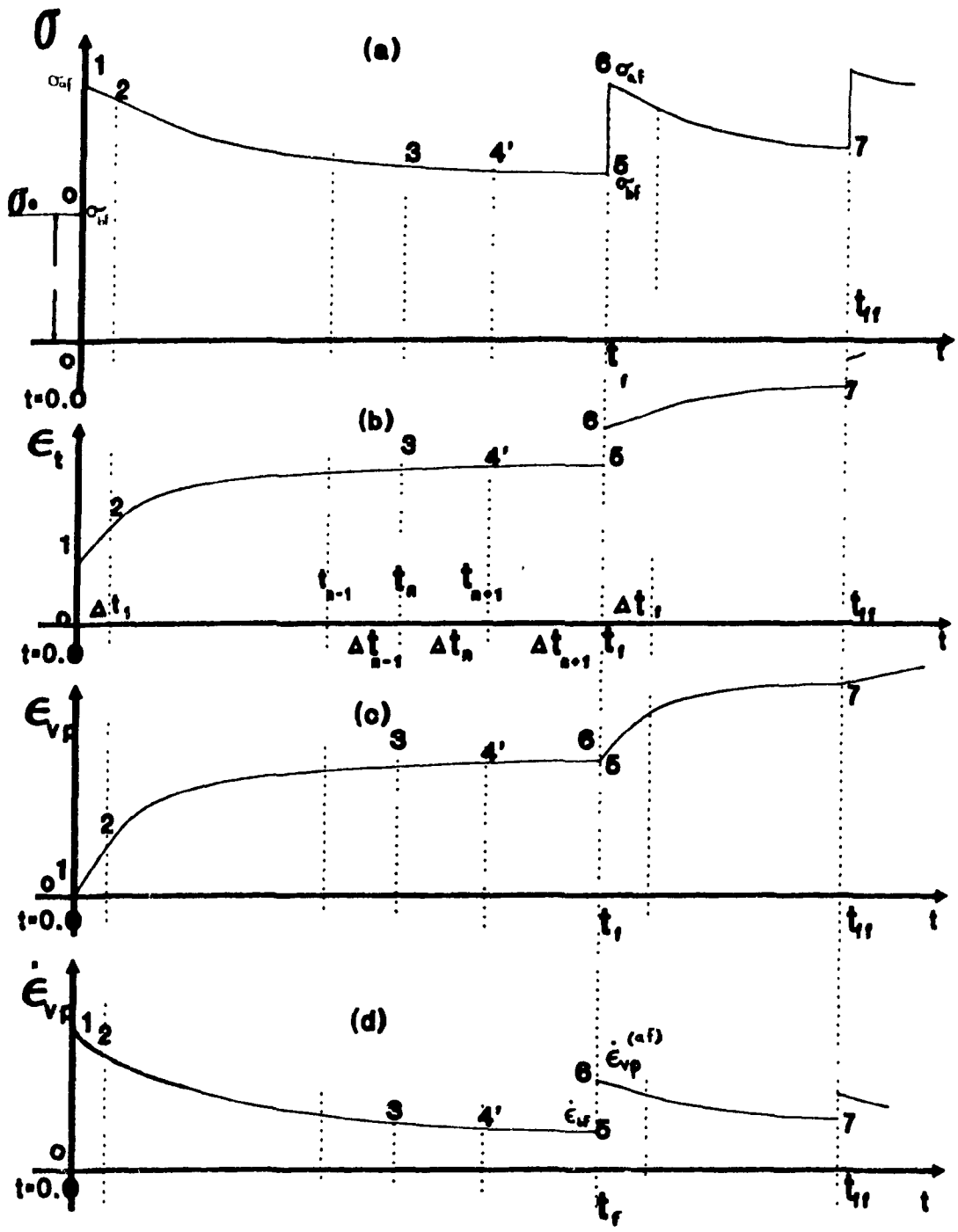

A qualitative diagram of the change of stress and viscous strain at a relaxing (critical) point in the rock mass
(Figure 3.1)

Referring to equation 3.1 , as a first (fast) iteration the viscoplastic strain increment is determined from conditions at time t_n i.e θ=0.0. Other iterations follow to improve accuracy with θ=0.7.

Referring to Figure 3.1 the analysis starts at point **o** before excavation at t=0.0 and viscoplastic modelling starts and continues to time station $\underline{t}_f$ at which an instantaneous change is applied (e.g elements cut or filled) then viscoplastic modelling continues and so on.

3.2.1 TIME DEPENDENT ANALYSIS:

SEGMENT 1: INSTANTANEOUS RESPONSE

Calculate the total load vector due to the sudden changes after excavation and hence solve the system under this loading conditions. This is given by :-

$$P + \int_{\Omega} N^T b \, d\Omega + \int_{\Gamma} N^T \bar{g} \, d\Gamma - \int_{\Omega} B^T \sigma_o \, d\Omega - K \Delta u \qquad (3.2)$$

where $\mathbf{N}^T$, $\mathbf{B}^T$ are the element shape function and strain matrices relating the nodal displacement of an element with the deformation **u** and strain vector respectively at a point within this element. The formulation of element shape functions are described elsewhere [32]. **P** is the load vector due to applied point loads, $\int_{\Omega} N^T b \, d\Omega$ is the global load vector due to body forces (own weight), $\int_{\Gamma} N^T \bar{g} \, d\Gamma$ represents

surface traction loading (side pressures and shears) global load vector, and $\int_{\Omega} B^T \sigma_o \, d\Omega$ is the balancing initial stress load vector which might not be in total balance with the first three terms because of a created cavity.

K is the global stiffness matrix and **Δu** is the required nodal displacements.

The set of equilibrium equations of the global degrees of freedom in 3.2 is solved by a Gauss elimination equation solver [33] which divides the global stiffness matrix into a number of blocks in order to alleviate the storage limit problem while using a banded symmetric stiffness matrix. The equation solver has been modified for the optimization of the iterative explicit time integration scheme in which the triangularized (or decomposed) global stiffness is stored for further use in the viscoplastic analysis (like equation 3.8) and only the load vector enters the process of Gauss elimination.

Direct access, unformatted files are used to store the element data and the calculated matrices like $[\mathbf{DxB}]_{4x8}$ for use in the coming viscoplastic analysis to reduce execution time . For each element, one direct access unformatted record is used to read, update and write the stress σ and viscoplastic strain vectors etc .. at all integration points in order to minimize the computer storage requirements .

SEGMENT 2: UPDATE THE STRESSES AND THE VISCOPLASTIC STRAIN

RATE DUE TO THE INSTANTANEOUS CHANGE AT $t=0.0$ (OR $= t_f$ IF ANALYSIS IS AT POINT 5) :

In the following steps integrations are actually done using numerical integration at four Gauss points within each element However for simplicity of interpretation the formulas presented below use the integration symbol $\int$.

Repeat the following steps for each element:

Known: σ_{bf} or (σ_o at t=0.0) , ϵ_{vp}^{bf}, $\dot{\epsilon}_{vp}^{bf}$ (see Figure 3.1), the element assigned material number (mat) to access the appropriate constitutive law ; $E^{mat}, \upsilon^{mat}, D^{mat}$ and if the material is specified as a creeping one, the non zero integers: NY(MAT) and NCR(MAT) are used to access the forms F^{mat}, Q^{mat}, ϕ^{mat}. and their constants which are stored per material.(see Section 4.3 cards 3,4)

a)- Use the element nodal displacement increments resulting from segment 1 to update stresses from σ_{bf} to σ_{af} ;

$$\sigma_{af} = \sigma_{bf} + D B \Delta u \quad . \quad . \quad . \quad . \quad . \quad (3.3)$$

If the material of this element is specified by the user to be treated elastically ; skip steps **b,c,d,e,f,g.**

b)- Use σ_{bf} , ϵ_{vp}^{bf} to calculate the numerical value of the specified yield function $F^{mat}(\epsilon_{vp}, \sigma)$;

If $F < 0.0$ → no creep at this point → skip steps **c,d, e,f,**(and step **g** - is skipped if this happened at the four gauss points)

c)- Get the viscoplastic strain rate vector $\dot{\epsilon}_{vp}^{af}$.

Calculate the value of the scalar creep rate ϕ according to the creep law assigned to the current material type. If the creep implies more than one yield function (like for each friction slider in Figure 2.19) the program checks the yield (or creep) of each mechanism to finally substitute in the appropriate form of ϕ .

Calculate the viscoplastic strain rate vector by using the specified plastic potential $Q^{mat}(\sigma, \epsilon_{vp})$.

$$\dot{\epsilon}_{vp_{ij}} = \phi \frac{\partial Q^{mat}}{\partial \sigma_{ij}} \tag{3.4}$$

If the viscoplastic strain rate vector $\dot{\epsilon}_{vp}$ is composed of different mechanisms with different flow rules like in Figure 2.17 ;

$$\dot{\epsilon}_{vp_{ij}} = \phi_1^{mat} \frac{\partial Q_1^{mat}}{\partial \sigma_{ij}} + \phi_2^{mat} \frac{\partial Q_2^{mat}}{\partial \sigma_{ij}} + \ldots\ldots\ldots \phi_n^{mat} \frac{\partial Q_n^{mat}}{\partial \sigma_{ij}} \tag{3.5}$$

(The updated values of σ and $\dot{\epsilon}_{vp}$ correspond to $\sigma_{af}, \dot{\epsilon}_{vp}^{af}$ in Figure 3.1 respectively).

d)- Get the value of $\frac{\partial \phi}{\partial F}$, $\frac{\partial F}{\partial \sigma_d}$, $\frac{\partial F}{\partial \sigma_T}$, $\frac{\partial Q}{\partial \sigma_d}$, $\frac{\partial Q}{\partial \sigma_T}$ (if the yield function and plastic potential depend on J_1, J_{2D} , they replace σ_T , σ_d respectively) which are important for monitoring the numerical stability during Δt_f (or Δt_1 after t=0.0) .see Section 3.3 for details and exceptions.

e)- Use the viscoplastic strain increment during a unit time ($\Delta\epsilon_{vp}=\dot{\epsilon}_{vp}*1$) to calculate the load vector due to stress relaxation or relief per unit time of Δt_1 (or Δt_f after t_f) which is still unknown;

$$v_{el.} = -\int_{\Omega} B^T D\dot{e}_{vp}\, d\Omega \qquad (3.6)$$

f)- Calculate the maximum allowable time increment according to the current state of element i ;$\Delta t_{max(i)}$ using equations of Section 3.3, and compare it with the minimum value of the preceding elements Δt_{MINMAX}.

g)- Add the element out of balance load vector $v_{el.}$ (equation 3.6) to the global out of balance load vector.

*End of loop over elements

Referring to Figure 3.1, the execution is at point **1** or point **6**.

SEGMENT 3:

a)- Use the maximum allowable time increment at the most critical point Δt_{MINMAX} (see step **f** segment 2) to get the value of the time increment Δt_f (Δt_1 at t= 0.0) by following the flow chart inside segment 3 in Figure 3.2 (In the flow chart if the analysis is at t=0.0 then t_f represents t=0.0 and t_{ff} represents t_f). Making sure when $t=t_f$ that $t+\Delta t_f \leq t_{ff}$ (or when t=0.0 that $t+\Delta t_1 \leq t_f$).

b)- Get the true value of the global relaxation load vector;

$$V = V\,\Delta t_f \qquad (3.7)$$

c)- Solve and get the global displacements Δu from

$$\boldsymbol{K}\,\Delta \boldsymbol{u} = \boldsymbol{V} \qquad (3.8)$$

The system is solved under **V** only and the stored triangularized form of the stiffness matrix is used.

Update the total displacements; $\boldsymbol{u} = \boldsymbol{u} + \Delta \boldsymbol{u}$ (3.9)

In the following segment t_f and Δt_f will serve as t_n , Δt_n respectively.

SEGMENT 4: Integration of the creep rate over the time increment Δt_n

Repeat the following steps for each element.

At the end of a time increment say Δt_{n-1} and the beginning of new one Δt_n :σ_n , ϵ_{vp}^n, $\dot{\epsilon}_{vp}^n$, Δt_n are known at t_n (after an instantaneous change these knowns at $t=t_f$ are :σ_{af} , ϵ_{vp}^{af}, $\dot{\epsilon}_{vp}^{af}$, Δt_f (see Figure 3.1) or at t=0.0 σ_1, ϵ_{vp}^1, $\dot{\epsilon}_{vp}^1$, Δt_f calculated at segment 2).

a)-If the material is elastic skip this step. Otherwise;

The first trial over Δt_n uses a fully explicit stepping i.e $\dot{\epsilon}_{vp}=\dot{\epsilon}_{vp}^n$ and assuming full relaxation in this step only

$$\Delta \boldsymbol{\epsilon}_{vp}^{(1)} = \dot{\boldsymbol{\epsilon}}_{vp}^{n}\,\Delta\, t_n \quad . \quad . \quad . \quad . \quad . \quad . \qquad (3.10)$$

$$\boldsymbol{\epsilon}_{vp}^{n+1(1)} = \boldsymbol{\epsilon}_{vp}^{n} + \Delta \boldsymbol{\epsilon}_{vp}^{(1)} \quad . \quad . \quad . \quad . \quad . \quad . \qquad (3.11)$$

$$\boldsymbol{\sigma} = \boldsymbol{\sigma} - \boldsymbol{D}\,\Delta\,\boldsymbol{\epsilon}_{vp}^{(1)} \quad . \quad . \quad . \quad . \quad . \quad . \qquad (3.12)$$

b)- Update σ_n for $\Delta\epsilon$ resulting from the application of the out of balance load vector (which was assumed 0.0 in step **a** if this is the first iteration or in step **g** of the first iteration if this is the second iteration) ;

$$\sigma = \sigma + D\,B\,\Delta u \qquad (3.13)$$

If the material of this element is specified by the user to be linear elastic , skip the following steps for the current element and start step **a** for another element.

c)- Use σ_{n+1} , $\epsilon_{vp}^{n+1(1)}$ to calculate the numerical value of the specified yield function $F^{mat}(\epsilon_{vp},\sigma)$;

If $F < 0.0$ → no creep (or no viscoplastic strain rate)at this point → skip steps **d,e,f,g,h,i,j,** (and step **k** if this happens at the four gauss points).

d)- Perform step c in segment 2 to get the plastic strain rate vector $\dot{\epsilon}_{vp}^{n+1}$ based on $\sigma_{n+1}, \epsilon_{vp}^{n+1}$.

e)- obtain an improved estimate of ϵ_{vp}^{n+1} using $\dot{\epsilon}_{vp}^{n}$ and $\dot{\epsilon}_{vp}^{n+1}$;

$$\epsilon_{vp}^{n+1} = \epsilon_{vp}^{n} + (\dot{\epsilon}_{vp}^{n} (1-\theta) + \dot{\epsilon}_{vp}^{n+1}\ \theta)\ \Delta t_n \qquad (3.14)$$

Repeat steps:- **c** (with ϵ_{vp}^{n+1} in place of $\epsilon_{vp}^{n+1(1)}$),**d,e** to get an improved estimate of $\epsilon_{vp}^{n+1}, \dot{\epsilon}_{vp}^{n+1}$.

Referring to Figure 3.1 , analysis may be at point **2** or **4** or in between.

f)-Get the correction of the total viscoplastic strain at this point;

$$\delta\epsilon_{vp} = \epsilon_{vp}^{n+1} - \epsilon_{vp}^{n+1\,(1)} \quad . \ . \ . \ . \ . \ . \qquad (3.15)$$

Where $\epsilon_{vp}^{n+1(1)}$ is the estimate of the previous iteration i.e step **a** of the first iteration if this is the Second iteration or step **e** of the second iteration if this is the third iteration and so on.

g)- Update stresses for $\delta\epsilon_{vp}$ (assuming full confinement $\delta\epsilon_t$=0.0):

$$\sigma-\sigma_{n+1} - \sigma_{n+1} - D\delta\epsilon_{vp} \quad \ldots\ldots \quad (3.16)$$

h)- Obtain the out of balance load vector caused by $\delta\epsilon_{vp}$

$$\delta v_{el} \cdot -\int_{\Omega} B^T D\, \delta\epsilon_{vp}\, d\Omega \quad \ldots\ldots \quad (3.17)$$

Obtain the values of $\frac{\partial\phi}{\partial F}$, $\frac{\partial F}{\partial\sigma_d}$, $\frac{\partial F}{\partial\sigma_T}$, $\frac{\partial Q}{\partial\sigma_d}$, $\frac{\partial Q}{\partial\sigma_T}$ (if the yield function and plastic potential depend on J_1,J_{2D} ,they replace σ_T ,σ_d respectively) based on σ_{n+1} and ϵ_{vp}^{n+1}, which are important for monitoring the numerical stability during Δt_{n+1} .see Section 3.3 for details and exceptions.

i)- Use the viscoplastic strain increment during a unit time ($\Delta\epsilon_{vp}=\dot{\epsilon}_{vp}^{n+1}*1$) to get the out of balance load vector per unit time of Δt_{n+1} which is still unknown.

$$v_{el}.^{n+1} -\int_{\Omega} B^T D\dot{\epsilon}_{vp}^{n+1}\, d\Omega \quad (3.18)$$

j)- Get the maximum allowable time increment according to the current state of element i $\Delta t_{max(i)}$ using equations of Section 3.3, and compare it with the minimum value of the preceding elements Δt_{MINMAX}.

k)- Assemble the load vectors $\delta v_{el.}$,$v_{el.}^{n+1}$ into the global relaxation load vector δV,V^{n+1} :

*End of loop over elements

SEGMENT 5:

If accuracy is satisfied or the required number of iterations over Δt_n are done (whatever happens first) go to step **b**.

a)- Apply the global out of balance load vector δV to solve for the resulting global displacements;

$$K \delta u = \delta V$$

Update the total displacements ; $u = u + \delta u$ (3.20)

To do a second or third iteration over the same time increment Δt_n ; repeat the loop over all elements in segment 4 from step **b** to step **k**.

Referring to Figure 3.1 the execution would be entering the 2^{nd} (or 3^{rd} or 4^{th}....) iteration over Δt_n to get an improved estimate of σ , ϵ_{vp}^{n+1} and $\dot{\epsilon}_{vp}^{n+1}$.

b)- Now the required number of iterations over time step Δt_n are done (or accuracy is satisfied whatever happens first) and we reach t_{n+1} i.e $t=t+\Delta t_n=t_{n+1}$. The value of Δt_{n+1} is defined by following the chart in Figure 3.2 where Δt_{MINMAX} is the minimum of time increment limits ($\Delta t_{max(i)}$) for numerical stability at each integration point in the rock mass and t_f the time station at which a sudden change may take place or the program may stop.

c)- Arriving at the start of Δt_{n+1}, the program calculates the true out of balance load vector based on the first estimate of; $\Delta \epsilon_{vp}^{n+1} = \dot{\epsilon}_{vp}^{n+1} \Delta t_{n+1}$.

$$V = V^{n+1} \Delta t_{n+1} + \delta V \qquad (3.21)$$

where δV is the residual of the previous Δt_n .

- Apply the global out of balance load vector V to get the resulting global displacements;

$$k \Delta u = V \quad . . . . . \quad (3.22)$$

$$u = u + \Delta u \quad . . . . . \quad (3.23)$$

- Go to segment 4 and repeat what was done for Δt_n with Δt_{n+1} as Δt_n, ϵ_{vp}^{n+1} as ϵ_{vp}^{n} , $\dot{\epsilon}_{vp}^{n+1}$ as $\dot{\epsilon}_{vp}^{n}$ and σ and u.

SEGMENT 6:

The analysis arrives at point 5 in Figure 3.1 where an instantaneous changes like cutting elements (additional excavation) or adding elements (adding backfill) may be applied. It can also include adding external nodal loads or surface loading.

A general equation would be as follows;

$$P + \int_{\Omega} N^T b \, d\Omega + \int_{\Gamma} N^T \bar{s} \, d\Gamma - \int_{\Omega} B^T \sigma \, d\Omega + P_{added} + \int_{\Gamma} N^T \bar{s}^{added} \, d\Gamma - K \Delta u \qquad (3.24)$$

The first three terms; P, $\int_{\Omega} N^T b \, d\Omega$, $\int_{\Gamma} N^T \bar{s} \, d\Gamma$ represent external applied loads at time t=0.0 (including the added changes at previous time stations), σ represents the

stresses just before t_f (at point 5 in Figure 3.1)

-If the changes include <u>cut elements only</u> the applied load would come from the unbalance between the external loads and the internal stresses σ_5 (see Figure 3.1) because of the absence of elements cut <u>at this time station</u> ;

$$P + \int_{\Omega} N^T b \, d\Omega + \int_{\Gamma} N^T \bar{s} \, d\Gamma - \int_{\Omega} B^T \sigma_5 \, d\Omega - K \Delta u \qquad (3.25)$$

and the cut elements are skipped when the global stiffness matrix **K** is reconstructed form the element stiffness matrices ($k_e = \int_{\Omega} B^T D B \, d\Omega$) and stored for the subsequent viscoplastic analysis.

-If the changes include only added loads (surface or nodal) equation 3.24 is written as follows;

$$P_{added} + \int_{\Gamma} N^T \bar{s}^{added} \, d\Gamma + \delta V - K_o \Delta u \qquad (3.26)$$

where K_o is the initial global stiffness matrix which remains unchanged. The creep process redistribute the stresses throughout the rock mass but it does not affect the equilibrium between the external forces and the internal stresses so in this case equation 3.26 is used because in equation 3.24 when there is no cut $\int_{\Omega} B^T \sigma \, d\Omega - \int_{\Omega} B^T \sigma_5 \, d\Omega - \int_{\Omega} B^T \sigma_1 \, d\Omega$ is in total equilibrium with $P + \int_{\Omega} N^T b \, d\Omega + \int_{\Gamma} N^T \bar{t} \, d\Gamma$. The residual out of balance load vector (from the last iteration of the previous time increment) has to be added in equation 3.24 only, because in equation 3.24 or 3.25 its effect is

included in ($-\int_{\Omega} B^T \sigma_5 \, d\Omega$) (see equation 3.16).

- The backfill is represented by adding or replacing existing elements with elements of new properties and zero internal stresses ($\sigma \rightarrow 0.0$) . The program reads their properties and construct their records of data needed for the coming analysis and adds the related loads (body or surface loads) to the global load vector The backfill stiffness is added to the global stiffness matrix tc contribute in the response to any external or future relaxation loads (like in equation 3.22) . The three types of changes ;cut,fill and added loads can be specified simultaneously at t_f (see Section 4.3 cards 8,9,10,11). This is particularly useful in the analysis of rocksalt mines.

After obtaining the elastic displacements (Δu) in response to the applied sudden loading, the program updates the stresses and viscous strain rate by executing the loop in segment 2 after which the analysis may continue or stop according to what is specified by the user (in card 12 of Section 4.3).

3.2.2 TIME INDEPENDENT ANALYSIS

When the viscoplastic model is used to predict an elastoplastic response , the time is a fictitious variable and

t_f does not exist in the input data (see Section 4.3 card 1). The applied load of the instantaneous change (Equation 3.24) is divided into a number of increments NINCR (specified in the input data file card 5.) in order to obtain the incremental viscous plasticity solution , see Figure 9. In this case the first increment of the global load vector;

$$\boldsymbol{L}_{incr} = \frac{1}{NINCR}\left(\boldsymbol{P}+\int_{\Omega}\boldsymbol{N}^T\boldsymbol{b}\,d\Omega+\int_{\Gamma}\boldsymbol{N}^T\bar{\boldsymbol{t}}\,d\Gamma-\int_{\Omega}\boldsymbol{B}^T\boldsymbol{\sigma}_o\,d\Omega\right) \quad (3.27)$$

is applied and the elastic displacements response obtained from $\mathbf{K}_o\ \Delta\mathbf{u} = \mathbf{L}_{incr}$ are used to update the stresses and viscoplastic strain rate in the loop of segment 2 . If the yield limit is exceeded at any point of the structure the viscoplastic stepping starts and the relaxation due to the viscous strain rate is redistributed throughout the rock mass by executing segment 4 and segment 5 (step a,b only) for the successive time increments (Δt_1 , Δt_2,....) untill the yield function $F(\sigma, \epsilon_{vp})$ at the most critical element of the rock mass is less than a small positive number (depending on the stress unit used in Card 2 of Section 4.3). At this point, the execution is transferred to segment 5 where the following load increment is applied ; $\mathbf{L}_{incr2} = \mathbf{L}_{incr} + \delta\mathbf{V}$ where $\delta\mathbf{V}$ is the residuaL out of balance load vector of the last iteration over the preceding Δt. The elastic response is obtained from $\mathbf{K}_o\ \Delta\mathbf{u} = \mathbf{L}_{incr2}$ is obtained The stresses and viscoplastic

strain rate are updated in the loop of segment 2 and so on. The program stops when a stabilization is obtained after the full load $\left(P+\int_{\Omega} N^T b\, d\Omega + \int_{\Gamma} N \cdot \bar{t}\, d\Gamma - \int_{\Omega} B^T \sigma_o\, d\Omega\right)$ is already applied.

3.2.3 MORE ABOUT THE PROGRAM

Whenever the program produces results of the stresses and deformation at any time station using segment , it calculates the sign of $\frac{\partial \phi}{\partial \varepsilon_{vp}} \cdot \dot{\varepsilon}_{vp}$ which is the same as $\frac{\partial \phi}{\partial \varepsilon_{vp_{ij}}} \cdot \frac{\partial Q}{\partial \sigma_{ij}}$ to determine if the behaviour at this point is stable (negative) or unstable (positive) (see Figure 4.16). The analysis may be performed for elastoplastic response (by the theory of elasto-viscoplasticity) then the creep analysis starts based on the obtained elastoplastic distribution of stresses. In this case for each material the user has the option to specify a yield function for the elastoplastic simulation and a yield function and creep law for the creep behavior (see Section 4.3 cards 6/,7/). If after the elastoplastic analysis the behaviour of an element was checked using the postprocessor to be softening (or perfectly plastic) one might specify properties of incompressible weak material (high poisson's ratio) for this element at the start of the creep analysis to avoid adding stresses over its yield limit during

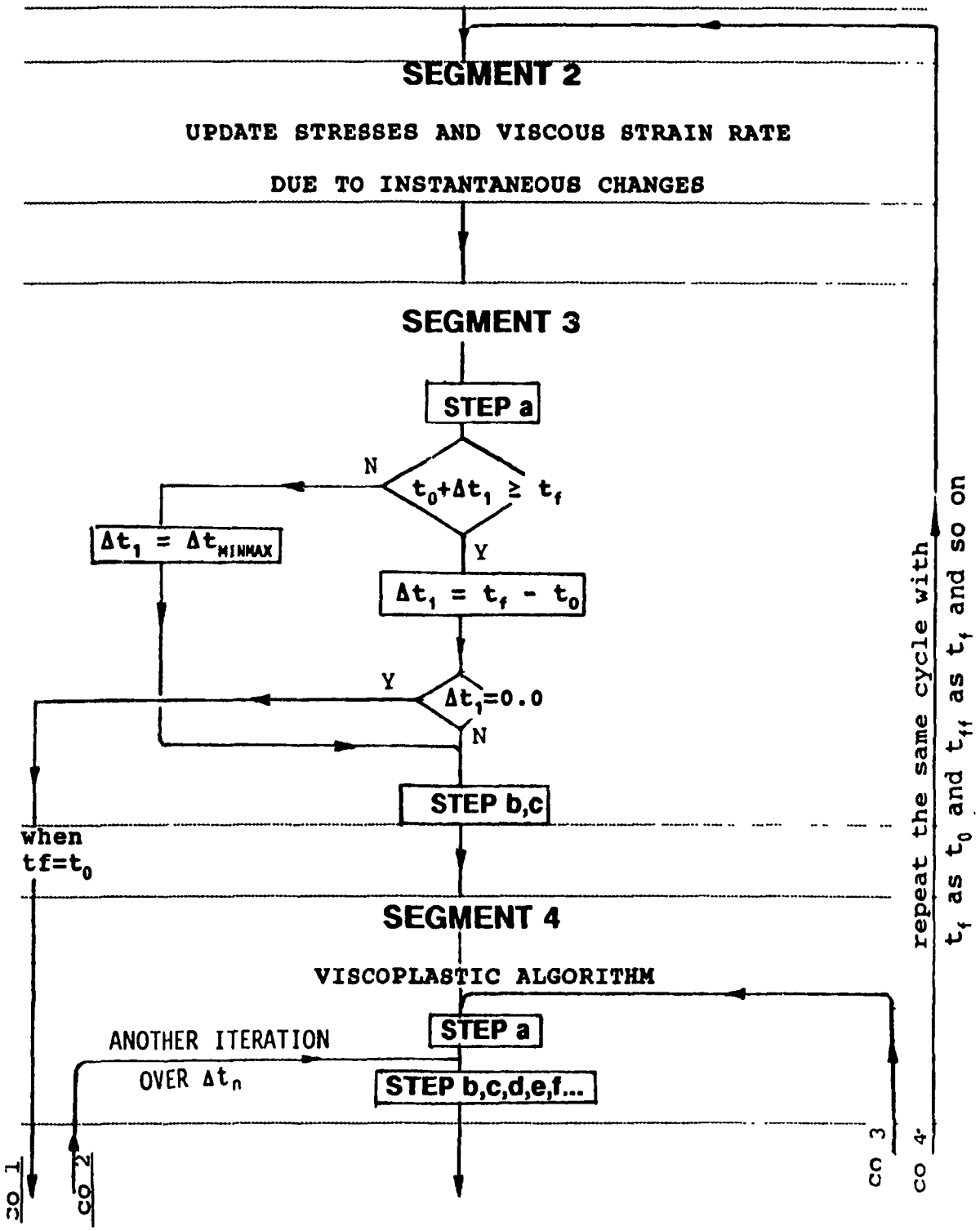

FLOW CHART OF PROGRAM VISA2D
(continued in the following page)
(Figure 3.2)

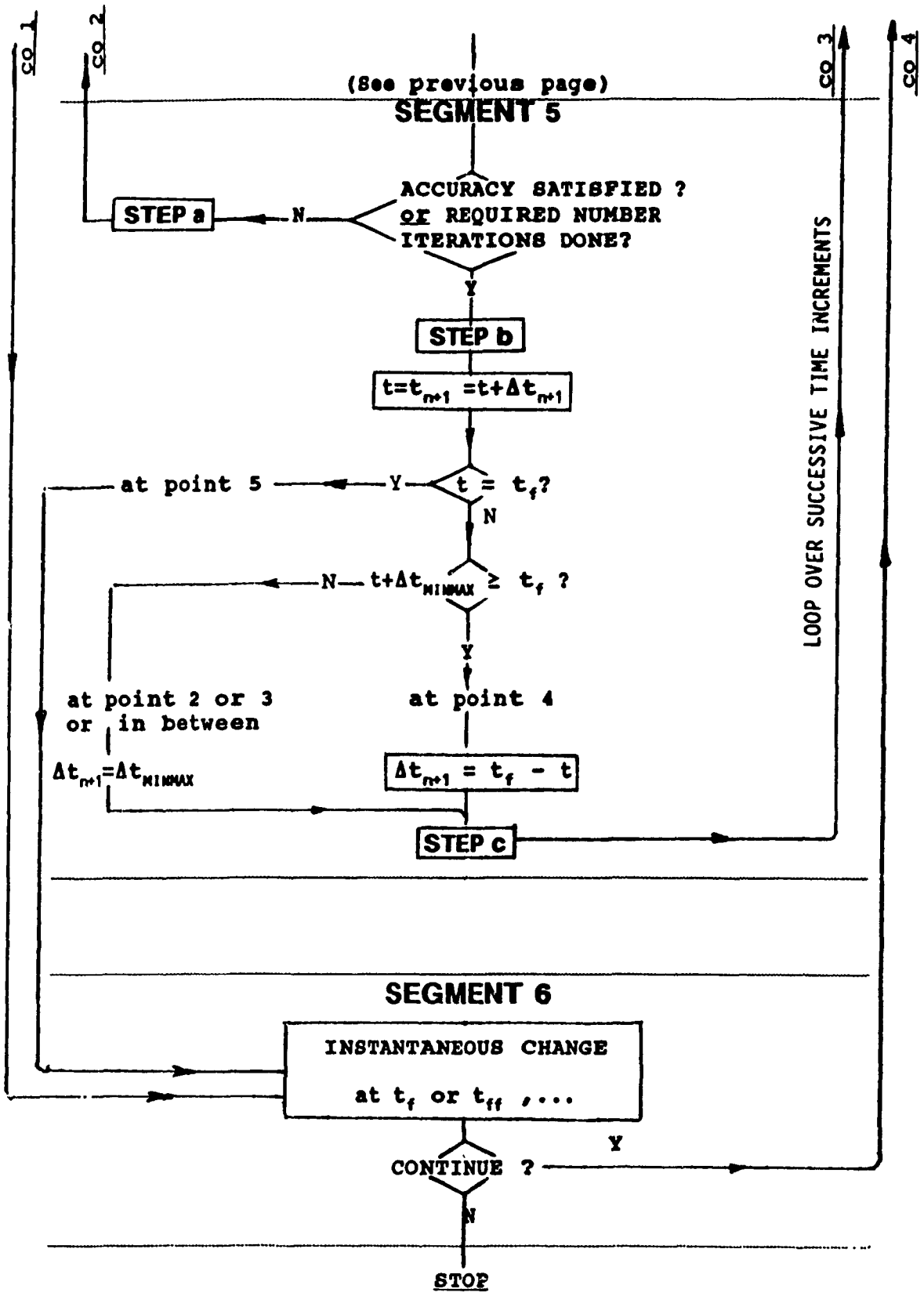

Flow chart of program **VISA2D**
(Figure 3.2)

the creep process. Or instead, one may specify for this element, a creep law giving ($\partial\phi/\partial F$) equal to the surrounding rock as being function of the same yield function used for the elastoplastic behaviour (to avoid numerical instability) .

In this way the effect of the short term and time dependent plasticity are simulated by an iterative explicit time integration scheme with some interference by the user while automating this feature inside the program is not done yet._ In the above discussion there is no focus on a specific constitutive law because the numerical model can with ease adopt different kinds of yield functions and creep laws suitable for the different rock types under different conditions and possibly in the same problem as mentioned in Section 2.3,2.4. The subject of numerical stability is reviewed in the following Section.

3.2 NUMERICAL STABILITY OF A FULLY EXPLICIT TIME STEPPING SCHEME

The value of the time increment used inside the program depends on the creep law ,yield function and plastic potential dictating the rate of viscoplastic strain rate as in equation 2.11 The concept used here is the same used in reference [17].

In a nonlinear viscoplastic strain behavior at which the stresses change with time and for rocklike materials , the stress σ is the most effective variable in the viscoplastic rate and the numerical instability which is the oscillatory change of the creep rate is caused by the oscillatory change of stresses . If $\dot{\phi}$ is the change in the creep rate during a unit time, as a first step, we try to express it in terms of the creep rate itself ϕ ;

$$\dot{\phi} = -\eta_1 \phi \qquad (3.28)$$

Therefore let us first consider in the following that $F=F(\sigma)$ and ; $\dot{\epsilon}_{vp_{ij}} = \phi(F) \frac{\partial Q}{\partial \sigma_{ij}}$. Assuming that Q depends on $\bar{\sigma}=J_{2D}^{1/2}$, J_1 only which is the common case of plastic potentials having a revolutionary surface around the axis of the hydrostatic stress conditions ($\sigma_1 = \sigma_2 = \sigma_3$) the stress and plastic strains become coaxial in the plane of $\bar{\sigma}$,J_1 and it

can easily be shown that the inelastic strain corresponding to $\bar{\sigma}, J_1$ are ;

$$\dot{\epsilon}_d = \left(\frac{1}{2} e_{ij} e_{ij}\right)^{1/2} = \frac{1}{2} \phi \frac{\partial Q}{\partial \bar{\sigma}} \quad \ldots . \quad (3.29)$$

$$\dot{\epsilon}_v^p = \dot{\epsilon}_1^j + \dot{\epsilon}_2^p + \dot{\epsilon}_3^p = 3 \phi \frac{\partial Q}{\partial J_1} \quad \ldots . \quad (3.30)$$

It is assumed that the viscous strain increment causes pure relaxation i.e $\Delta\epsilon_t = \Delta\epsilon_e + \Delta\epsilon_{vp} = 0.0$ at the most critical points of the rock mass which is a theoretical conservative assumption. Using this assumption $(d\epsilon_t = 0.0) \rightarrow d\epsilon_e = -d\epsilon^I$ at a critical point of the rock mass and the corresponding change of stresses is obtained by using the elasticity relations of an isotropic material ;

$$\dot{\bar{\sigma}} = -\dot{\epsilon}_d^p (2G) = -\frac{1}{2} \phi \frac{E}{1+\nu} \frac{\partial Q}{\partial \bar{\sigma}} \quad (3.31)$$

$$\dot{J}_1 = -\dot{\epsilon}_v^p \frac{E}{1-2\nu} = -3 \phi \frac{E}{1-2\nu} \frac{\partial Q}{\partial J_1} \quad (3.32)$$

Taking also the common case that the yield function is dependent on $\bar{\sigma}$, J_1 only (like Drucker and Prager yield function) the change in F during unit time of Δt can be expressed as follows ;

$$dF = \frac{\partial F}{\partial \bar{\sigma}} d\bar{\sigma} + \frac{\partial F}{\partial J_1} dJ_1$$

$$\dot{F} = -\frac{\partial F}{\partial \bar{\sigma}} \left(\frac{1}{2} \phi \frac{E}{1+\nu} \frac{\partial Q}{\partial \bar{\sigma}}\right) - \frac{\partial F}{\partial J_1} \left(3 \phi \frac{E}{1-2\nu} \frac{\partial Q}{\partial J_1}\right) \quad (3.34)$$

In equation 3.34 it is assumed that the viscoplastic strain is not causing hardening or softening by changing the value of F or directly affecting ϕ (this case will be explained later) For now we get ;

$$\frac{d\phi}{dt} = \dot{\phi} = \frac{\partial \phi}{\partial F}\dot{F}$$

$$\frac{d\phi}{dt} = -\frac{\partial \phi}{\partial F}\left(\frac{1}{2}\frac{E}{1+\nu}\frac{\partial F}{\partial \bar{\sigma}}\frac{\partial Q}{\partial \bar{\sigma}} + 3\frac{E}{1-2\nu}\frac{\partial F}{\partial J_1}\frac{\partial Q}{\partial J_1}\right)\phi \quad (3.35)$$

comparing equation 3.35 with equation 3.28 we get η_1 as follows;

$$\eta_1 = \frac{\partial \phi}{\partial F}\left(\frac{1}{2}\frac{E}{1+\nu}\frac{\partial F}{\partial \bar{\sigma}}\frac{\partial Q}{\partial \bar{\sigma}} + 3\frac{E}{1-2\nu}\frac{\partial F}{\partial J_1}\frac{\partial Q}{\partial J_1}\right) \quad (3.36)$$

The equation $\dot{Y} = -\eta\ Y$ is popular mathematically (see Figure 3.2 [17]). If this equation is integrated using a fully explicit time integration scheme the time increments should be less than a certain limit $\Delta t_{crit}=2/\eta$ which admits stable oscillatory convergence to steady state and $\Delta t_{max} = \Delta t_{crit}/2$ represents an upper bound for non oscillatory stable predictions [17]. In our case the value of Y which corresponds to ϕ can never be negative i.e $\dot{\phi} = -\eta_1 \phi$ is not unstable numerically by itself.

But if the time increment used to integrate this equation and multiplied by the viscous rate to get the relaxation stress increment at all the critical elements of the rock mass is

higher than Δt_{crit} an oscillation in the transfer of the relaxation load from one element to another occurs, i.e referring to Figure 3.3 the stress σ of an element relaxes during Δt_n to reach point 1, but carries the relaxation loads of the adjacent elements during Δt_{n+1} to reach point 2 and so on. Based on that, equation 3.37 gives $\Delta t_{max}=\Delta t_{crit}/2$ for yield functions and plastic potentials depending on J_1 and $\bar{\sigma}$ only :

$$\Delta t_{crit} = \frac{(1+\nu)(1-2\nu)}{\frac{\partial \phi}{\partial F} E \left(\frac{1}{2}(1-2\nu) \frac{\partial F}{\partial \bar{\sigma}} \frac{\partial Q}{\partial \bar{\sigma}} + 3(1+\nu) \frac{\partial F}{\partial J_1} \frac{\partial Q}{\partial J_1} \right)} \quad (3.37)$$

Applying this general form to Drucker-Prager associated viscoplasticity where the yield function is of the form :

$$F = \frac{2\sin\psi}{3-\sin\psi} J_1 + \sqrt{3}\,\bar{\sigma} - const \quad (3.38)$$

where ψ is the angle of internal friction , it can easily be shown that :

$$\frac{\partial F}{\partial \bar{\sigma}} = \frac{\partial Q}{\partial \bar{\sigma}} = \sqrt{3}$$

$$\frac{\partial F}{\partial J_1} = \frac{\partial Q}{\partial J_1} = \frac{2\sin\psi}{3-\sin\psi}$$

Δt_{crit} is obtained by substituting in equation 3.37 as follows :

$$\Delta t_{crit} = \frac{2(1+\nu)(1-2\nu)(3-\sin\psi)^2}{\frac{\partial \phi}{\partial F} E \left(\frac{3}{2}(1-2\nu)(3-\sin\psi)^2 + 12(1+\nu)\sin^2\psi \right)} \quad (3.39)$$

This result is the same as that given by Cormeau [4] for Drucker-Prager yield function. However this approach is more

general and easier to be applied to a variety of yield functions and flow rules.

When the yield function and plastic potential are concerned with the plane of minimum and maximum principal stresses like Mohr-Coulomb, Tresca, or the yield function of reference [13] the total stress $\sigma_T=\sigma_1+\sigma_3$ and the differential stress $\sigma_d=|\sigma_1-\sigma_3|/2$ monitor the hydrostatic and deviatoric component of the applied stress in place of J_1 and $J_{2D}^{1/2}$.

In this case the corresponding plastic strain increments are;

$$\dot{\epsilon}_d^p = \sqrt{\left(\frac{\dot{\epsilon}_x^p-\dot{\epsilon}_y^p}{2}\right)^2 + \dot{\epsilon}_{xy}^{p\,2}} = \frac{1}{2}\frac{\partial Q}{\partial \sigma_d}\,\phi \qquad (3.40)$$

$$\dot{\epsilon}_T^p = \dot{\epsilon}_1^p + \dot{\epsilon}_3^p = 2\,\frac{\partial Q}{\partial \sigma_d}\,\phi \qquad (3.41)$$

Using the same assumption of $\dot{\epsilon}_t = \dot{\epsilon}_e + \dot{\epsilon}^p = 0$ and the elasticity relations for an isotropic material in plane the negative change (relaxation) in the dynamic yield function is controlled by the σ_d, σ_T as follows ;

$$\dot{\sigma}_d = (-)\sqrt{\left(\frac{\dot{\sigma}_x-\dot{\sigma}_y}{2}\right)^2 + \dot{\tau}_{xy}^2} = (-)\,\frac{E}{1+\nu}\dot{\epsilon}_d^p = (-)\,\frac{1}{2}\frac{E}{1+\nu}\frac{\partial Q}{\partial \sigma_d}\,\phi \qquad (3.42)$$

$$\dot{\sigma}_T = \dot{\sigma}_1+\dot{\sigma}_3 = (-)\,\frac{E}{(1+\nu)\,(1-2\nu)}\dot{\epsilon}_T^p = (-)\,2\frac{E}{(1+\nu)\,(1-2\nu)}\frac{\partial Q}{\partial \sigma_T}\,\phi \qquad (3.43)$$

And proceeding in the same way as equation 3.37 the critical time limit Δt_{crit} for oscillatory stable response is given by;

$$\Delta t_{crit} = \frac{2\,(1+\nu)\,(1-2\nu)}{\frac{\partial \phi}{\partial F}\,E\left(\frac{1}{2}\frac{\partial F}{\partial \sigma_d}\frac{\partial Q}{\partial \sigma_d}\,(1-2\nu) + 2\,\frac{\partial F}{\partial \sigma_T}\frac{\partial Q}{\partial \sigma_T}\right)} \qquad (3.44)$$

where $\sigma_T=\sigma_1+\sigma_3$ and the differential stress $\sigma_d=|\sigma_1-\sigma_3|/2$. Considering Mohr-coulomb yield function ,

$$F = |\sigma_1-\sigma_3| + (\sigma_1+\sigma_3)\sin\psi - const. \qquad (3.45)$$

where ψ is the angle of internal friction , and considering a plastic potential in a similar form ;

$$Q = |\sigma_1-\sigma_2| + (\sigma_1+\sigma_2)\sin\alpha - const = 0.0 \qquad (3.46)$$

where α here is the dilation angle . In this case ;

$$\frac{\partial F}{\partial \sigma_d}=2 \quad , \quad \frac{\partial Q}{\partial \sigma_d}=2$$

$$\frac{\partial F}{\partial \sigma_T}=\sin\psi \quad , \quad \frac{\partial Q}{\partial \sigma_T}=\sin\alpha$$

Substituting in equation 3.44 we reach the same expression found in reference [17] for Δt_{max} ;

$$\Delta t_{crit} = \frac{(1+\nu)\ (1-2\nu)}{2\ \frac{\partial \phi}{\partial F}\ E\ (1-2\nu+\sin\psi\sin\alpha)} \qquad (3.47)$$

In the derivation of equation 3.37 or 3.44 it is assumed that $\Delta\epsilon=0.0$ meaning a full relaxation caused by the yielding at the most critical point which is on the safe side . When $\Delta\epsilon \neq 0.0$ the numerical stability becomes less critical and higher limits for Δt_{max} can be used . For example in case of constant stress creep experiment where $\Delta\epsilon = \Delta\epsilon_{vp}$ Δt is not limited by equation 3.37 or 3.44.

The strain hardening affects the accuracy of the solution but not the numerical stability. In order to take the effect of

strain hardening or softening in the equation $\dot{\phi} = -\eta\,\phi$ where $\Delta t_{max}=1/\eta$ and noting that $\frac{\partial \phi}{\partial \epsilon_{vp}} \cdot \dot{\epsilon}_{vp} = \left(\frac{\partial \phi}{\partial \epsilon_{vp_{ij}}} \cdot \frac{\partial Q}{\partial \sigma_{ij}} \right) \phi$ and equation 3.28 is rewritten as follows:

$$\dot{\phi} = -\eta\,\phi = -\left(\eta_1 - \frac{\partial \phi}{\partial \epsilon_{vp}} \cdot \frac{\partial Q}{\partial \sigma_{ij}} \right) \phi \qquad \ldots \quad (3.48)$$

where η_1 is given by equation 3.36 when the yield function is dependent on $\bar{\sigma}, J_1$. And when the plastic flow is in the plane of maximum and minimum principal stresses and if the strain hardening or softening variables are ϵ^I_d and ϵ^I_T which are the allowable plastic strain parameters for isotropic hardening;

$$\dot{\phi} = -\left(\eta_1 - \frac{1}{2} \frac{\partial \phi}{\partial \epsilon^I_d} \frac{\partial Q}{\partial \sigma_d} - 2 \frac{\partial \phi}{\partial \epsilon^I_T} \frac{\partial Q}{\partial \sigma_T} \right) \phi \qquad (3.49)$$

where;

$$\eta_1 = \frac{\frac{\partial \phi}{\partial F} E}{(1+\nu)\,(1-2\nu)} \left(\frac{1}{2} (1-2\nu) \frac{\partial F}{\partial \sigma_d} \frac{\partial Q}{\partial \sigma_d} + 2 \frac{\partial F}{\partial \sigma_T} \frac{\partial Q}{\partial \sigma_T} \right) \qquad (3.50)$$

In the above equations if ϵ^I_d and ϵ^I_v or ϵ^I_T appear in F rather than ϕ : $\frac{\partial \phi}{\partial \epsilon^I_d} = \frac{\partial \phi}{\partial F} \frac{\partial F}{\partial \epsilon^I_d}$ and $\frac{\partial \phi}{\partial \epsilon^I_v} = \frac{\partial \phi}{\partial F} \frac{\partial F}{\partial \epsilon^I_v}$ with strain harding η increases but with strain softening η decreases and Δt_{max} increases. Using the same approach the work hardening can also be considered in Δt_{max}.

However in both cases for early stages of primary creep giving considerable hardening the accuracy of the solution has to be considered especially for low values of E (soft rock and soil-like materials, see equation 3.44) like examples 1,2 in Section 4.4

The preceding form of Δt is simplified and easy to program

especially in the 3 dimensional state of stress. If the yield function or the plastic potential are anisotropic like equation 2.31 or contains the effect of J_{3D}, the general form given in reference [17] should be used :

$$\Delta t_{max} = \frac{1}{\frac{\partial \Phi}{\partial F}(H_e + H_p)} \quad \ldots\ldots \quad (3.51)$$

where $H_e = (\partial F/\partial \sigma) D (\partial Q/\partial \sigma)$ H_p is a viscoplastic strain hardening parameter (see reference [17]).

It has to be noted that effect of the assumed relaxation in the deviatoric stress increment during Δt_{max} is considerably higher than the volumetric one . The simplicity of considering only the deviatoric part may justify using a simplified form of Δt_{max} in case of complicated forms of yield functions and plastic potentials as a factor of Δt_{crit} is used.

Another limit on numerical stability is imposed by the numerical integration itself. Transferring the relaxation stress increments from each integration point within an element to nodal forces and the vice versa with the nodal displacements (after solving) to get the redistributed stresses (equation 3.13) , is based on a linearized process which imposes a limit on Δt for the explicit as well as the implicit scheme especially when the change of the internal stresses (and hence the viscous relaxation rate) are high within relatively big elements.

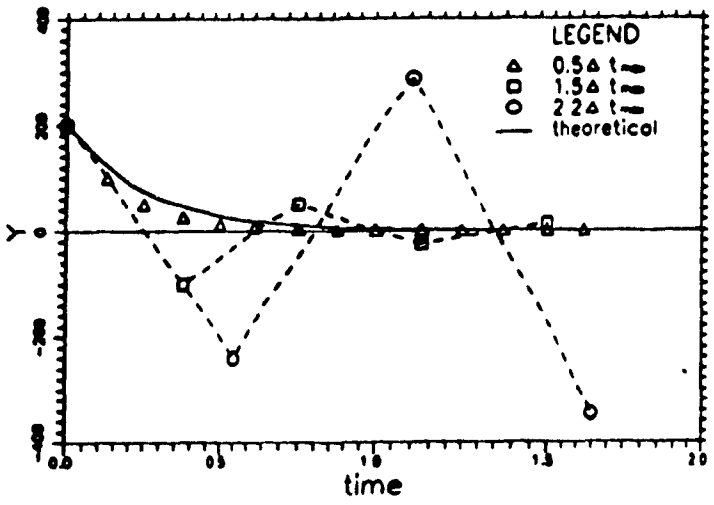

Numerical prediction for $\frac{dy}{dt} = -\eta y$ using the explicit scheme

(Figure 3.3)[17]

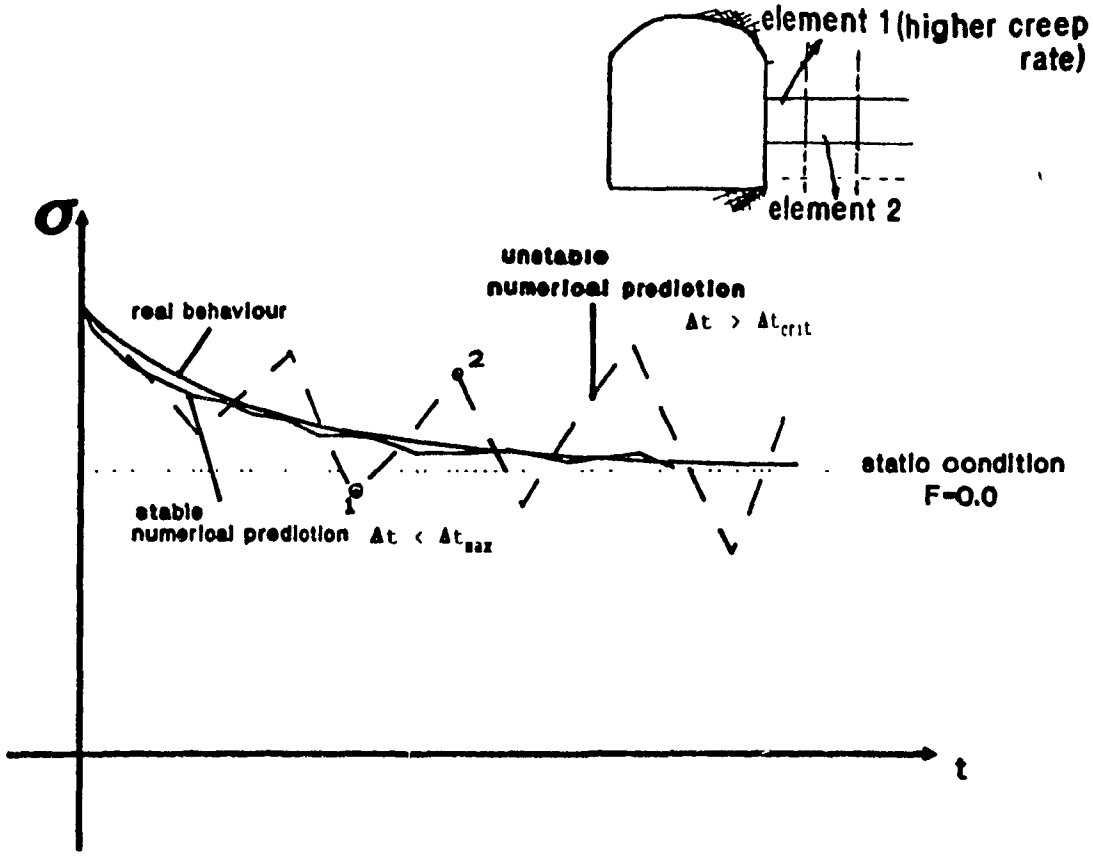

The effect of the time increment on numerical stability
(Figure 3.4)

CHAPTER 4

USER'S GUIDE TO COMPUTER PROGRAM

4.1 INTRODUCTION

The input data of the program **VISA2D** goes in parallel with the elasto-viscoplastic analysis to be performed. The program starts by reading the necessary data for the elastic analysis so that the user may examine first the elastic response without having to enter data for viscoplastic analysis. So the major part of the input file (file.VSC) includes data like nodal coordinates , degrees of freedom , element connectivities, elastic properties of materials, distribution of initial stresses σ_0 and initially applied loads. This part is generated using the preprocessor program **PRESAP**. It reads a free format file (file.dat) and generates the first part of (file.vsc). The same data file can be used for viscoplastic analysis by adding a few more data cards as described in Section 4.3. If an input error is detected, the program stops giving the user an error message to rectify the error. The program can then be resta-ted from where this mistake occurred and the previous analysis is not lost. The program is assisted by three graphical programs to check the input files and to illustrate the output as will be explained later. In Section 4.4, the model verification and two

examples are demonstrated.

4.2 DESCRIPTION OF INPUT DATA FOR ELASTIC ANALYSIS

In this Section, the input data required for the computer program is described. Inputting the data is usually time consuming and also requires considerable effort for error checking if the user is not assisted by a preprocessor. The user writes a simplified free format data file (file.dat) configuring the problem layout as zones of different material properties, grid density and simulating the openings and possible mining sequence. First, the user runs a graphics program called **ZONE** to view the problem layout (zones and opening) on the computer screen. Program **PRESAP** reads this user-written file (file.dat) and generates the finite element grid with the required mesh density and grading for each zone and specifying openings and different rock types to the computer program in file (file.vsc).

In the following the sequence of input data(file.dat) to the mesh generator **PRESAP** is given. The use of the program is demonstrated through numerical examples in Section 4.4 This program generates the output file of program **SAP2D** for which LL=1 and NPROB = 1 is also the first section of the input file (file.vsc).

Card 1. Heading card

TITLE The master heading information for use in labelling the output

CARD 2. Control card for finite element mesh generation

NZNP	Number of zone nodal points
NVZONE	Number of non-void zones
NSPAN1	Number of spans in ξ direction
NSPAN2	Number of spans in η direction
NPROB	Number of subproblems simulating a mining sequence. (Enter 1). For mining sequence in viscoplastic analysis, see Section 4.3
NFOLD	= 1 if mesh is fanning = 0 if mesh is rectangular
ANGLE	Angle between gravity and x axis (measured according to the X-Y axis used)

Card 3. Subdivision of zones in ξ direction

NSBDV1(NSPAN1)	Array defining the number of subdivisions in ξ direction. (see Figure 4.1,4.2)

Card 4. Subdivision of zones in η direction

NSBDV1(NSPAN1)	Array defining the number of subdevisions in η direction. (see Figure 4.1,4.2)

CARD 5. Data of zone nodal points (NZNP cards)

N	Node number
NCODZP(N)	code for degrees of freedom (DOF) at the node = 0 , both X and Y DOF are free

= 1 ,X fixed and Y free
= 2 ,X free and Y fixed
= 3 ,both X and Y DOF are fixed

XZP(N)	X coordinate
YZP(N)	Y coordinate

CARD 6. Data of zone node numbers and boundary loading

(NVZONE cards + loading cards)

a) Nodes

N	Zone number
IZ(8,N)	Node number defining the zone ; see Fig. 4.3 for order or sequence
MATZ(N)	Material number associated with zone N.
NCUTZ(N)	Cut number associated with this zone of elements. NCUTZ(N) is compared with NCOUNT entered in card 6 of Section 4.3 (for each time station) If NCUTZ(N) = 0 the elements are cut in the elastic analysis.
NUMPC	Number of sides subjected to surface loading.(0 to 4)

b) Loads - NUMPC cards (If NUMPC=0 , skip this card)

NSIDE	Side number (=1, 2, 3 or 4); see Fig. 4.4 for details.
P1	Pressure at the first node
P2	Pressure at the second node
S1	Shear at the first node

S2	Shear at the second node

CARD 7. Control card for finite element analysis

NBE	Boundary elements (=0 **here**)
LL	Number of load cases (= 1 **here**)
NPRNT(1)	=1 to print input data
	=0 otherwise
NPRNT(2)	=1 to print nodal displacements
	=0 otherwise
NPRNT(3)	=1 to print stresses
	=0 otherwise
NRES	=1 to include initial stresses;
	=0 otherwise
ICONC	=1 to include concentrated forces;
	=0 otherwise
SCALE	Geometric scale factor to be multiplied by
	X and Y co-ordinates of points
NUMMAT	Number of materials used
NSTR	=0, axisymmetric analysis
	=1, plane starin analysis

CARD 8. Data of materials used (NUMMAT * 2 cards)

(a) Material Classification

M	Material number
WT (M)	Weight per unit volume
ISO (M)	=1, isotropic material

=2, anisotropic material (elastic analysis only)

(b) Isotropic material properties (If ISO (M)=2, skip this card)

E	Young's modulus of elasticity
R	Poisson's Ratio

CARD 9. Initial stress data (If NRES = 0 skip this card)

AINIT(8) Array defining 8 coefficients to be used for the calculation of initial stresses σ_{ox} , σ_{oy}, σ_{oz}, τ_{oxy} respectively as linear functions of Y. Each stress component requires two coefficients a, b

such that $\sigma = a + b\ Y$

For the case of initial stresses developed in a plane strain condition ;

$\sigma_{oz}=\nu\ (\ \sigma_{ox} + \sigma_{oy})$

For the case of initial hydrostatic state; $\sigma_{ox} = \sigma_{oy} = \sigma_{oz}$. In an axisymmetric problem σ_r replaces x , z replaces y and σ_θ replaces σ_z

CARD 10 Concentrated loads - any number of cards ending with a blank card

If ICONC = 0, skip this card group

N	Node number
L	Load case (=1 **here**)
FX(L,N)	Force in X-direction at N for load case L

FY(L,N) Force in Y-direction at N for load case L

CARD 11. Force multipliers used by MSAP2D for each load case. (Put any 5 numbers separated by spaces here. These will not be used in program VISA2D)

The input data generated by **PRESAP** represents, in case of a dense mesh, about 95% the size of (file.vsc) which can be checked graphically by program MESH2D. This graphical program shows the finite element grid with node numbering and elements connectivity. Because some of the input data of Section 4.3 might be linked to specific elements or node numbers of the actual finite element grid, it became convenient to generate the finite element grid first in (file.vsc) (based on file.dat) then the user (after checking it) proceeds to the viscoplastic analysis by appending a free-format viscoplastic input data to file.vsc. Any reference to elements or nodes would then be possible (a zoomed-in plot of the grid as in Figure 4.9 is useful).

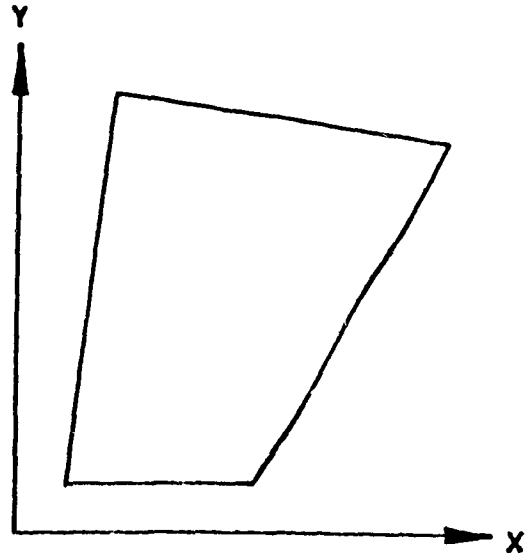

(a) Physical domain

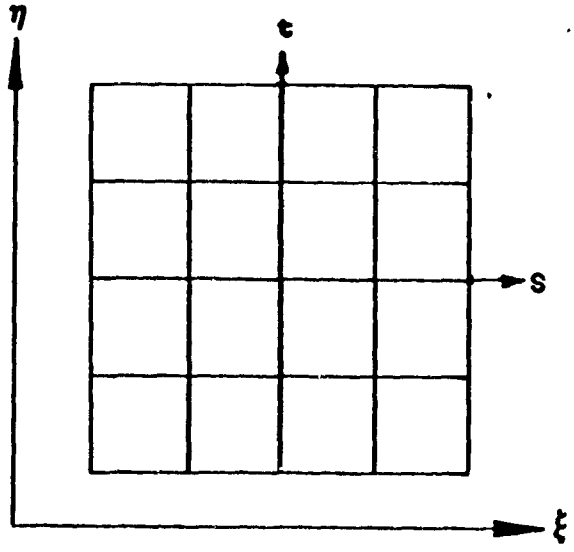

(b) Key diagram
&Mesh discretizing

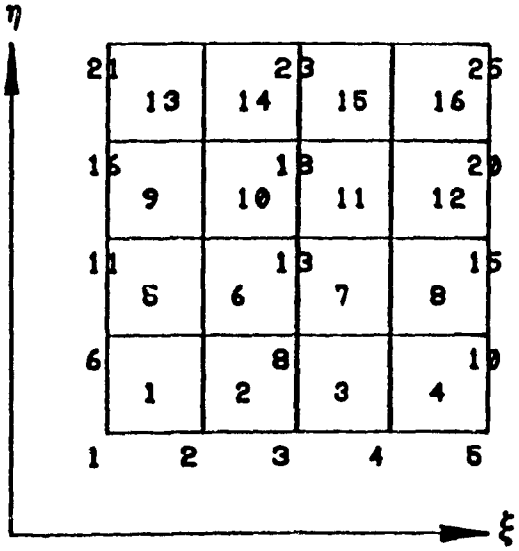

(c) Node and element numbering

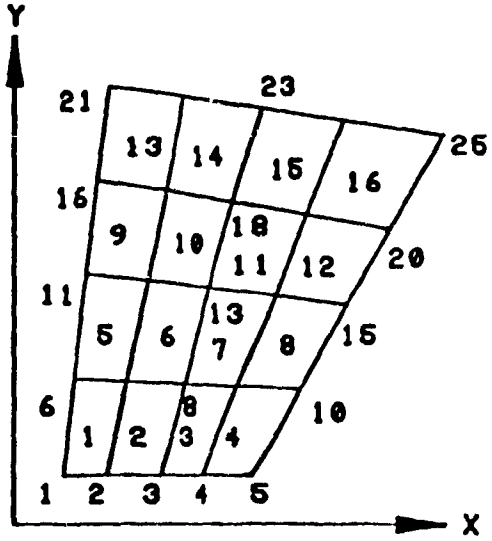

(d) Physical domain after being discretized

Mesh generation scheme
(Figure 4.1)

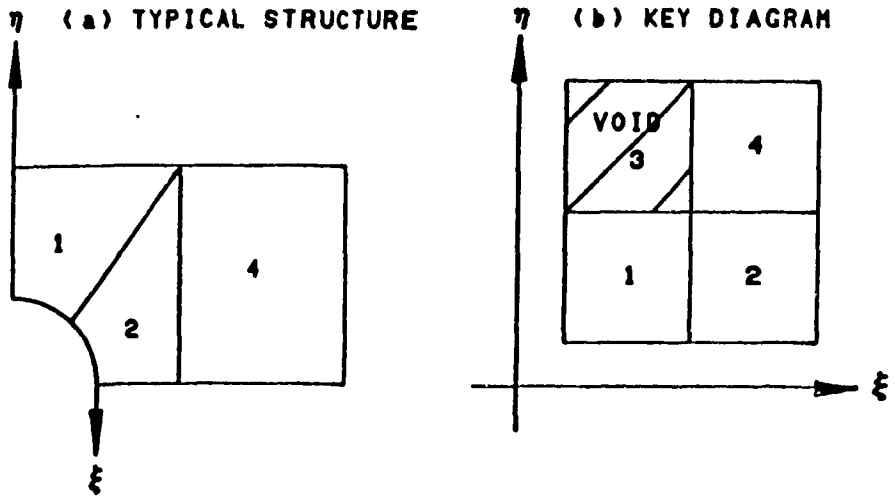

Mapping a typical structure to a key diagram
(Figure 4.2)

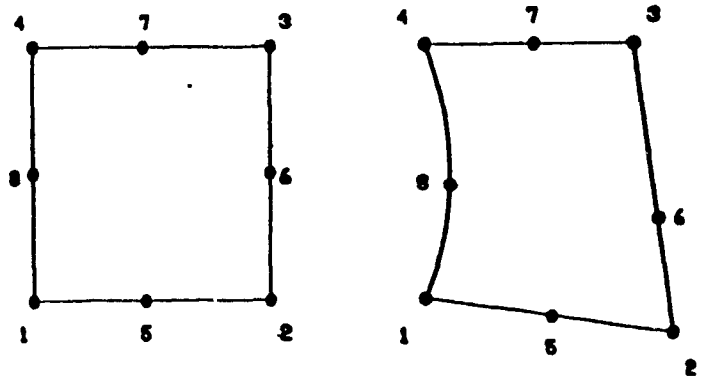

Model zones
(Figure 4.3)

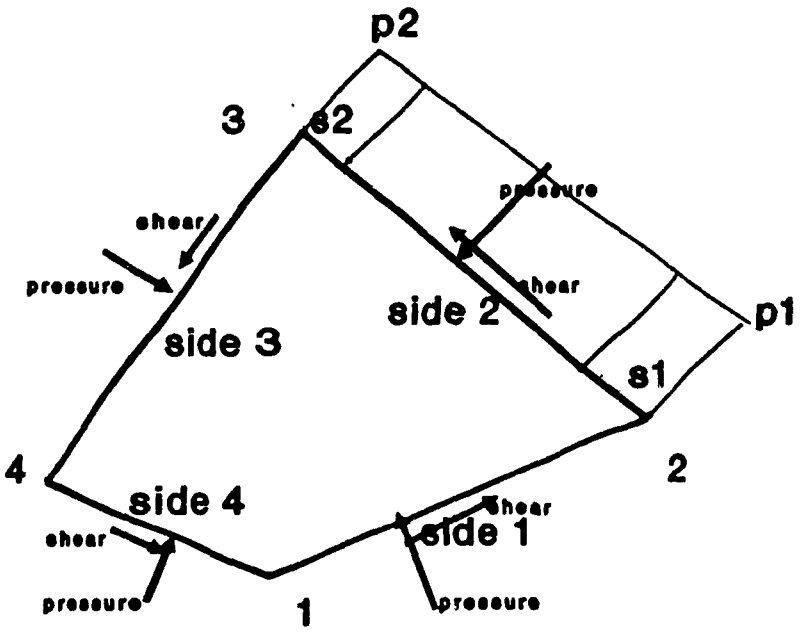

Positive sign directions of surface loading (load/unit area) acting at element or zone sides
(Figure 4.4)

4.3 VISCOPLASTIC INPUT DATA

This Section describes the simple free format input file of the viscoplastic data written directly to the input file (file.vsc) (see Appendix) after the formatted data has been generated by PRESAP.

CARD 1 WHAT TO DO AFTER SOLVING FOR THE ELASTIC RESPONSE

STATUS END or STOP[2] :The program stops after the elastic analysis. or;

CONT :The program proceeds to time dependent analysis or;

OUP&CONT :The program proceeds to time dependent analysis after generating output files.

or;

VISCO : The program uses viscoplasticity to obtain elastoplastic response.

CARD 2 SOME UNITS USED TO CONVERT THE CONSTANTS USED BY THE PROGRAM AS LOWER LIMITS INSTEAD OF AN ABSOLUTE ZERO FOR THE ASYMPTOTIC CONVERGING EXPRESSIONS

STUN The stress unit expressed in MPa (for checking the yield function against .005 MPa)

FUN The force unit expressed in Mega-Newtons;1E+6 N.

TMUN The time unit of the creep strain rate ϕ $[time]^{-1}$ expressed in seconds . This is used through the time dependent analysis and is not important if card 1 is entered as VISCO.

Example: if Young's modulus (E) and stresses are in psi → STUN=1/145, FUN=9.81/2.21/10e+6 and if ϕ is strain per day enter TMUN=24*60*60=86400 .

MXTR The maximum number of time increments after which the program gives the maximum yield function and asks the user whether to stop or to continue .

NOTR The number of iterations per time increment Δt which is effective from t=0.0 to t_f

NOTR = 1 → fully explicit and faster

NOTR > 1 → Iterative explicit with higher accuracy. (use 2 or 3..)

TMMUL A factor multiplied by Δt_{max} (given by Equation 3.37 or 3.44) which is effective only from t=0.0 to t_f. Normally put this factor = 1.0 unless higher accuracy is required for primary creep of rock with low Young's modulus E (see example 1 in section 4.4).

CARD 3 Viscoplastic properties of material number MAT

MAT Material number for which the following data is entered

TENS(MAT) The tensile resistance of this material (use a high tensile resistance if not interested in tension checking and relief)

NY(MAT) A number corresponding to the type of yield

function and plastic potential used and in some cases the creep law as well

NY(MAT)=1 → Mohr-Coulomb Equation 2.4a and as a plastic potential without strain hardening($Y_1=Y_o$).

NY(MAT)=2 → Drucker-Prager Equation 2.4b and as a plastic potential without strain hardening($Y_2=Y_o$)

NY(MAT)=3→10 are planned to point to other common types of yield functions .

NY(MAT)=11 → Tresca Equation 4.4 is used (case of the axisymmetric analysis of example 2) with Y_1=0.0 and is used also as a plastic potential. At the same time it directs the execution to Equation 4.4 as a constitutive law.

NCR(MAT) A number pointing to a creep law from a library of creep laws (When NY(MAT) > 10, it directs the execution to the creep law as well)

NCR(MAT)=1 → ϕ is given by equation 2.26a (time hardening)

NCR(MAT)=2 → ϕ= F for time independent plasticity

NCR(MAT)=3 → ϕ is given by equation 2.26c (strain hardening)

CARD 4 This might be one or two cards (lines) giving the constants of the forms of yield function, plastic potential, and creep law assigned to this material type (by NY(MAT) ,NCR(MAT)).

When NY(MAT)=11 (example 2) Card 4 is two lines the first

contains α_1 , Y_{10} of equation 2.4a and the second contains the constants of equation 4.1 In example 3 of Section 4.4, NY(MAT) is entered 2 and card 4 is one line containing α_1, Y_{10} (see Appendix) while NCR(MAT)=2 implies no input.

Cards 3,4 should be repeated until MAT in card 3 is input as 0 at which the program jumps to card 6 with materials not specified remaining elastic through the viscoplastic analysis.

Decision : If card 1 is specified as VISC, the program jumps to card 5'.

The following cards are entered for each time station t_f , t_{ff},etc. In the following t_0=0.0 is assumed as the current time station and t_f is the coming time station (see Figure 3.1).

CARD 5 This is a blank card serving as a separator between cards of successive time stations (see Appendix).

CARD 6 :

NCOUNT This is a number associated with the current time station t_f . It is entered such that when compared with the cut number of each element $NCUT_i$, which is basically that of its zone (see Section 4.2 card 6), determines if the element is to be cut or to remain active according to the following relation:

$NCUT_i \leq NCOUNT$ → the element is cut

$NCUT_i > NCOUNT$ → the element is active

CARD 7:

tf — The time (t_f) at which the changes occur (Fig. 3.1)

UNIT — A character variable defining the time unit used to enter t_f and should be one of the following:

'SE' → t_f is in seconds

'MI' → t_f is in minutes

'HR' → t_f is in hours

'DA' → t_f is in days

'WE' → t_f is in weeks

'MO' → t_f is in months

'YE' → t_f is in years

NOTR — The number of iterations per time increment Δt which becomes effective from t_f to t_{ff}

NOTR = 1 → fully explicit and faster

NOTR > 1 → Iterative explicit with higher accuracy.(put =2 or 3 or 4)

TMMUL — A factor multiplied by Δt_{max} given by Equation 3.37 or 3.44 which will become effective only from t_f to t_{ff}. Normally put this factor = 1.0 unless higher accuracy is required for primary creep of rock with low Young's modulus E (see example 1 in section 4.4).

NCUYN — Indicator to the program to reconstruct the global stiffness matrix in case of excavation sequence. Use NCUYN = 1 if the relation of card

6, which is checked for each element, will result in some elements (active before tf) to become cut at this time or if card 8 is used to specify a range of element numbers to be cut at this time. Otherwise enter NCUYN = 0 . This is important because the program will not spend time in reconstructing the stiffness matrix and getting its triangular decomposed form unless NCUYN = 1 or the first occurence of card 9 ≠ 0 (i.e case of backfilling)

After reading card 7 the execution proceeds for viscoplastic analysis and adds time increments till when $t=t_f$ at which ;

If NCUYN = 1 it reads card 8, otherwise it jumps to card 9.

CARD 8 In this card, a range of elements are implicitly specified as cut by changing their cut number.

MCTi the first element in the range MCTi:MCTj

MCTj the last element in the range MCTi:MCTj

NCUT the cut number of the range of elements MCTi:MCTj

For example if NCOUNT = 3 (see card 6) , specify NCUT = 3 for these elements to be excavated at t_f and remain cut afterwards.

This card should be repeated for different ranges of elements untill MCTi is entered 0.

For example if NCUYN=1 and the cut sequence of card 6 in Section 4.2 is sufficient for excavation steps put 0 in the

first occurence of this card.(see Appendix).

CARD 9 In this card a range of elements are specified to to be filled.

MFli	the first element in the range MFLi:MFLj
MFLj	the last element in the range MFLi:MFLj
MAT	the material number of the backfill in the elements range MFLi:MFLj

This card should be repeated for different ranges of elements backfilled at t_f untill MFLi is entered as 0. For example if there is no backfill at t_f put 0 in the first occurence of this card.(see Appendix). If at the current time station a group of elements M_1:M_2 are <u>cut and filled</u>, this card would be enough.

CARD 10 Nodal loads added at this time station

INO	node number at which the added nodal load is applied
Rx	X component of the point load
Ry	Y component of the point load

This card should be repeated till it is entered as 0 .(see Appendix).

CARD 11 This card describes the <u>added</u> <u>surface</u> loads at one or more sides of element M.

M	element number (a non cut element)
NPRSD	number of sides subjected o pressure or shear.

The following should be repeated NPRSD times (in the same

line).

k Side number (see Figure 4.4)

P1(k) pressure at node 1 of this side

P2(k) pressure at node 2 of this side

S1(k) shear at node 1 of this side

S2(k) shear at node 2 of this side see Figure 4.4

This card (card 11) should be repeated until M is entered 0

After reading card(s) 11, the program applies the instantaneous changes at (t_f) and computes the displacements as described in Section 3.3 (Equation 3.24 or 3.25or 3.26), then it reads the following card to know what to do next.

CARD 12 what to do next ?

STATUS STOP[1] → the program stops

or

OUP&CONT → the program reads card 5,6,7 mainly to identify the next time station (say t_{ff}). It updates the stresses, viscoplastic strain rate due to changes at t_f and produces output (Segment 2 in Section 3.2) then continues the viscoplastic analysis till arriving at $t=t_{ff}$ where it reads cards 8,9,10,11 of t_{ff} and so on. Note that t_{ff} should be $\geq t_f$

or

CONT → the same as above except no output is generated at t_f.

The program stops when card 12 is entered as STOP[1]. If an error in the input file is encountered, the program stops after identifying the line of input error. Once the input data is corrected the program restarts the reading from that line and the previous analysis is not lost.

The following cards are related to the case of time <u>independent</u> analysis and entered after card 4;

CARD 5/ ;

NINCR The number of increments required to simulate the incremental plasticity by the theory of viscoplasticity (see Subsection 3.2.2 and Figure 2.9).

CARD 6/, 7/ If the user is not interested in creep behavior after the nonlinear (short term) behavior he/she simply puts card 6/ as 0 and skips card 7/. The two cards are the same as cards 3 and 4, and they are used to input yield functions and creep laws of materials which will exhibit time dependent behaviour after the elastoplastic analysis.

---

2 Whenever STOP or END is read the program updates the stresses, viscoplastic strain rate and total displacements. It produces output and stores the data necessary for continuing the same analysis later (after asking the user if he wants so.

4.4 MODEL VERIFICATION AND ILLUSTRATIVE EXAMPLES

4.4.1 INTRODUCTION:

In this chapter a comparison between the model prediction and an analytical solution, which may be viewed as a way to verify the model, is presented. Two other examples are used to illustrate the use of the program to model cut sequence and its use to model the elastoplastic behaviour using the theory of elasto-viscoplasticity.

4.4.2 EXAMPLE 1: (MODEL VERIFICATION)

In the following, a comparison between the numerical model predictions and the analytical solution derived by Sulem et al. [14] is presented. The solution derived is for an axisymmetric problem involving a circular tunnel opening of radius r_0 in a hydrostatic ground stress field σ_0. Assuming that the rate of creep or the total creep strain to be linearly proportional with $(\sigma_\theta - \sigma_r)$, i.e.

$$-\epsilon_{r\,vp} = (\sigma_\theta - \sigma_r) \cdot \frac{f(t)}{A} = \epsilon_{\theta\,vp} \qquad (4.1)$$

it was shown that,

$$\sigma_r = \sigma_0 \left[1 - \lambda \left(\frac{r_0}{r}\right)^2\right] , \quad \sigma_\theta = \sigma_0 \left[1 + \lambda \left(\frac{r_0}{r}\right)^2\right] \qquad (4.2)$$

and

$$\frac{u}{r} = \frac{2\lambda\sigma_0}{A} \cdot f(t) \cdot \left(\frac{r_0}{r}\right)^2 + \frac{\lambda\sigma_0}{2G}\left(\frac{r_0}{r}\right)^2 \qquad (4.3)$$

where $\lambda = 1$ when neglecting the face advance effect, A is a constant and G is the shear modulus of elasticity. In order to run the comparison of results, a finite element grid was constructed for the purpose of numerical modelling; see Figure 4.5 The following data has been used to generate the results shown in Figure 4.6:

$\sigma_0 = 2$ MPa, A = 256 MPa, E = 360 MPa, G = 150 MPa, $\nu = 0.2$,

$f(t) = 1 - [0.2/(0.2 + t)]^{0.3}$

$Q = F = \sigma_1 - \sigma_3$

and,

$$\dot{\varepsilon}_{vp} = 7.2308 \times 10^{-4} (t + 0.2)^{-1.3} \cdot F \cdot \frac{\partial F}{\partial \sigma_{ij}} \qquad (4.4)$$

The effect of θ, used in Equation 3.1 on the integration scheme is very significant at early stages of primary creep whereby a considerable time hardening takes place. A value of θ of (0.7 - 0.8) gives more accurate integration scheme than $\theta = 0.5$. The value of the stresses remained constant throughout the numerical time dependent analysis in agreement with Equation 4.2. This shows that for similar problems, an

iterative explicit time integration scheme is more effective than an implicit one, because the change of stress over Δt = 0.0 The time increment is limited by the hardening occurring from time t_n to t_{n+1}. In this example, a factor of 0.036 was multiplied by Δt given by Equation 3.44 used to maintain the accuracy of time hardening because E is low. The input data (axisym.dat and axisym.vsc) are provided in the Appendix.

4.4.3 EXAMPLE 2: THE USE OF CUT SEQUENCE TO SIMULATE FACE ADVANCE

To take the effect of the face advance in Equations 4.2, Sulem et al. [14] used a factor $\lambda(x)$ varying from 0 to 1 as the distance to the tunnel face (x) becomes longer. This assumes that the effect of face advance on the stresses and displacements can be separated from the effect of creep. However they cannot be separated, as the rate of creep is a direct function of the applied stresses which in turn depend on the face advance. Thus, instead of depending on this parameter to simulate the face advance one can use the program to analyze a section along the tunnel axis presented by the finite element grid shown in Figure 4.8. This is also an axisymmetric problem where a point is defined by $\underline{r}$, $\underline{z}$ in the plane of the finite element grid and similar planes rotating around the tunnel axis (in θ direction) should have the same properties (axisymmetric). Like above, the initial state of

stress is assumed hydrostatic and constant. Program **PRESAP** was used to generate the first part of file tunnel.vsc which is checked graphically as in Figure 4.9 and the viscoplastic part is written directly to tunnel.vsc (see Appendix) using a reminding comment at the end of each free format record. Curve 3 in Figure 4.6 represents a plot of the radial deformation with time when the cut sequences along the tunnel are considered as per Figure 4.8. The deformation is measured at point 1 and tunnel face advances at a rate of 1 m/day in intervals from 1 m (up to day 10) to 10 m. At each time station NCOUNT entered at card 6 of Section 4.3 is compared with the cut number of each element to cut the necessary elements (see Appendix). In Figure 4.9, the finite element grid has no openings, however, at t=0.0 (the initial elastic analysis) the elements having cut number =0 are cut to simulate an initial face advance of 1 meter. The viscoplastic analysis is conducted till t=1 day where no instantaneous changes are dictated so it just produces output and continues. But the following time station t_{ff}= 1 day also, so the program reads directly the associated changes , applies them produces output and continues creep till t_{faff} = 2 days and so on. Like that we have two outputs at t= 1 day one before the cut and another after it thus having the stepped response of curve 3 due to the sudden change in deformation rate following the start of each time interval accompanied by a cut sequence. Clearly, this modelling capability developed in the numerical

model results in a prediction that is more coherent with what may be observed in practice.

Figures 4.10,4.11 present the stress and deformation fields at different times where it may be noticed that the stress concentration in the longitudinal section at the corner of the tunnel face which increases with the creep relation of adjacent sections farther from the tunnel face. This means that this three dimensional stress concentration which is more critical than the prediction of the conventional plane strain analysis might cause premature failure at the tunnel walls immediately after the face advance. According to Figure 2.18, a strain hardening law is well suited to nonlinear creep behaviour like this case and should give better results than the time hardening creep law which is used here only for demonstrating some features of the present computer program.

4.4.4 EXAMPLE 3 ELASTOPLASTIC ANALYSIS

In this example, the computer program is used to Model the elastoplastic behaviour of a circular tunnel using the theory of elasto-viscoplasticity. The input file of the mesh generator (circular.dat) is attached in the Appendix. It is checked using the program **ZONE** as shown in Figure 4.12 which shows the super elements or zone diagram. The initial stresses $\sigma_h=\sigma_v=55$ MPA and E=40 GPa and $\nu=.2$. The finite element grid and elastic properties contained in the first

part of file circular.vsc generated by **PRESAP** is also checked graphically using program **MESH2D** as in Figure 4.13. The short free form viscoplastic part is appended to file circular.vsc. Mohr-Coulomb yield function is used as a plastic potential as well. In this case the viscoplastic strain rate is given function of the current state of stress as : $\dot{\epsilon}_{vp}=F(\partial F/\partial\sigma)$ where

$$F = |\sigma_1-\sigma_2| + .4\,(\sigma_1+\sigma_2) - 20 \qquad (4.5)$$

The fictitious time increments (Δt) are chosen according to Equation 3.44 . The load is divided to 20 steps (see Figure 2.19 and Equation 3.27) with a maximum of 100 time increments per load step except for the last one which ended after 125 time increment with F=.2 MPa.

Figures 4.14,4.15 present the stress , deformation fields after plastic yielding. Figure 4.16 illustrates the material behavior around the circular tunnel which in this case is only; either elastic or perfectly plastic because no strain hardening or softening variables were implemented in the yield function F or the viscoplastic rate law ϕ. The user can use the post processor to check the state of stress of Figure 4.15 using a failure criteria or another yield function as seen in Figure 4.17.

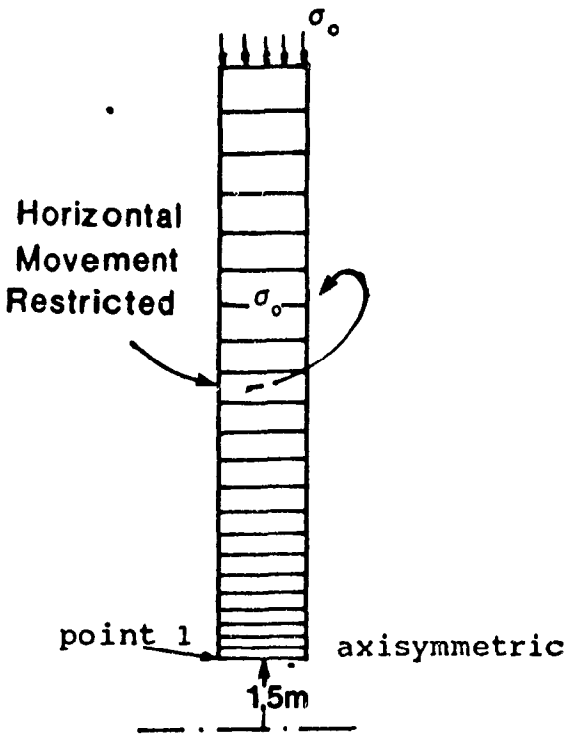

Finite element grid of example 1
(Figure 4.5)

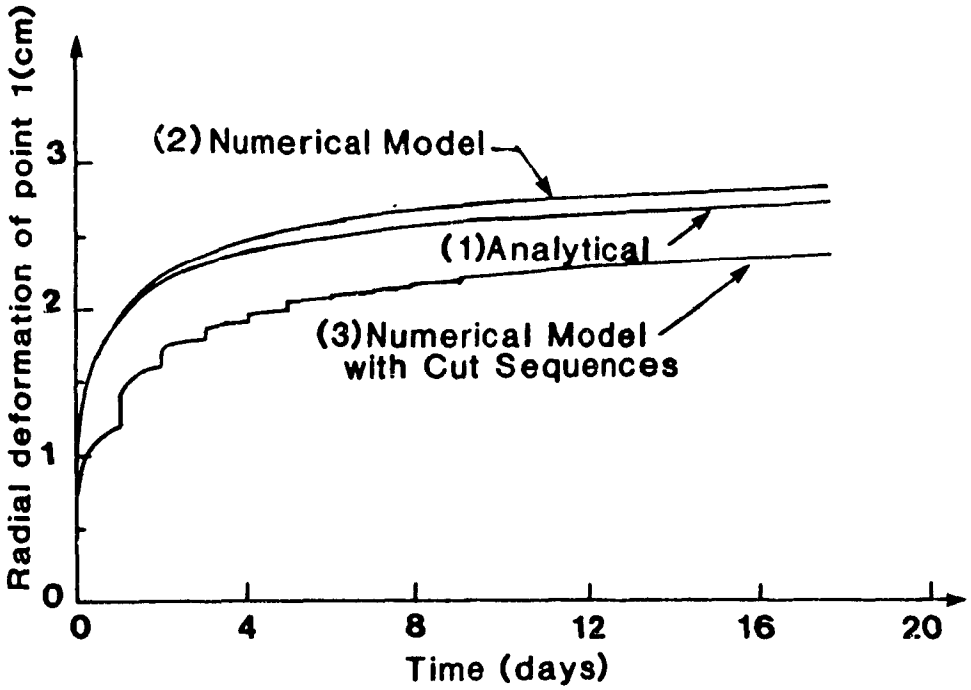

Comparison between numerical and
analytical results
(Figure 4.6)

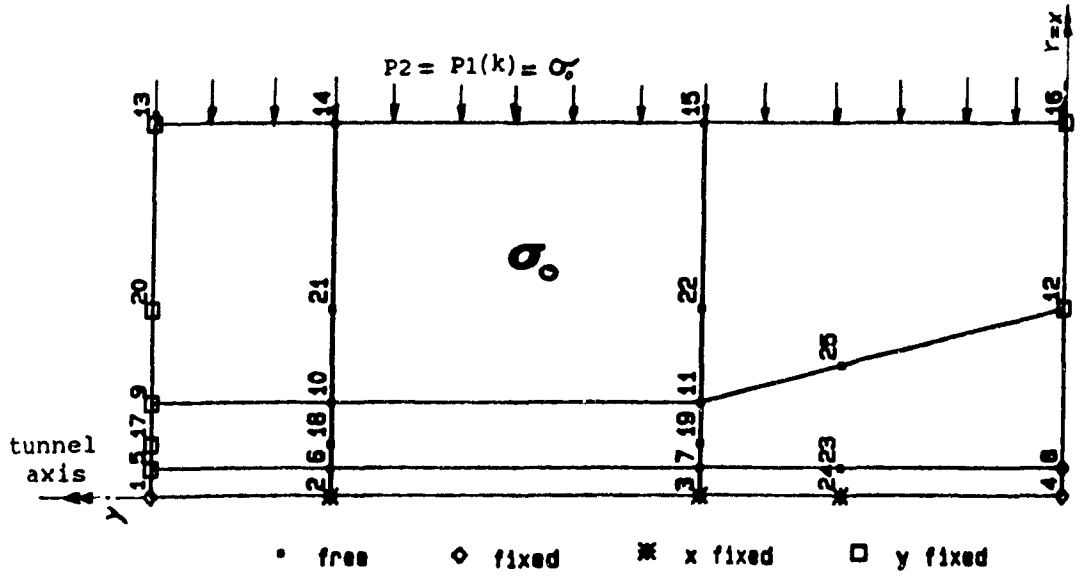

Zone diagram of example 2
(Figure 4.7)

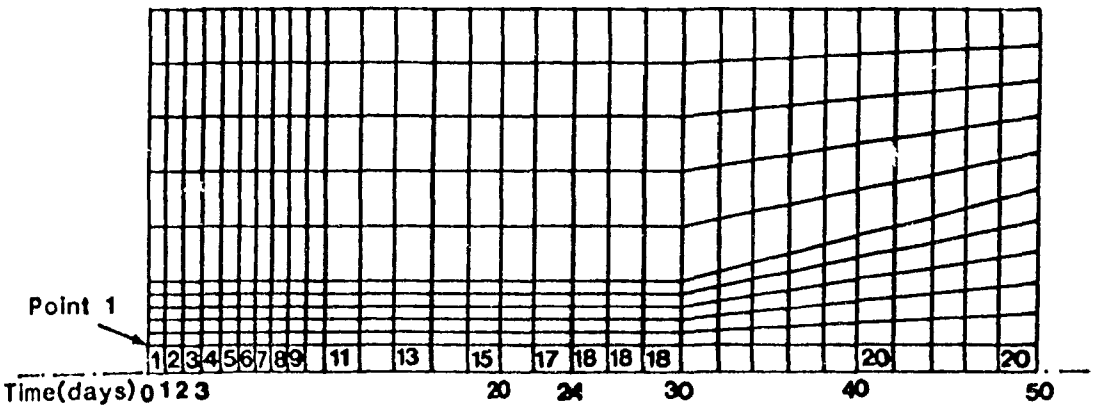

Cut sequences along the time scale (example 2)
(Figure 4.8)

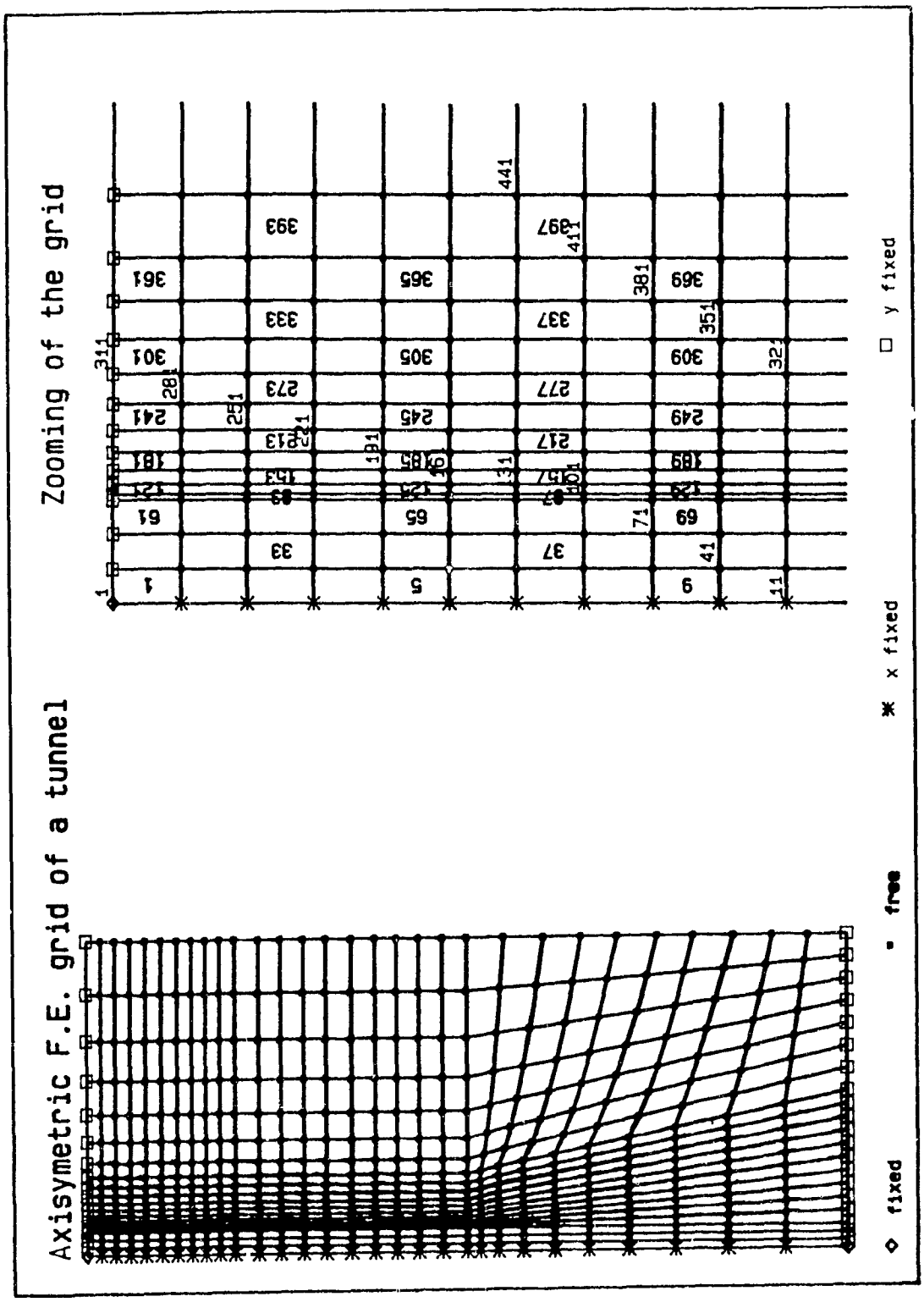

Finite element grid of example 2
(Figure 4.9)

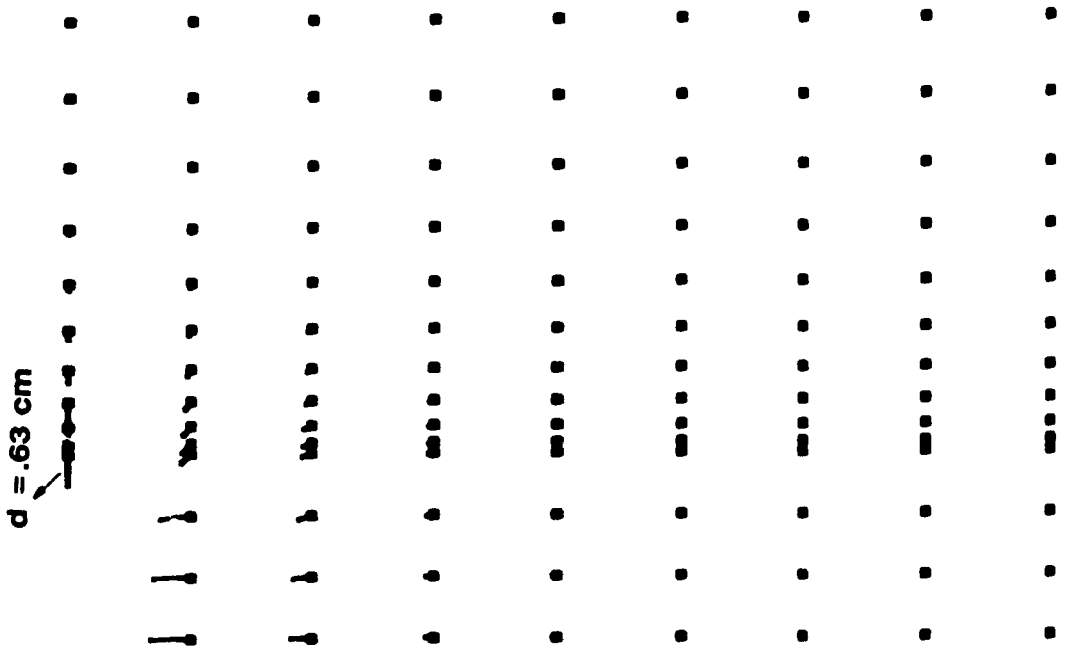

Displacements after blasting at t=0.0
(Figure 4.10a)

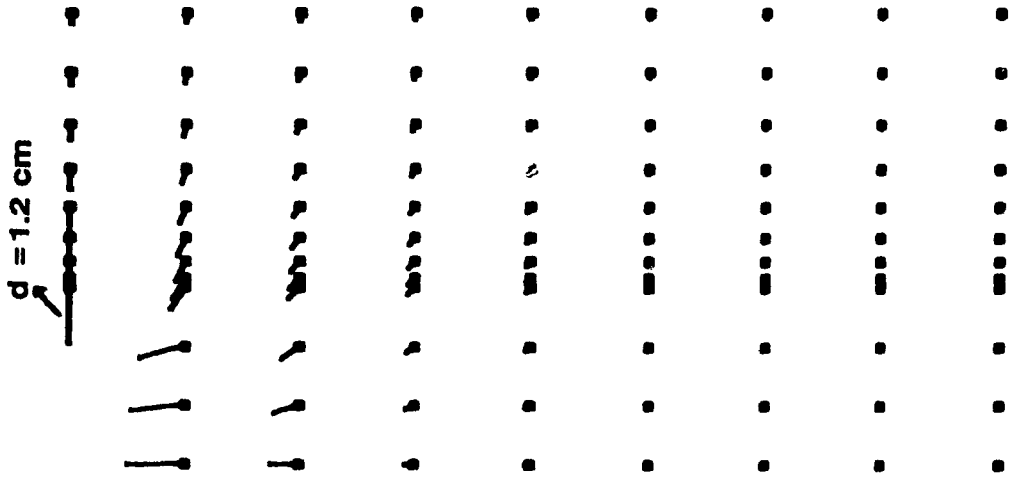

Displacements after one day creep
(Figure 4.10b)

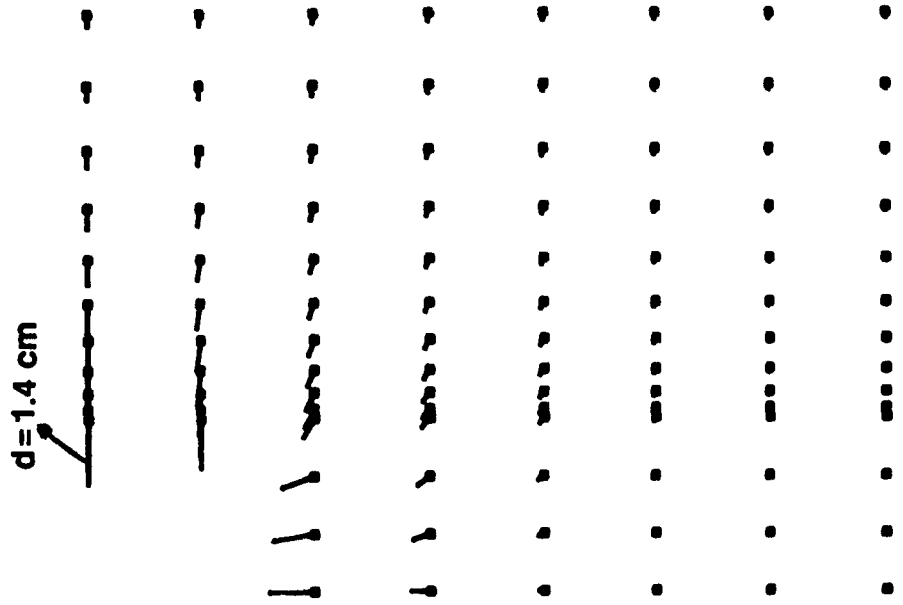

Displacements after cut at t=1 day
(Figure 4.10c)

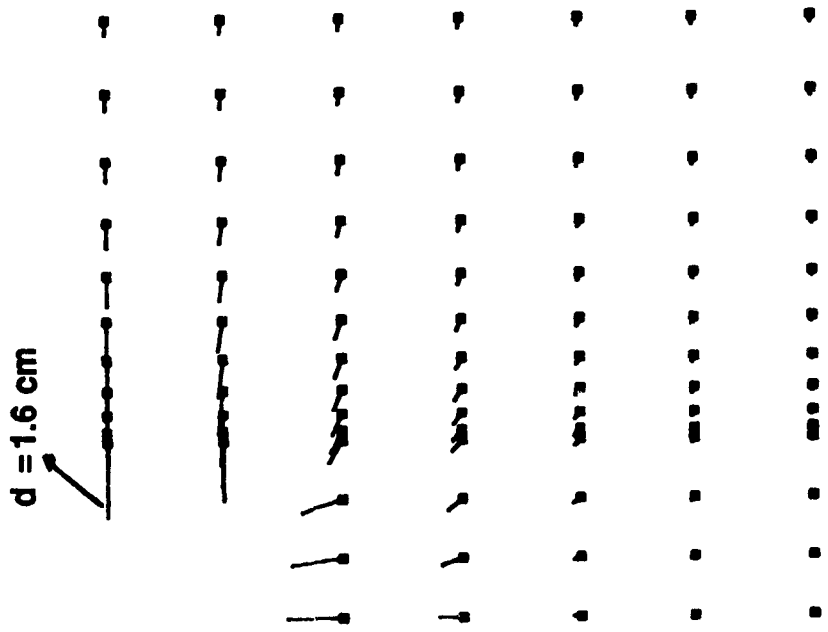

Displacements before cut at t=2 days
(Figure 4.10d)

e

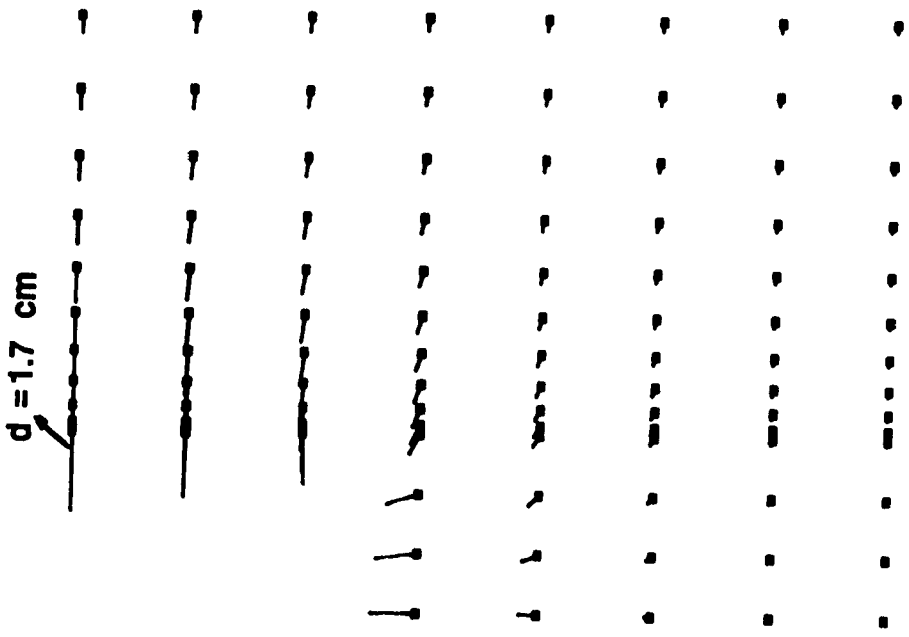

Displacements after cut at t=2 days
(Figure 4.10e)

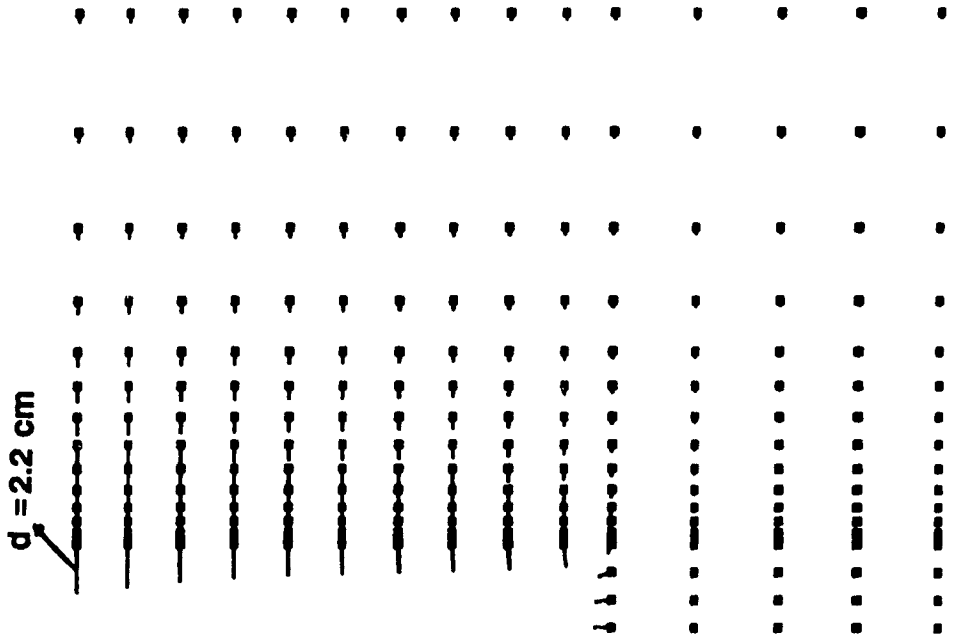

Displacements after cut at t=9 days
(Figure 4.10f)

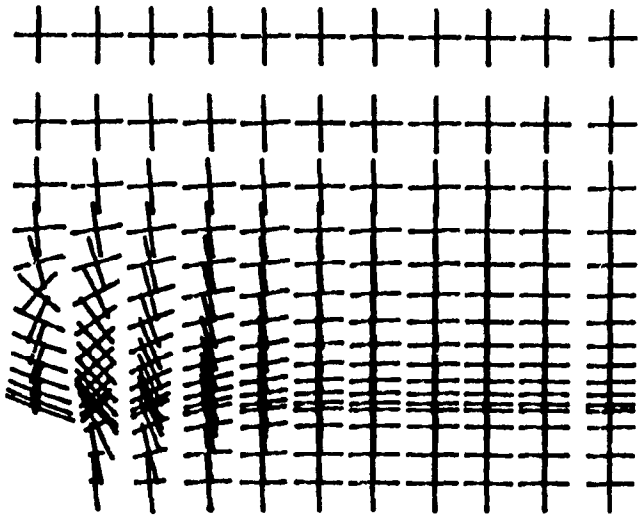

Principal stresses at time (0.0)
(Figure 4.10a)

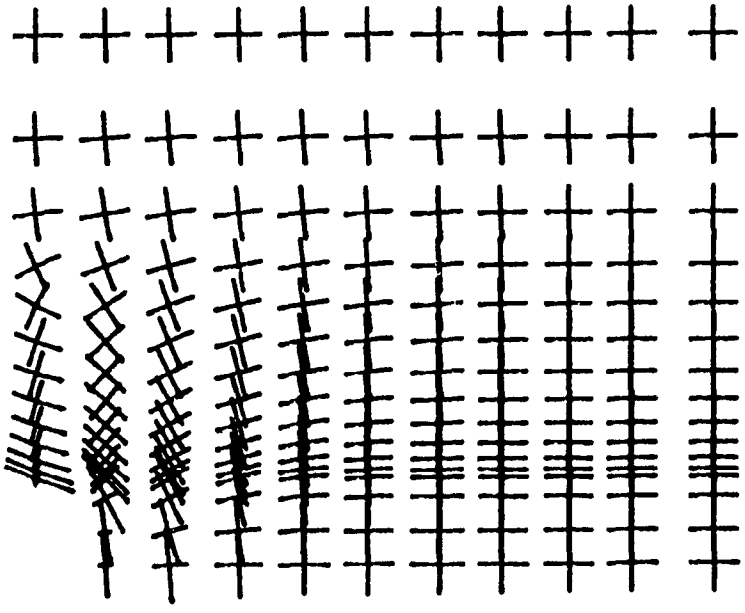

Principal stresses before cut at t=1 day
(Figure 4.11b)

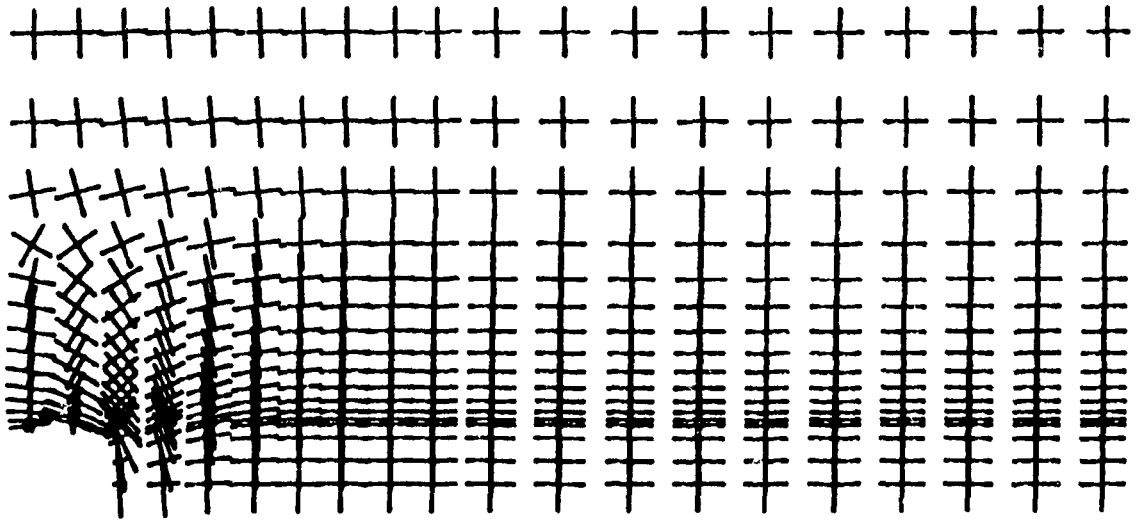

Principal stresses after cut at t=1 day
(Figure 4.11c)

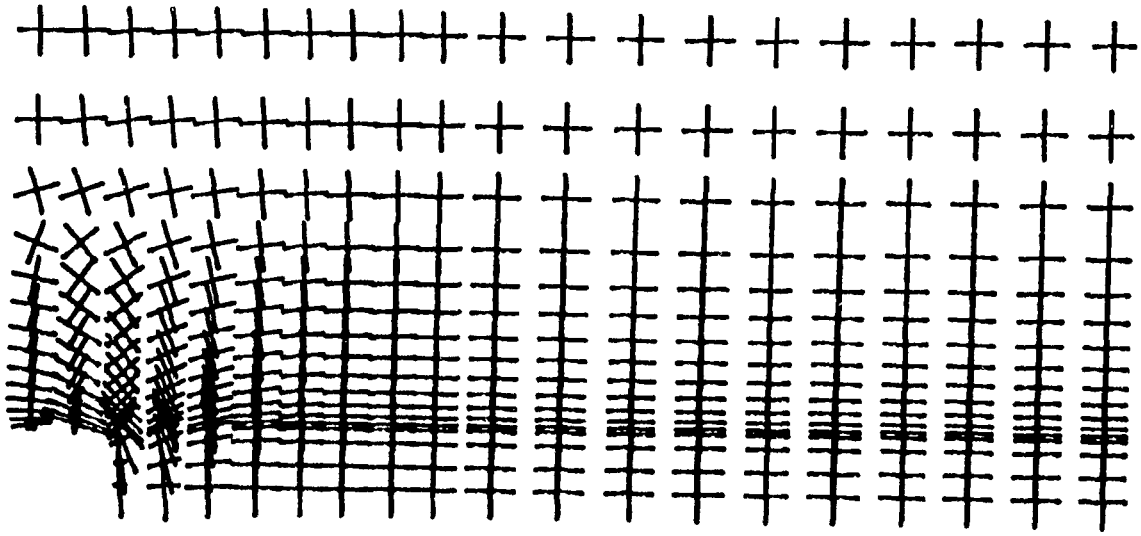

Principal stresses before cut at t= 2 days
(Figure 4.11d)

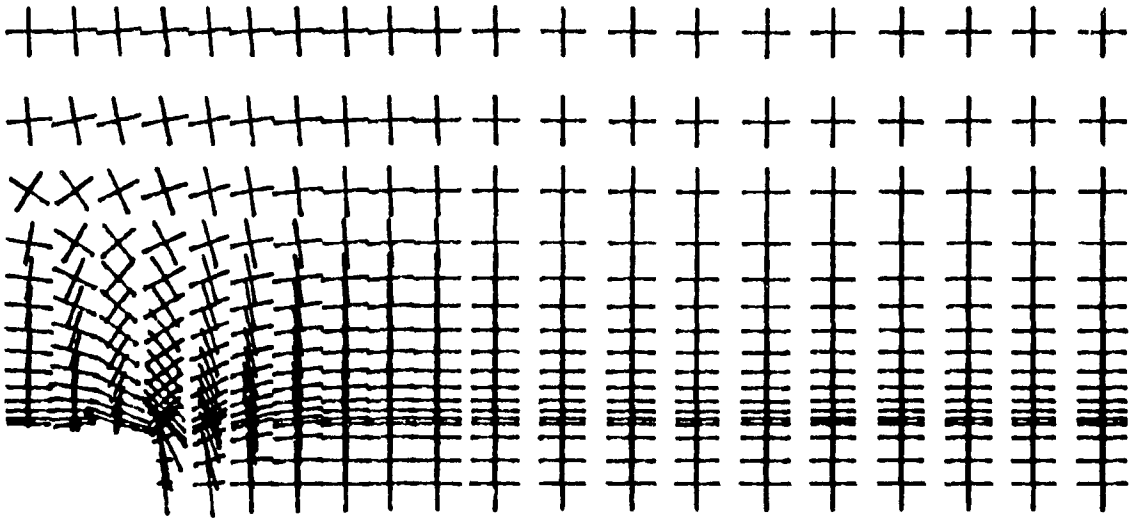

Principal stresses after cut at t=2 days
(Figure 4.11e)

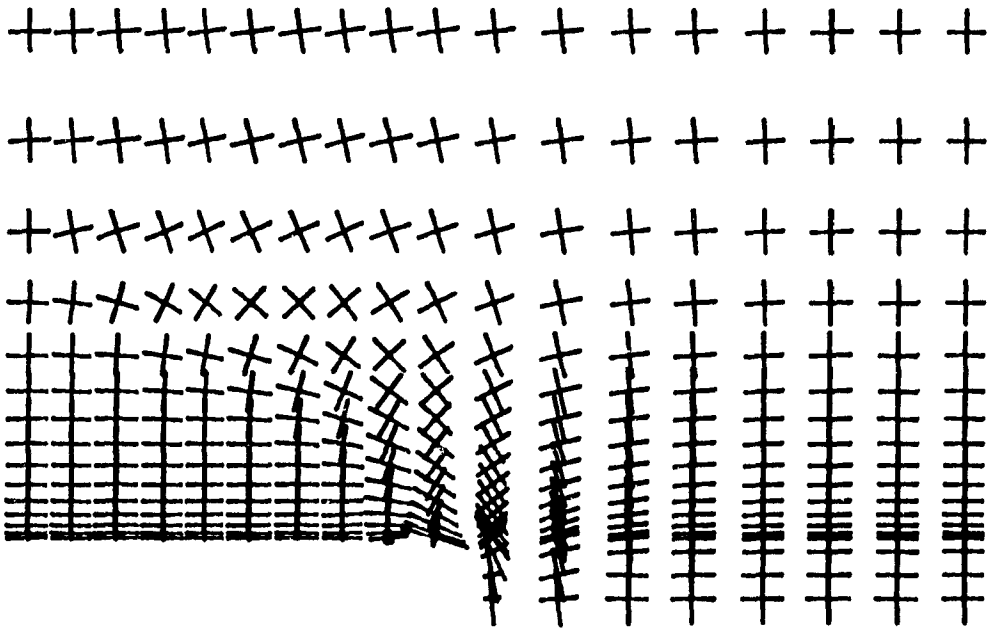

Principal stresses before cut at t=9 days
(Figure 4.11f)

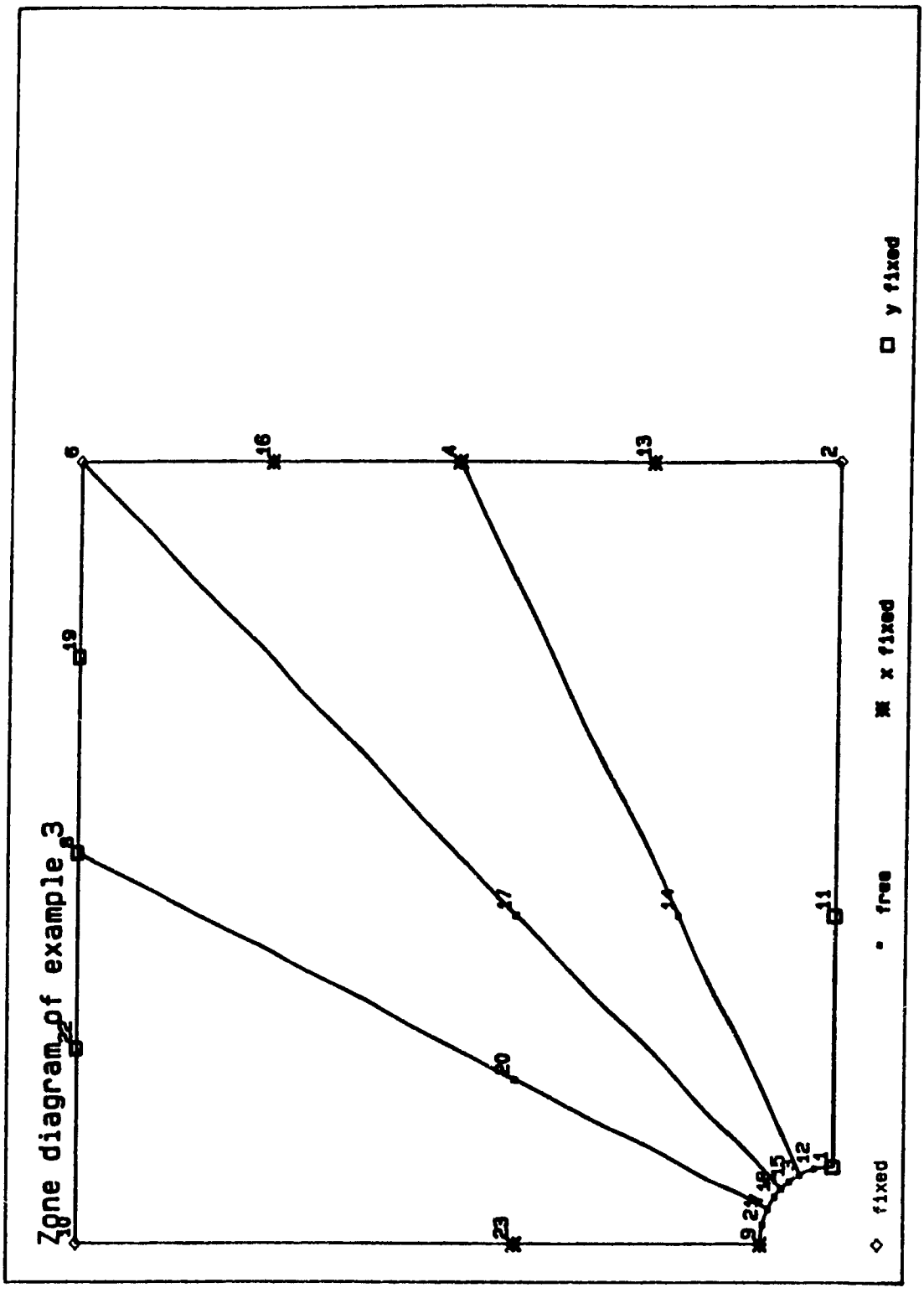

Zone diagram of example 3
(Figure 4.12)

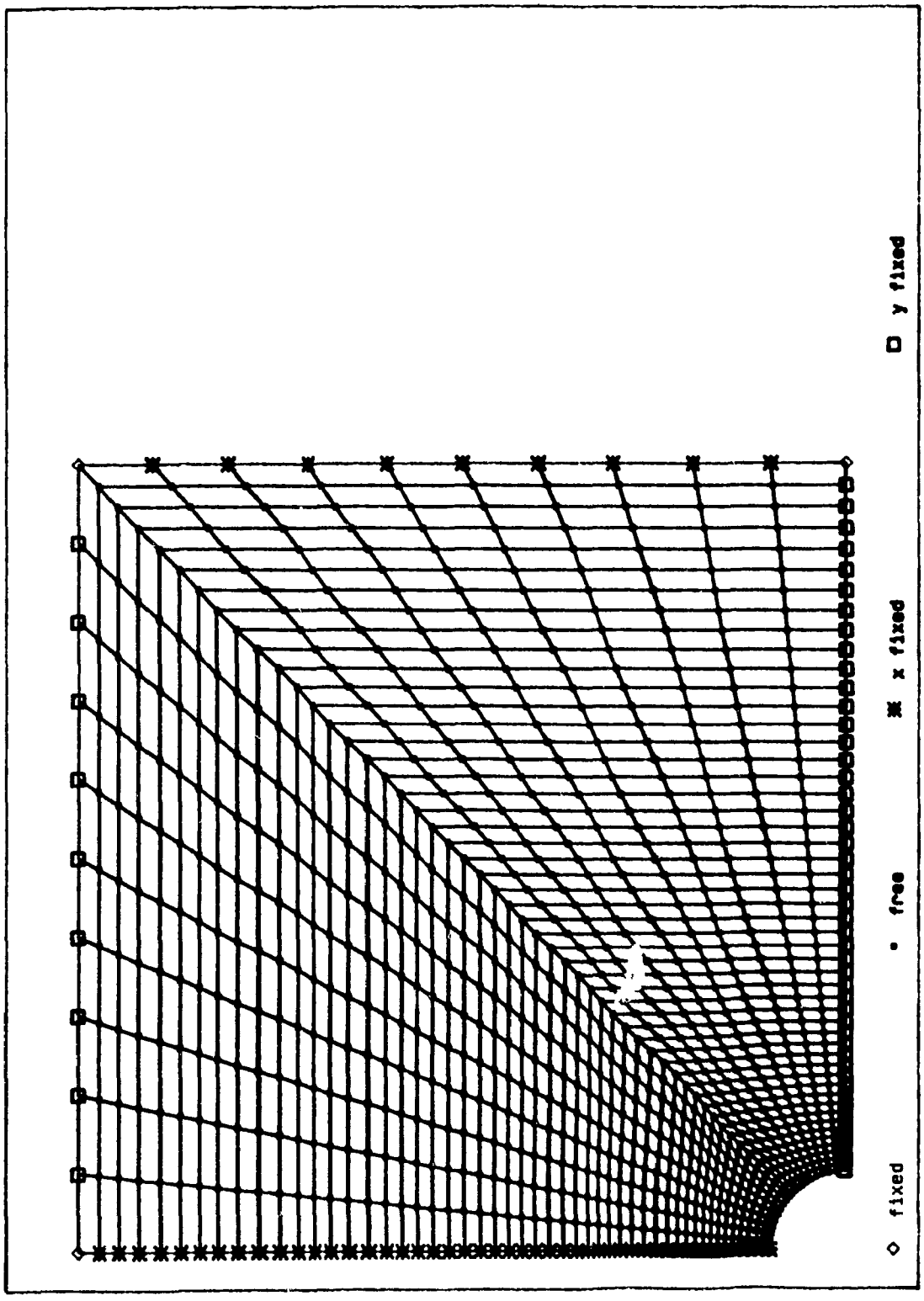

Finite element grid of example 3
(Figure 4.13)

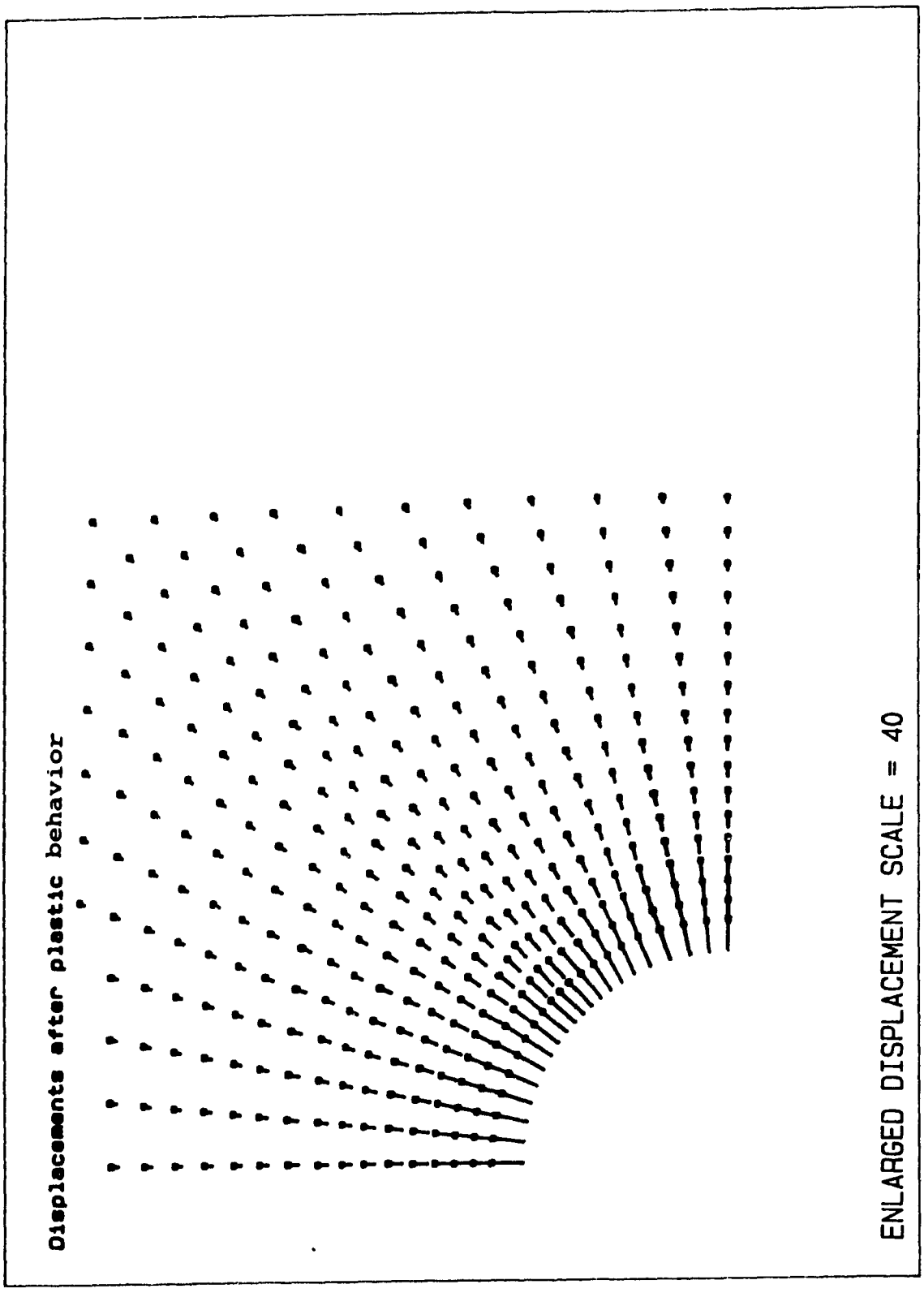

Displacements after plastic behavior
(Figure 4.14a)

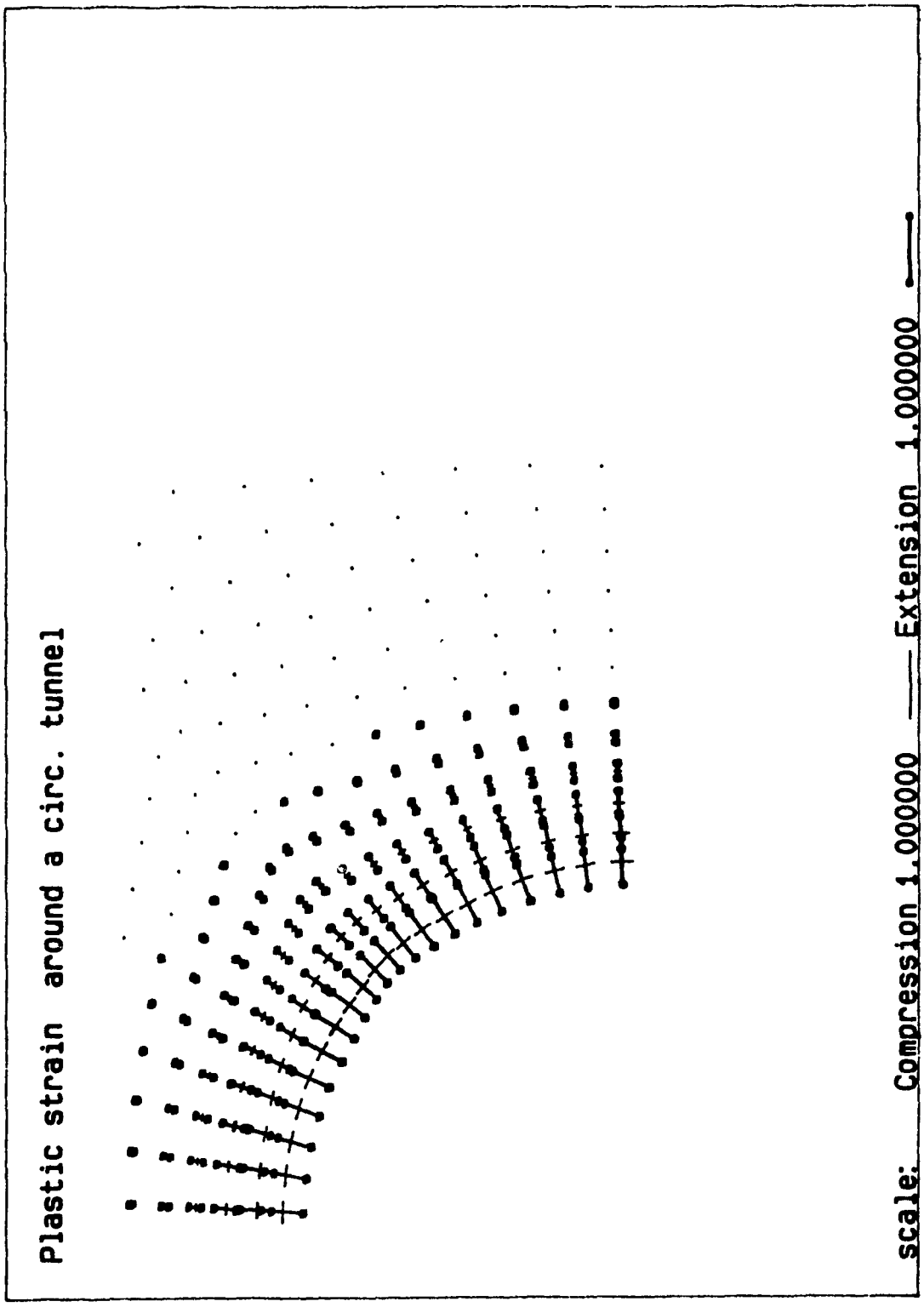

Principal plastic strain with dilation, around the circular tunnel of example 3
(Figure 4.14b)

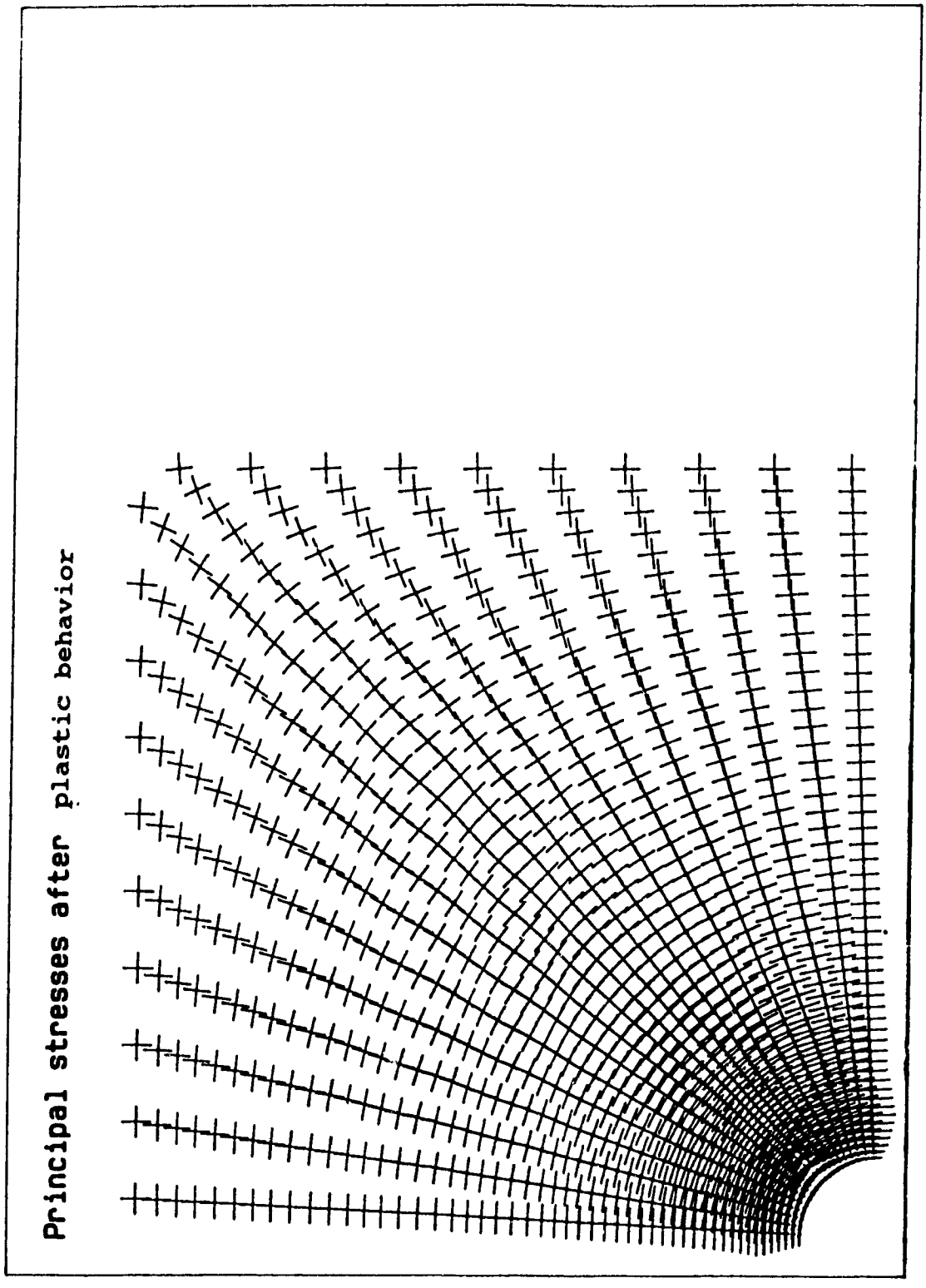

Principal stresses after the plastic behavior
(Figure 4.15)

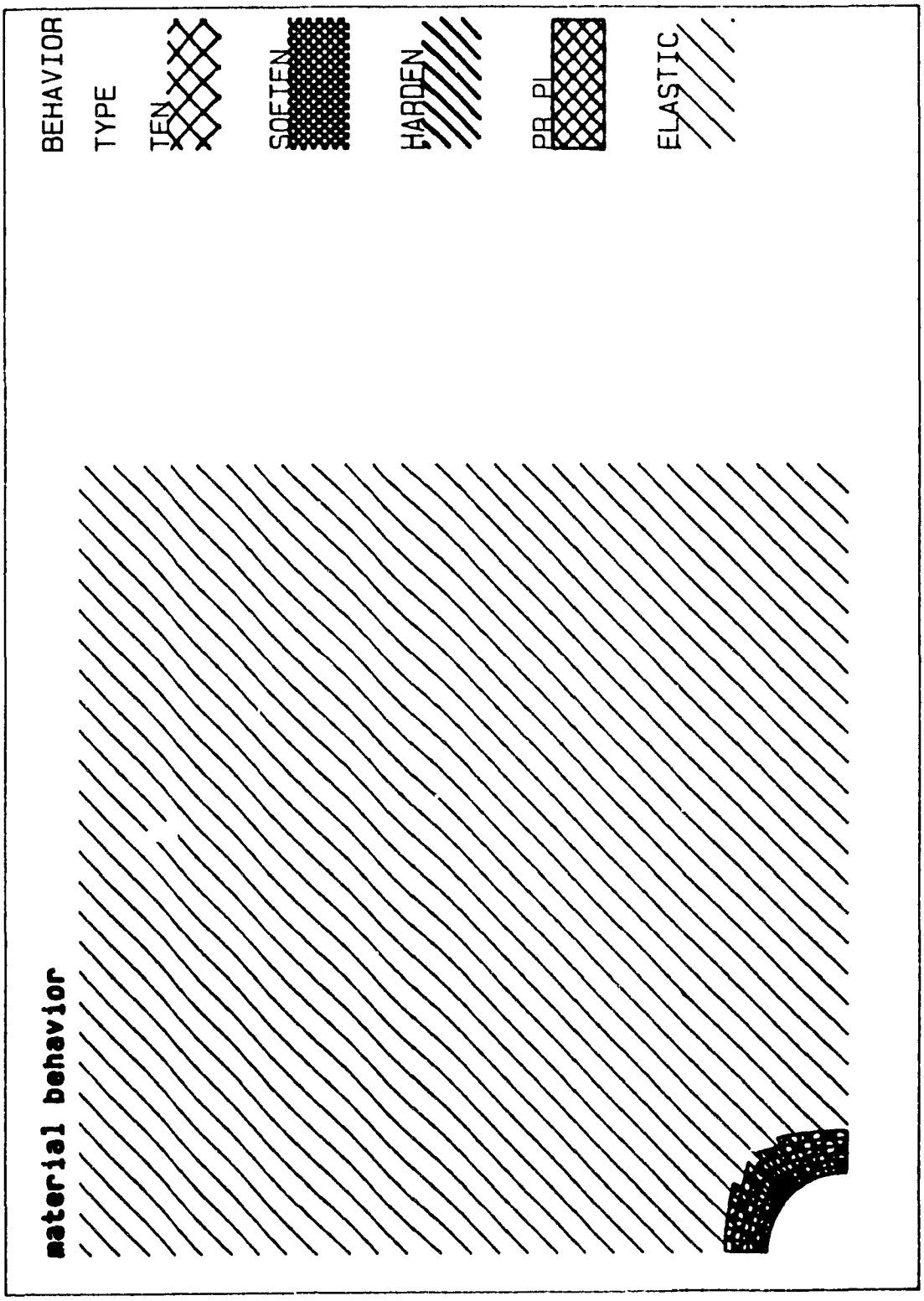

Rock behavior around the circular tunnel
(Figure 4.16)

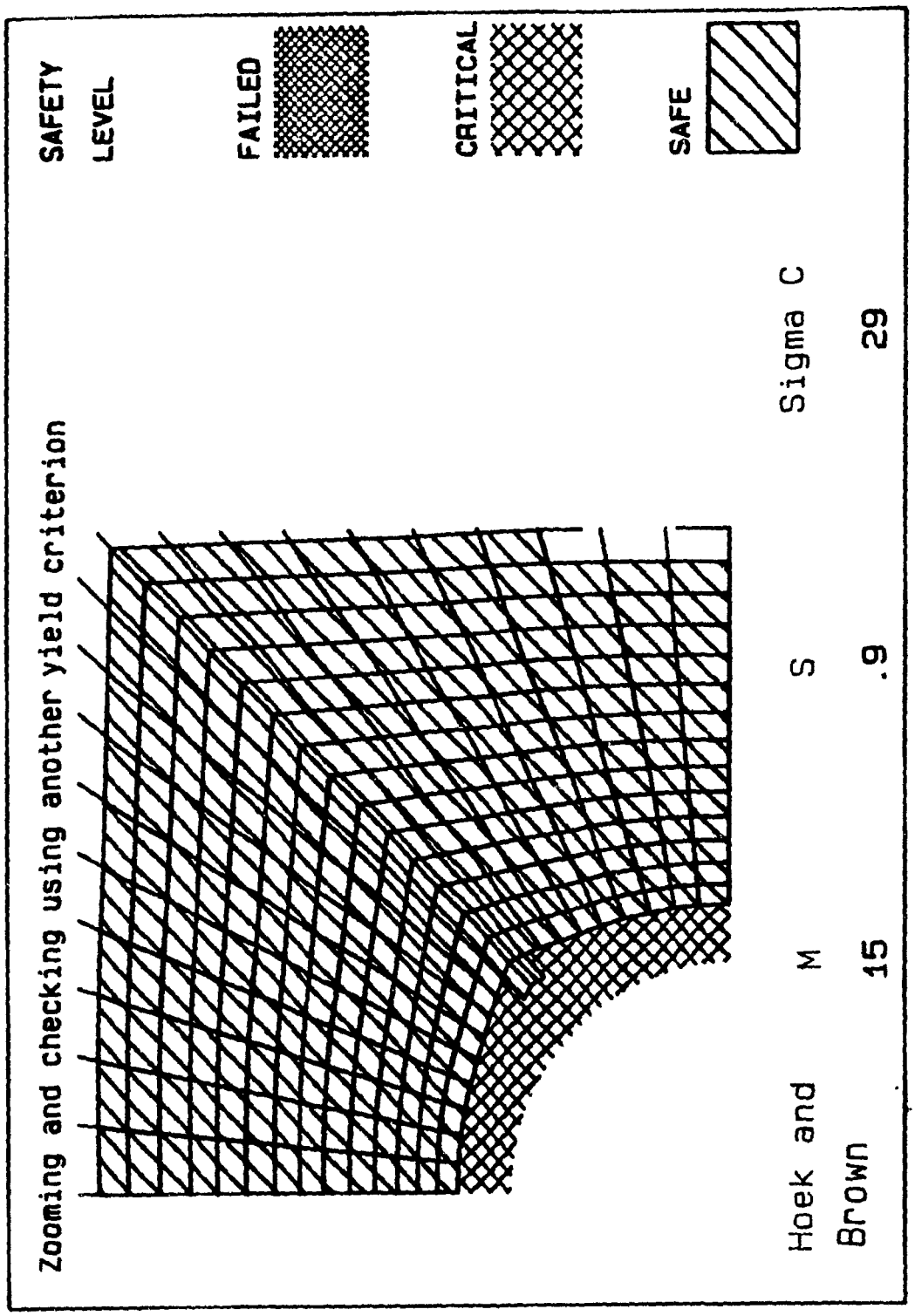

Using Hoek & Brown failure criterion to make sure that the state of stress after plastic yield is also safe within its limits . Otherwise a decision is taken.
(Figure 4.17)

CHAPTER 5

CONCLUSIONS

Both the theory of viscoplasticity and a variety of constitutive models used for different rock types have been reviewed in detail in Chapter 2 in an attempt to present a global perspective on the subject and highlight the main contributions by various authors in recent years.

A 2-dimensional elasto-viscoplastic finite element program incorporating linear and nonlinear yield functions and an iterative explicit time marching scheme has been developed. The program is designed primarily for mining engineering applications; it is written using Microsoft version FORTRAN 5.0 which utilizes the features of the 80286 processors. This program occupies 260 kb of RAM when it handles 2000 elements. At the same time, it makes use of both direct and sequential access files . One prime concern was to minimize execution time which is of importance for this kind of nonlinear analysis. Unformatted and binary files are used for internal use to speed up the read write operations. Repeated calculations are avoided by reading and writing a direct access unformatted record per element (containing data of all integration points). Also binary files were implemented to store long data like the global total displacements vector. This helped to avoid excessive structuring of the program

code (calls to subroutines) which adds to the execution time especially when a call is located in a nested do loop (like Segment 4 in Section 3.2).

There is no limit imposed on the number of time stations at which instantaneous changes occur like elements cut, elements backfilled, applied loads or simply an output is required. A time station t_f can be specified more than one time with different associated cards. This is useful when outputs just before and just after a cut or a fill are required. This feature might also be useful if premining stresses are not uniform because of the surrounding geology. In this case, the user can run the program to get the non uniform stress distribution (caused by own weight and tectonic effect) before mining at t=0.0 . Then, specify cards 5 → 12 with t_f = 0.0 and cut the elements representing the excavation. The user can stop the program at this point and use the postprocessor to see the results. The same analysis could be pursued later for time dependent behavior when he appends cards of $t_f > 0.0$ to the input file (file.vsc).

The program simulates cut elements by skipping them when constructing the global stiffness and the global total load vector while the installation of backfill by taking into account the changed element properties and their initialized internal stresses in reconstructing the global stiffness and load vectors.

When the input data is read in parallel with the analysis,

the user can simulate compound behaviour by stopping the analysis, examining the results graphically and restarting it again and possibly after making a decision to be implemented in the subsequent appended input like adding a backfill at a given time station. The user can run the program to perform nonlinear behaviour (time independent) which is one basic use of viscoplasticity. The creep (time dependent) analysis might start afterwards based on the stresses obtained from the nonlinear behaviour.

The iterative explicit time integration scheme is simple and can accommodate a variety of constitutive models. The scheme is iterative to allow the improvement of solution accuracy. The user can speed the execution by optimizing the number of iterations per time increment for a period between two consecutive time stations.

The program uses an automatic time-step calculator in an attempt to prevent solution instability. Section 3.4 uses the concept adopted in reference [17] to derive easy to program equations giving the maximum time step insuring stability for common forms of yield functions and plastic potentials.

The program input and output are made compatible with those of program **SAP2D** to make use of its preprocessor and graphical programs. However, some modifications had to be done to the postprocessor to accommodate time dependent analysis output. Section 4.4 presented three illustrative examples . The

program was debugged using Microsoft Fortran debugger when it was used to simulate other problems for verification . Using this interactive debugger makes it easier to program and verify the coding in detail.

Despite the good correlation between numerical and analytical results, much remains to be done on the model sensitivity analysis and validation with actual geomechanical data.

Anisotropic (transversally isotropic) elastic properties will be included. The program should expand to 3 dimensions (the program structure encourages that) and should incorporate ground support elements as with rock bolts and cable bolts. Only then will the present numerical model have the potential for becoming a general mine design tool.

LIST OF REFERENCES

1. Pande, G.N., Beer, G. and Williams, J.R., 1990. Numerical methods in rock mechanics. John Wiley & Sons Ltd., New York.
2 Brady, B.H.G and Brown, E.T.,1980. Rock Mechanics For underground Mining. George Allen & Unwin, London.
3. Owen, D.R. and Hinton, E., 1980. Finite Element In Plasticity. Pineridge Press Limited, Swansea, U.K.
4. Zienkiewicz, O.C. and Cormeau, 1974, Viscoplasticity - plasticity and creep in elastic solids - a unified numerical solution approach. Int. J. Num. Meth. Engng., 8:821-845.
5. Mendelson, A., 1968. Plasticity Theory And Application.
6. Aubertin, M., Gill, D. and Ladanyi, B., 1987. Le comportement rheologique du sel: revue bibliographique - Tome I Essais en laboratoire et modelisation empirique.-Tome II Mechanismes de deformation, modelisation physique, rupture, essais en place et comportement in situ. Ecole Polytechnique de Montreal, Quebec, Canada.
7. Brown, E.T. and Michelis, P.N,1978. A critical state yield equation for strain softening rock. Proc. 19th U. S. Sympos. On Rock Mech. , 515-519, Lake Tahoe Nevada.
8. Suzuki, K. and Desai, C.S., 1985. Finite element analysis using an elasto-plastic anisotropic hardening model. Fifth International Conference On Num. Meth. In Geomechanics, Nagoya. 317-324

9. Axelsson, K. and Samuelsson, A., 1979. Finite element analysis of elastoplastic materials displaying mixed hardening. Int. J. Num. Meth. Engng., 14; 211-225.

10. Cristescu, N., 1987. Elasto/Viscoplastic constitutive equations for rock. Int. J. Rock Mech. Min. Sci. & Geomech. Abstr. 24; 271-282

11. Oka, F., Adachi, T. and Okano, Y., 1986. Two-dimensional consolidation analysis using an elasto-viscoplastic constitutive equation. Int. J. Num. Anal. Meth. Geomech., 10:1-16.

12. Dragon, A. and Mroz, Z., 1979. A continuum model for plastic-brittle behaviour of rock and concrete. Int. J. Engng. Sci., 17: 121-137.

13. Pietruszczak, S. and Mroz, Z., 1980. Numerical analysis of elastic-plastic compression of pillars accounting for material hardening and softening. Int. J. Rock Mech. Min. Sci. & Geomech. Abstr. 17: 199-207.

14. Smith, B.M. and Cheatham Jr., J.B., 1980. An anisotropic compacting yield condition applied to porous limestone. Int. J. Rock Mech. Min. Sci. & Geomech. Abstr., 17: 159-165.

15. Microsoft corporation, 1989. Microsoft Fortran Advanced Topics.

16. Chau, K.S.P., 1988. A finite element model for stress analysis of underground openings. M.Eng. Thesis, Mining Enigineering, McGill University, Montreal, Canada.

17. Stolle, D.E. and Higgins, J.E., 1989. Viscoplasticity and plasticity - numerical stability revisited. Numerical Models in Geomechanics NUMOG III, Niagara

Falls, Canada, Elsevier Science Publishers, 431-438.

18. Nayak, G.C., Zienkiewicz, O.C., 1972. Elasto-plastic stress analysis - a generalization for various constitutive relations including strain softening. Int. J. Num. Meth. Engng., 5:113-135.

19. Sun, J. and Lee, Y.S., 1985. A viscous elastoplastic numerical analysis of the underground structure interacted with families of multi-laminate rock mass using FEM. Fifth International Conference On Num. Meth. In Geomechanics, Nagoya. 1127-1134

20. Gerogiannopoulos, N.G. and Brown, E.T., 1978. The critical state concept applied to rock. Int. J. Rock Mech. Min. Sci. & Geomech. Abstr. 15:1-10.

21. Gioda, G., 1981. A finite element solution of non-linear creep problems in rocks. Int. J. Rock Mech. Min. Sci. & Geomech. Abstr., 18:35-46.

22. Cristescu, N., 1985. Plasticity of compressible dilatant rock-like materials. Int. J. Engng Science 23; 1091-1100

23. Schofield, A.N. and Wroth, C.P., 1968. Critical state soil mechanics, McGraw-Hill.

24. Desai, C.S. and Salami, M.R., 1987. A constitutive model and associated testing for soft rock. Int. J. Rock Mech. Min. Sci. & Geomech. Abstr. 24; 299-307

25. Langer, M. ,1984. The rheological behaviour of rock salt. Proc. 1st Int. conf. on the mech. behavior of salt (Nov. 1981), Trans Tech Pub. 201-240.

26. Horseman, S.and Passaris, E., 1984. Creep tests for storage cavity closure prediction. Proc. 1st Int.

conf. on the mech. behavior of salt (Nov. 1981), Trans Tech Pub. 119-157.

27. Munson, D.E.,Dawson, P.R., 1979. Constitutive model for the low temperature creep of salt. Sandia National Laboratories, SAND-79-1853 .

28. Sulem, J., Panet, M. and Guenot, A., 1987. An analytical solution for time-dependent displacements in a circular tunnel. Int. J. Rock Mech. Min. Sci. & Geomech. Abstr., 24; 155-164.

29. Serata, S., 1968. Application of continuum mechanics to design of potash mines in canada. Int. J. Rock Mech. Min. Sci. 5; 293-314.

30. Dragon, A. and Mroz, Z., 1979. A model for plastic creep of rock-like materials accounting for the kinetic of fractures. Int. J. Rock Mech. Min. Sci. & Geomech. Abstr. 16; 253-259

31. Zienkiewicz, O.C., Valliappan, S. and King, I.P., 1969. Elasto-plastic solutions of engineering problems "Initial Stress" finite element method. Int. J. Num. Meth. Engng., 1:75-100

32. Mitri, H.S. and Scoble, M.J., 1989. A numerical procedure for stability analysis of hardrock mine structures. Min. Sci. Technol., 9:187-195.

33. Mitri, H.S.,1988. Finite element applications in mining engineering. Professional Development Seminar Notes, Department of Mining & Metallurgical Engineering , McGill University, June 2-6, Montreal.

APPENDIX I. EXAMPLES OF INPUT DATA FILES

The following is the preprocessor's input data file (FILE.DAT) of example 1:

```
AXISYMMETRIC TUNNEL IN PLANE STRAIN (EXAMPLE 1)                    →CARD 1
6 1 1 1 1 0 -90                                                    →CARD 2
1                                                                  →CARD 3
100                                                                →CARD 4
1 2 1 0                                                            →CARD 5
2 2 20 0                                                           →CARD 5
3 2 1 .5                                                           →CARD 5
4 2 20 .5                                                          →CARD 5
5 2 6.5 0                                                          →CARD 5
6 2 6.5 .5                                                         →CARD 5
1 3 1 2 4  0 5 0 6  1 2 1                                          →CARD 6a
3 2 2 0 0                                                          →CARD 6b
0  1  0 0 0  0  0 0  1  1  0 1 1                                   →CARD 7
1 .0 1                                                             →CARD 8a
360 .2                                                             →CARD 8b
-2 0 -2 0 -2 0 0 0                                                 →CARD 9
1 1 1 1 1                                                          →CARD 11
```

This is the input data file of program VISA2D ; the first part is generated by the preprocessor PRESAP based on the above data and the second is user written.

```
AXISYMMETRIC TUNNEL IN PLANE STRAIN (EXAMPLE 1)
202  1  1  0  0  0  1  1  0 -90 000                          →control card
  1  0  1 .1000000E+01  .1000000E+01                         nodal points data and
  2  0  1 .1000000E+01  .0000000E+00                         degrees of freedom (generated)
  3  0  1 .1031600E+01  .9999999E+00
  4  0  1 .1031600E+01  .0000000E+00
  5  0  1 .1066400E+01  .1000000E+01
  6  0  1 .1066400E+01  .0000000E+00
  7  0  1 .1104400E+01  .1000000E+01
  8  0  1 .1104400E+01  .0000000E+00
and so on till;
199  0  1 .1965159E+02  .1000000E+01
200  0  1 .1965159E+02  .0000000E+00
201  0  1 .2000000E+02  .1000000E+01
202  0  1 .2000000E+02  .0000000E+00
 4 100  1  1  0  1                                           control card (generated)
 1  1 .0000000E+00 .0000000E+00
.3600000E+03 .3600000E+03 .3600000E+03 .2000000E+00 .2000000E+00   →elastic material
.2000000E+00 .1500000E+03                                    properties
-2000000E+01 .0000000E+00 -2000000E+01 .0000000E+00         initial stresses (generated)
-2000000E+01  0000000E+00
 1  1  2  4  3  1  2  0  0   .000   1.000                     elements data and
 2  3  4  6  5  1  2  0  0   .000   1 000                     and connectivity (generated)
 3  5  6  8  7  1  2  0  0   .000   1.000
and so on till;
 97 193 194 196 195  1  2  0  0   .000  1 000
 98 195 196 198 197  1  2  0  0   .000  1.000
 99 197 198 200 199  1  2  0  0   .000  1.000
100 199 200 202 201  1  2  1  0   .000  1.000
 3   2 000   2 000   .000   .000                  pressure on side 3 of element 100 (generated)

   .000   1.000   1 000   1.000   1.000   1.000    multipliers of loading are not used by VISA2D
PRN&CONT                  CARD 1 (these are time dependent data cards written by the user)
1. 1. 86400  100 3 .036                                      CARD 2
1 200  11 0                                                  CARD 3
7.2308e-4                                                    CARD 4
0                                                            CARD 3 is put 0 to end its occurrence
****************** CARD 5
1                                  CARD 6 →NCOUNT is put = 1 and all elements remain active
.010 'DA'  3 .036 0                CARD 7 a factor of .036 is used because E is very small
0 for added fill                                             CARD 9
0 for added ndld                                             CARD 10
```

```
0  for added sur. pr.                                          CARD 11
PRN&CONT                                                       CARD 12
*******************as a seperator***************
1                                                              CARD 6 of time .3days
.30 'DA'  3  036 0                                             CARD 7 of time .3days
0                                                              CARD 9 of time .3 days
0                                                              CARD 10 of time .3 days
0                                                              CARD 11 of time  3 days
PRN&CONT                                                       CARD 12 of time .3 days
****************
1
.430 'DA'  3 .036 0
0  for added fill
0  for added ndld
0  for added sur. pr.
PRN&CONT
*****************
1
 730 'DA'  3 .036 0
0  for added fill
0  for added ndld
0  for added sur. pr.
PRN&CONT
```

and so on till 10 days time:

```
*****************
1
10  'DA'  3 .036 0
0
0
0
oup&cont
*****************
1
50  'DA'  3 .036 0
0
0
0
oup&cont
*****************
1
100  'DA'  3 .036 0
0
0
0
STOP
```

The following is the preprocessor's input data file (FILE.DAT) of example 2:

```
AXISYMETRIC ANALYSIS OF A CIRCULAR TUNNEL                    CARD 1
25 9 3 3 3 0 -90                                             CARD 2
10 10 10                                                     CARD 3
3 10 7                                                       CARD 4

1  3  0  70                                                  CARD 5
2  1  0  60                                                  CARD 5
3  1  0  40                                                  CARD 5
4  3  0  20

5  2  1.5  70                                                CARD 5
6  0  1.5  60                                                CARD 5
7  0  1.5  40                                                CARD 5
8  3  1.5  20                                                CARD 5

9   2  5  70                                                 CARD 5
10  0  5  60                                                 CARD 5
11  0  5  40                                                 CARD 5
12  2  10 20                                                 CARD 5

13  2  20  70                                                CARD 5
14  0  20  60                                                CARD 5
15  0  20  40                                                CARD 5
16  2  20  20                                                CARD 5

17  2  2.8   70                                             CARD 5
18  0  2.8   60                                             CARD 5
19  0  2.8   40                                             CARD 5
20  2  10  70                                                CARD 5
21  0  10  60                                                CARD 5
22  0  10  40                                                CARD 5
23  0  1.5  32                                               CARD 5
24  1  0   32                                               CARD 5
25  0  7   32                                               CARD 5

1  1   2  6  5    0 0 0 0  1  0  0                          CARD 6
2  2   3  7  6    0 0 0 0  1  0  0                          CARD 6
3  3   4  8  7    24 0 23 0  1  0  0
4  5   6  10 9    0 18 0 17 1  20  0
5  6   7  11 10   0 19 0 18  1  20  0
6  7   8  12 11   23 0  25 19  1  20  0
7  9   10 14 13   0 21 0 20  1  20  1                       CARD 6 a
3  2 2 0 0                                                  CARD 6 b
8  10  11 15 14   0 22 0 21  1  20  1                       CARD 6a
3  2 2 0 0                                                  CARD 6b
```

```
9 11 12 16 15  25 0 0 22 1 20 1
3 2 2 0 0                                   Side pressure of 2 Mpa at side 3 of zone 9

0 1 0 0 0  0 0 0 1 1 1 0 1 1                                          CARD 7
1 .0 1                                                                CARD 8a
360 2                                                                 CARD 8b
2 0 2 0 2 0 0 0                                                       CARD 9
1 1 1 1 1                                                             CARD 11
```

This is the input data file of program **VISA2D** ; the first part is generated by the preprocessor **PRESAP** based on the above data and the second is user written.

```
AXISYMETRIC ANALYSIS OF A CIRCULAR TUNNEL WITH CUT SEQUENCE
 651   1   1   0   0   0   3   1   0 -90.000
   1   1   1  .0000000E+00  .7000000E+02
   2   1   0  .0000000E+00  6899999E+02
   3   1   0  .0000000E+00  6800000E+02
   4   1   0  .0000000E+00  .6700000E+02
   5   1   0   0000000E+00  6600000E+02
   6   1   0  .0000000E+00  .6500000E+02
   7   1   0  .0000000E+00  6400000E+02
and so on till;
 649   0   0  2000000E+02  2500000E+02
 650   0   0  2000000E+02  2250000E+02
 651   0   1  .2000000E+02  2000000E+02
   4 600   1   1   0   1
   1   1  .0000000E+00  .0000000E+00
 .3600000E+03  .3600000E+03  .3600000E+03  .2000000E+00  .2000000E+00
 .2000000E+00  .1500000E+03
-.2000000E+01  .0000000E+00 -.1800000E+01  .0000000E+00
-.2000000E+01  .0000000E+00
   1   1   2  33  32   1   0   0   0   .000   1.000                  elements data and
   2   2   3  34  33   1   1   0   0   .000   1.000                  and connectivity (generated)
   3   3   4  35  34   1   2   0   0   .000   1.000
   4   4   5  36  35   1   3   0   0   .000   1.000
   5   5   6  37  36   1   4   0   0   .000   1.000
   6   6   7  38  37   1   5   0   0   .000   1.000
   7   7   8  39  38   1   6   0   0   .000   1.000
   8   8   9  40  39   1   7   0   0   .000   1.000
   9   9  10  41  40   1   8   0   0   .000   1.000
  10  10  11  42  41   1   9   0   0   .000   1.000
  11  11  12  43  42   1  10   0   0   .000   1.000
  12  12  13  44  43   1  10   0   0   .000   1.000                  an element of cut no. 10
  13  13  14  45  44   1  11   0   0   .000   1.000                  an element of cut no 11
```

```
 14  14  15  46  45  1  11  0  0   .000   1 000
 15  15  16  47  46  1  12  0  0   .000   1 000
 16  16  17  48  47  1  12  0  0   .000   1 000
 17  17  18  49  48  1  13  0  0   .000   1 000
 18  18  19  50  49  1  13  0  0   .000   1.000
 19  19  20  51  50  1  14  0  0   000    1 000
 20  20  21  52  51  1  14  0  0   .000   1.000
 21  21  22  53  52  1  15  0  0   000    1 000
 22  22  23  54  53  1  15  0  0   .000   1.000
 23  23  24  55  54  1  16  0  0   000    1.000
 24  24  25  56  55  1  16  C  0   000    1 000
 25  25  26  57  56  1  17  0  0   .000   1 000
 26  26  27  58  57  1  17  0  0   .000   1.000
 27  27  28  59  58  1  18  0  0   .000   1.000
 28  28  29  60  59  1  18  0  0   .000   1 000
 29  29  30  61  60  1  19  0  0   .000   1 000
 30  30  31  62  61  1  19  0  0   .000   1.000
 31  32  33  64  63  1  0   0  0   .000   1 000
 32  33  34  65  64  1  1   0  0   .000   1.000
 33  34  35  66  65  1  2   0  0   000    1.000
and so on ;
 87  89  90 121 120  1  18  0  0   .000   1.000
 88  90  91 122 121  1  18  0  0   .000   1.000
 89  91  92 123 122  1  19  0  0   .000   1.000
 90  92  93 124 123  1  19  0  0   .000   1.000
 91  94  95 126 125  1  20  0  0   .000   1.000
 92  95  96 127 126  1  20  0  0   .000   1.000
 93  96  97 128 127  1  20  0  0   .000   1 000
 94  97  98 129 128  1  20  0  0   000    1 000
and so on ;
568 586 587 618 617  1  20  0  0   000    1.000
569 587 588 619 618  1  20  0  0   .000   1.000
570 588 589 620 619  1  20  0  0   .000   1 000
571 590 591 622 621  1  20  1  0   .000   1.000
  3   2.000   2 000  .000   000
572 591 592 623 622  1  20  1  0   .000   1.000
  3   2.000   2 000  .000   000
and so on
598 617 618 649 648  1  20  1  0   .000   1.000
  3   2.000   2 000  .000   .000
599 618 619 650 649  1  20  1  0   .000   1.000
  3   2 000   2 000  .000   .000
600 619 620 651 650  1  20  1  0   .000   1.000
  3   2 000   2.000  .000   .000

   000   1.000   1.000   1.000   1 000   1.000
oup&cont
1.  1  86400. 100 3 .036
1 200  11 0
7.2308e-4
0
******************
0
```

an element of cut no.11
an element of cut no.12
an element of cut no.19
an element of cut no. 0
an element of cut no.1
an element of cut no. 2
elements around the tunnel have a cut no. 20

no point loads
load multiplier not used by VISA2D
to continue and print results
card 2
card 3:NY(1)=11 (and NCR(1)=0 but not used)
card 4: the constant of equation 4.4
card 3: put 0 to end its occurence
card 5: seperator for clarity

```
0 'DA' 0                                  for instantaneous elastic analysis output
0                                                                     no backfill
0                                                           no added nodal loads
0                                                       no added surface pressure
PRN&CNT.
@@@@@@@@@@@@@@@@@@@@@@@@@@@@@@@@@@@@@@@@@@@@@@@@@@
0
1 'DA' 3 .036 0                                       {till the end of the first day }
0                                                                   no backfill
0                                                           no  added nodal loads
0                                                       no added surface pressure
PRN&CNT.
******************
1                              {elements of cut number 1 are cut at t= 1 day}
1 'DA' 3 .036 1
0        no change of cut number of any element (the sequence above is sufficient)
0                                                                  for added fill
0                                                                  for added ndld
0                                                                for added sur. pr.
PRN&CNT.
******************
1
2 'DA' 3 .036 0   {till the end of the second day}
0
0
0
stop                                     the program is stopped here(at t=2 days)
******************                                          and is restarted here
2
2 'DA' 3 .036 1   !{elements of cut number 2 are cut at  t= 2 days}
0
0
0
0
PRN&CNT.
******************
3
3 'DA' 3 .036 1   {elements of cut number 3 are cut at t= 3 days}
0
0
0
0
PRN&CNT.
******************
4
4 'DA' 3 .036  1   {elements of cut number 4 are cut at  t= 4 days}
0
0
0
0
PRN&CNT.
******************
5        {elements of cut number 5 are cut at  t= 5 days}
5 'DA' 3 .036  1
```

```
0 for added cut
0 for added fill
0 for added ndld
0 for added sur. pr.
PRN&CNT.
*******************
6
6 'DA' 3  036  1   {elements of cut number 6 are cut at  t= 6 days}
0 for added cut
0 for added fill
0 for added ndld
0 for added sur. pr
PRN&CNT.
an so on till;
****************
18          means cut number 18 is cut at end of day 50
50 'DA' 3  036  1
0 for added cut
0 for added fill
0 for added ndld
0 for added sur. p
cont.
****************
19          means cut number 19 is cut at end of day 75
75 'DA' 3 .036  1
0 for added cut
0 for added fill
0 for added ndld
0 for added sur. p
cont.
****************
19          analysis continues tiil day 100
100 'DA' 3 .036  0
0 for added fill
0 for added ndld
0 for added sur. p
STOP
```

it is preferable to write a comment at the end of each free format record to help the program locate the error at the exact line if it happens.

The following is the preprocessor's input data file (FILE.DAT) of example 3:

```
ELASTO PLASTIC ANALYSIS OF A CIRCULAR TUNNEL USING VISCOPLASTICITY
23 4 1 4 1 0 -90
50
5 5 5 5
1 2 1 0
2 3 10 0
3 0 .894 .447
4 1 10 5
5 0 .707 .707
6 3 10 10
7 0 .447  894
8 2 5 10
9 1 0 1
10 3 0 10
11 2 3.2 0
12 0 .970 .243
13 1 10 2.5
14 0 3 2 1.6
15 0 .8 .6
16 1 10 7.5
17 0 3.2 3.2
18 0 .6 .8
19 2 7.5 10
20 0 1.6 3.2
21 0 .243 .970
22 2 2.5 10
23 1 0 3.2
1 1 2 4 3 11 13 14 12 1 2 0
2 3 4 6 5 14 16 17 15 1 2 0
3 5 6 8 7 17 19 20 18 1 2 0
4 7 8 10 9 20 22 23 21 1 2 0
0 1 1 1 1 0 1 0 1 1 1 1 1
1 .0 1
50000 .2
-55 .0  -55  .0 -55 .0 0 0
1 1 1 1 1
```

This is the input data file of program **VISA2D** ; the first part is generated by the preprocessor **PRESAP** based on the above data and the second is user written.

```
ELASTO PLASTIC ANALYSIS OF A CIRCULAR TUNNEL USING VISCOPLASTICITY
 1071   1   1   1   1   1   1   1   0    1.000
   1    0   1  .1000000E+01  .0000000E+00
   2    0   1  .1078080E+01  .0000000E+00
   3    0   1  .1160320E+01   0000000E+00
and so on till;
 1069   1   0  .0000000E+00  .9440323E+01 THESE DATA ARE GENERATED BY THE PREPROCESSOR
 1070   1   0  .0000000E+00  .9718082E+01
 1071   1   1   0000000E+00  .1000000E+02
   4 1000   1   1   1   1
   1   1  .0000000E+00  .0000000E+00
  .5000000E+05  .5000000E+05  5000000E+05  .2000000E+00  .2000000E+00
  .2000000E+00  .2083333E+05
 -.5500000E+02  .0000000E+00 - 5500000E+02   0000000E+00
 -.5500000E+02  .0000000E+00
   1   1   2  53  52   1   2   0   0     .000    1.000
   2   2   3  54  53   1   2   0   0     .000    1 000
and so on till;
 999 1018 1019 1070 1069   1   2   0   0     000    1.000
1000 1019 1020 1071 1070   1   2   0   0     .000    1.000

    .000    1 000    1.000    1.000    1.000    1 000
VISCO                                          CARD 1 OF VISCOPLASTIC INPUT
1  1 86400 100 2 .5                  !CARD 2: maximum of 100 time increments per load increment
1 2  1 2                                  !CARD3; 2MPa is the tension resistence and
.4  -20                          !CARD 4:Mohr Coulomb perfect plasticity for the unique material type
0                                                  !CARD3: no other materials
20                                  !CARD 5: The applied load is incremented to 20 steps
0                                                  !CARD 6:no creep data
```